Upper Labrador Sea Freshwater - Seasonal to Decadal Variability

Dissertation
zur Erlangung des Doktorgrades
der Mathematisch-Naturwissenschaftlichen Fakultät
der Christian-Albrechts-Universität
zu Kiel

vorgelegt von

Sunke Schmidt

Kiel
März 2008

Referent/in: .....

Korreferent/in: .....

Tag der mündlichen Prüfung: .....

Zum Druck genehmigt: Kiel, ...

Der Dekan

Abstract

The main focus of the thesis is the analysis of freshwater variability in the upper Labrador Sea on seasonal to decadal time scales. The seasonal freshening of the Labrador Sea and its variations play a key role in Labrador Sea deep water formation, since the freshwater has large impact on the stratification of the water column. This stratification as well as atmospheric forcing define in first order the intensity and density - thus depth - of the convection. Therefore it was the aim of this study to understand the origin, variability and path of the freshwater better.

A large amount of data sources got combined to get the best possible results, including two online databases of CTD data, float data from the "Labrador Sea Deep Convection Experiment" (1996-1999), ARGO-floats and thermosalinograph data from the North Atlantic. The analyzes concentrate on 9 region within the Labrador Sea that have low horizontal salinity gradients and represent all important surface water masses. The best possible climatological seasonal salinity cycle was constructed for every region. This is for instance important for judging on anomalies in decades with only isolated measurements in a few months. The climatological salinity cycles confirm qualitatively my preliminary work in Schmidt and Send (2007).

The further use of satellite SSH-anomaly measurements derived geostrophic surface currents and eddy kinetic energy (EKE) allowed a selection of high and low EKE years from the last 13 years of satellite data. These years show significant hydrographic differences in the central Labrador Sea. Years with low EKE in the Labrador Sea show an early freshening between April and May. The existence, variability and origin of this freshening was so far unsure. The freshwater pulse is not existing in years with high EKE. On the basis of changes in geostrophic surface current and variabilities within the seasonal cycle of some regions I develop a hypothesis. This hypothesis describes the origin, pathway and occurrence of the early freshening pulse in the central Labrador Sea. High EKE in the Labrador Sea seems to reduce the mean velocities of the southern West Greenland Current branch or even stops it. Since this branch is a pathway of freshwater into the northern Labrador Sea and the convection area, high EKE suppresses the freshwater flux into the Labrador Sea.

Finally I analyze the pathway of decadal variations in salinity like the Great Salinity Anomaly (GSA) of the 70's. Measurements in the West Greenland Current region during times of large anomalies in the central Labrador Sea ('57, '70, '85), show the origin of these anomalies in the salty Irminger Sea waters with salinities above 34.7. With an average lag of two years these anomalies are found in the fresh shelf water of polar origin, thus significantly past the occurrence in the central Labrador Sea. This order suggests that an origin in the source of the Irminger Current, the North Atlantic Current is more likely than in the Nordic Seas. This would contradict the general believe of Great Salinity Anomalies originating from the Arctic.

Zusammenfassung

Die vorliegende Arbeit untersucht die Salzgehaltsvariabilität in der Deckschicht der Labradorsee auf saisonalen bis dekadischen Zeitskalen. Variationen im Salzgehalt, insbesondere der saisonale Eintrag von Süßwasser in die zentrale Labradorsee, sowie seine Schwankungen, haben großen Einfluss auf die Stabilität der Schichtung. Diese wiederum hat - neben dem veränderlichen atmosphärischen Antrieb - den größten Einfluss auf die Menge und Dichte - und damit auch Tiefe - der Wassermassenbildung. Ziel dieser Arbeit ist es, Ursprung und Weg dieses Süßwassers nachzuzeichnen.

Basis dieser Arbeit ist - im Gegensatz zu bisherigen Studien mit ähnlicher Fragestellung - die Verarbeitung einer großen Menge von Messdaten. Herangezogen werden zwei Online-Datenbanken mit CTD-Profilen: Floatdaten aus den Zeiten des Labrador Sea Deep Convection Experiment (1996-1999) sowie ARGO-Floats und Thermosalinographen-Daten aus dem Nordatlantik. Die Analyse der Messdaten konzentriert sich auf neun Regionen, die für die Labradorsee von elementarer Bedeutung sind und sich durch geringe horizontale Salzgehaltsänderungen auszeichnen.

Da aus zurückliegenden Jahrzehnten teilweise nur Messungen aus einzelnen Monaten vorliegen, ist es von großer Bedeutung, zunächst den mittleren Jahresgang möglichst genau zu erheben, um Anomalien als solche erkennen zu können. Deshalb wird für jede der untersuchten Region der klimatologische Salzgehaltsjahresgang erstellt. Die klimatologischen Jahresgänge bestätigen quantitativ meine vorangegangenen Untersuchungen aus Schmidt and Send (2007).

Durch Hinzuziehen von Satellitenmessungen der SSH-Anomalien und den daraus berechneten geostrophischen Oberflächenströmungen und der Eddy Kinetic Energy (EKE), war eine Selektion von hohen und niedrigen EKE-Jahren aus dem Zeitraum der letzten dreizehn Jahre möglich (seit 1994). In ihren hydrographischen Eigenschaften sind diese Jahre in der zentralen Labradorsee deutlich zu unterscheiden. Jahre mit niedriger EKE haben einen frühen Süßwasserpuls zwischen April und Mai, dessen Existenz, Variabilität und Herkunft nicht eindeutig geklärt ist. Dieser Süßwasserpuls ist in Jahren mit hoher EKE nicht präsent. Anhand der Veränderungen in den geostrophischen Oberflächenströmungen und in der Variabilität des saisonalen Jahresgangs wird in dieser Arbeit eine Hypothese zur Ausbreitung und Herkunft dieses ersten bis dato noch unerklärten Pulses entwickelt: Hohe EKE scheint die mittlere Strömungsgeschwindigkeit des südlichen Westgrönlandstromabzweigs zu reduzieren und zeitweise zum Erliegen zu bringen. Dieser Strom ist jedoch ein Transportpfad von Süßwasser in die nördliche Labradorsee und in das Konvektionsgebiet.

Im letzten Teil dieser Arbeit werden die Ausbreitungspfade von dekadischen Salzgehaltsanomalien, wie zum Beispiel die große Salzgehaltsanomalie der 70er Jahre, untersucht. Messungen im Westgrönlandstromgebiet zu Zeiten großer Anomalien in der zentralen Labradorsee ('57, '70, '85) belegen eine Anomalie zuerst im salzigen Irmingerseewasser mit Salzgehalten über 34.7. Erst nach einer mittleren Verzögerung von etwa zwei Jahren sind die Anomalien im frischen Schelfwasser polaren Ursprungs zu sehen, also deutlich nach dem Auftreten in der zentralen Labradorsee. Diese zeitliche Abfolge legt nahe, dass die großen Salzgehaltsanomalien ihren Ursprung wahrscheinlicher im Irmingerstrom und damit im Nordatlantikstrom haben und nicht im polaren Wasser aus nordischen Meeren. Diese These widerspricht der vorherrschenden Meinung, dass die in der Labradorsee beobachteten Salzgehaltsanomalien ihren Ursprung in der Arktis haben.

Contents

Abstract **I**

Zusammenfassung **III**

1 Introduction **1**

2 Data **15**
2.1 Spatial and Temporal Resolution 15
2.2 Bathymetry 15
2.3 Hydrographic data 16
2.3.1 Floats 16
2.3.2 surface "underway" data 19
2.3.3 CTD-Measurements 20
2.3.4 Mooring Data 21
2.3.5 Processing and mapping of hydrography data 22
2.4 Altimetry data 24

3 Seasonal Salinity Cycle **27**
3.1 Data regions 27
3.1.1 Robust Seasonal Cycle 33
3.2 Labrador Sea salinity cycle 35
3.2.1 Central Labrador Sea (area cLS) 36
3.2.2 Northern Labrador Sea (LSn) 41
3.3 Boundary Currents 43
3.3.1 West Greenland Current shelf areas (WGC and WGCn) 43
3.3.2 West Greenland Current offshelf areas (WGC-ic and WGCn-ic) . . . 45
3.3.3 Southern West Greenland Current branch (sWGCb) 46
3.3.4 Labrador Current shelf area (LC) 46
3.3.5 Labrador Current offshelf area (LC-ic) 47
3.4 Discussion 47
3.5 Conclusion 52

4 Phases of EKE **53**
4.1 Spreading EKE in the Labrador Sea 53
4.2 EKE phases 59
4.3 Changes in Pathways and Transport 65
4.3.1 on-shelf geostrophic surface velocities 67

4.3.2 offshelf geostrophic surface velocities . . . 69
4.4 Hydrographic differences . . . 72
4.5 Pathway hypothesis and Conclusion . . . 77

5 Decadal variability **83**
5.1 Method . . . 83
5.2 Labrador Sea . . . 86
5.2.1 central Labrador Sea (area cLS) . . . 86
5.2.2 northwestern Labrador Sea (area LSn) . . . 87
5.3 West Greenland Current . . . 88
5.3.1 On shelf variations (area WGC and WGCn) . . . 88
5.3.2 offshelf trends (area WGC-ic and WGCn-ic) . . . 91
5.3.3 southern West Greenland Current branch (area sWGCb) . . . 93
5.4 Labrador Current . . . 93
5.4.1 On shelf trends (area LC) . . . 93
5.4.2 offshelf trends . . . 94
5.5 Inheritance and correlations . . . 96
5.6 Periodicities . . . 100
5.6.1 Occurrence of Great Salinity Anomalies . . . 100
5.6.2 Labrador Current periodicities . . . 101
5.7 Discussion . . . 103
5.8 Conclusions . . . 106

6 Conclusions and Outlook **109**

7 Bibliography **113**

Abbreviations **121**

Chapter 1

Introduction

The world's ocean plays a key role in our climate system. It has the capacity to uptake and transport large amount of heat and gases, like oxygen and in particular anthropogenic gases like carbon dioxide (CO_2). The ocean can act as a conveyor and buffer for atmospheric fluctuations on timescales from days to years or even centuries. The global thermohaline circulation is an important component in some of these processes. This circulation, often called "conveyor belt", transports large amount of heat northward. The subsequent loss of heat to the atmosphere results in loss of buoyancy and eventually convective formation of intermediate and deep water masses. The conservative properties and dissolved gasses, representing the last contact to the atmosphere, are buffered in these newly formed water masses on timescales from centuries to millennia. Influences decreasing this deep water formation significantly, might therefore accelerate changes in the world climate dramatically.

Rising global average temperatures in the atmosphere and ocean, widespread melting of snow and ice and rising global average sea level make warming of the climate system unequivocal (IPCC, 2007). The reason for this is mainly to be found in considerably increasing release of anthropogenic gases since the beginning of the industrial period. This "recent" increase of anthropogenic gases is buffered by the ocean, as an example only two thirds of newly emitted anthropogenic CO_2 remains in the atmosphere (Sabine et al., 2004). One aspect in a warming climate, next to biological and chemical change (Fasham, 2003) is a variance of deep water formation that could change this oceanic uptake dramatically (Sarmiento and Le Quéré, 1996; Sarmiento et al., 1998). The North Atlantic, due to formation of Labrador Sea Water and North Atlantic Deep Water, stores 23% of the global inventory, despite covering only 15% of the global ocean area (Sabine et al., 2004). Thus an understanding of the sensitivity of North Atlantic convection to effects that are capable of changing this ventilation is crucial for future climate prognosis.

Further this North Atlantic deep water formation is part of the Atlantic meridional overturning circulation (MOC) and for this reason part of the thermohaline circulation (THC), though the term thermohaline circulation is understood in many different ways (Wunsch, 2002). The simplified view of THC consists of an upper component of light warm waters and a deeper one of dense cold water masses. The upper component is mainly wind driven, with an excess of energy in the tropics and a deficit in polar regions caused by uneven solar heating. Warm saline water masses are transported poleward, heating the atmosphere. This thermal buoyancy loss causes the water column to become unstable, thus the cooled water sinks. The newly formed deep water recirculates towards

the equator, slowly diffuses upward throughout the world ocean and returns as northward flow of warm water (STOMMEL AND ARONS, 1960a,b). The dynamical characteristic of the THC is its nonlinear behavior, which is the basis of understanding possible existence of several equilibrium states and relatively rapid transitions between them (GANOPOLSKI AND RAHMSTORF, 2001).

Model simulation showed that the meridional ocean circulation system appeared to be particular vulnerable to changes in the freshwater balance (LE TREUT ET AL., 2007), for instance it is believed that the abrupt Dansgaard-Oeschger climate change events find their origin in rapid changes of the Atlantic meridional overturning circulation (GANOPOLSKI AND RAHMSTORF, 2001; RAHMSTORF, 2002). Therefore it is important to estimate how likely a radical change in the MOC into a different regime in near future is. BREWER ET AL. (1983); LAZIER (1995) and CURRY AND MAURITZEN (2005) show a dilution of the North Atlantic Water masses since the 60's. This raises the possibility of a shift of circulation into another stable regime in timescales of two centuries at the current freshening rate (STOMMEL, 1961; CURRY AND MAURITZEN, 2005; LE TREUT ET AL., 2007), though a more rapid change would be expected for a pooling and sudden release of freshwater.

Freshwater input in the North Atlantic consists of precipitation, continental runoff, Greenland ice shield melt and icebergs and annual and multi year sea ice melt. Freshwater is lost by evaporation, sea ice formation and export of intermediate and deep water masses. Evaporation and sea ice formation hardly export any freshwater from the North Atlantic including the arctic, thus deep water formation is the only possibility of effectively exporting freshwater from this region.

This deep water formation, convection, is the process of vertical mixing between upper and intermediate or deep layers. For convection to set in, several premises have to be fulfilled and thus only a few areas favor deep convection. These premises include a cyclonic circulation, which invokes doming isopycnals, and prevailing rigorous surface buoyancy loss. Regions that fulfill these are some bays of the Antarctic especially the Weddel Sea, the Mediterranean Sea in mid latitudes and the Greenland Sea and Labrador Sea in subpolar and polar regions. The whole convection process can be described in three steps, at which the actual intense vertical mixing, often referred to as convection, is second. These three steps can be sketched as follows:

preconditioning (on large scales, up to the order of several $100\,km$) Basin scale cyclonic circulation domes the isopycnals of the interior and exposes deeper water masses closer to the surface. Increasing oceanic heat loss to the atmosphere in autumn and early winter erodes the vertical density gradient between the upper layer and the weakly stratified water mass beneath, until the water column is weakly stratified from the surface to greater depth (e.g. MARSHALL AND SCHOTT, 1999).

deep convection (on scales the order of $\leq 1\,km$) Subsequent buoyancy loss associated with prevailing meteorologic conditions may cause a violent mixing down to great depths in numerous plumes that distribute the dense surface water in the vertical. These plumes form a deep mixed patch on scale from tens to $> 100\,km$ (e.g. SEND AND MARSHALL, 1995).

lateral exchange and spreading Increasing horizontal density gradients at the limits of the mixed patch lead to a "rim current". Thus baroclinic instabilities at the bound-

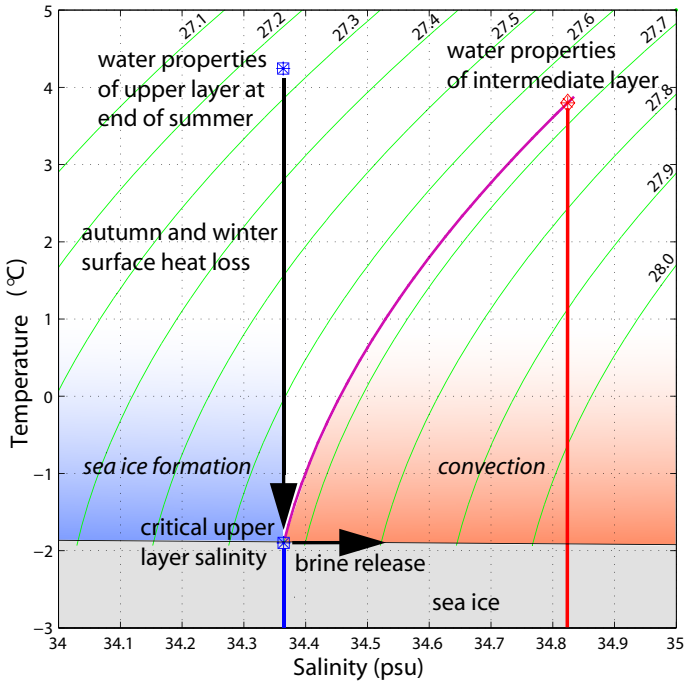

Figure 1.1: Sketch of water property changes in autumn with emphasis on the possibility of sea ice formation at low salinities. Blue marks the upper water layer salinity red the intermediate water.

aries of the convection patch can create eddies, in which the dense mixed water slowly sinks, (e.g. Jones and Marshall, 1997).

The vulnerability to freshwater is imminent in the preconditioning phase. A lighter fresher upper layer is more buoyant, thus preconditioning takes longer, leaving less time and less buoyancy loss for the subsequent convection. During phases of intense freshening deep convection can even be completely shut down. The convection can be shut down, if either the thermal forcing is not cooling vigorously enough, if the upper water layer is too buoyant, or if the upper layer reaches it freezing point before the vertical density gradient of upper layer and weakly stratified water mass beneath is eroded. In the latter case sea ice forms and thus isolates the ocean from the atmosphere, though brine release and turbulence do increase the chance of convection by inducing or mixing up salt (Rudels, 1990). An idealized sketch of this is illustrated in figure 1.1, an intermediate water layer with salinities of $34.83\,psu$ and a temperature of $3.8°\,C$ and an upper layer with salinities below $34.36\,psu$ would not convect but form sea ice in an idealized non turbulent water column. Such sea ice formation is observed in the Weddel Sea and Greenland Sea (Wadhams, 2000). In the Labrador Sea sea ice formation is mainly observed in the boundary currents, the central Labrador Sea stays so far free of sea ice (Mysak et al., 1990; Wang et al., 1994). The reason for this is the relative warm subsurface waters of the Irminger Current that enters the Labrador Sea beneath and offshelf from the West Greenland current.

The West Greenland Current and Labrador Current form the large scale cyclonic circulation of the Labrador Sea (figure 1.2) and are part of the subpolar gyre. Both currents have cold fresh polar waters on the shelf and warm saltier Irminger Sea Water above the

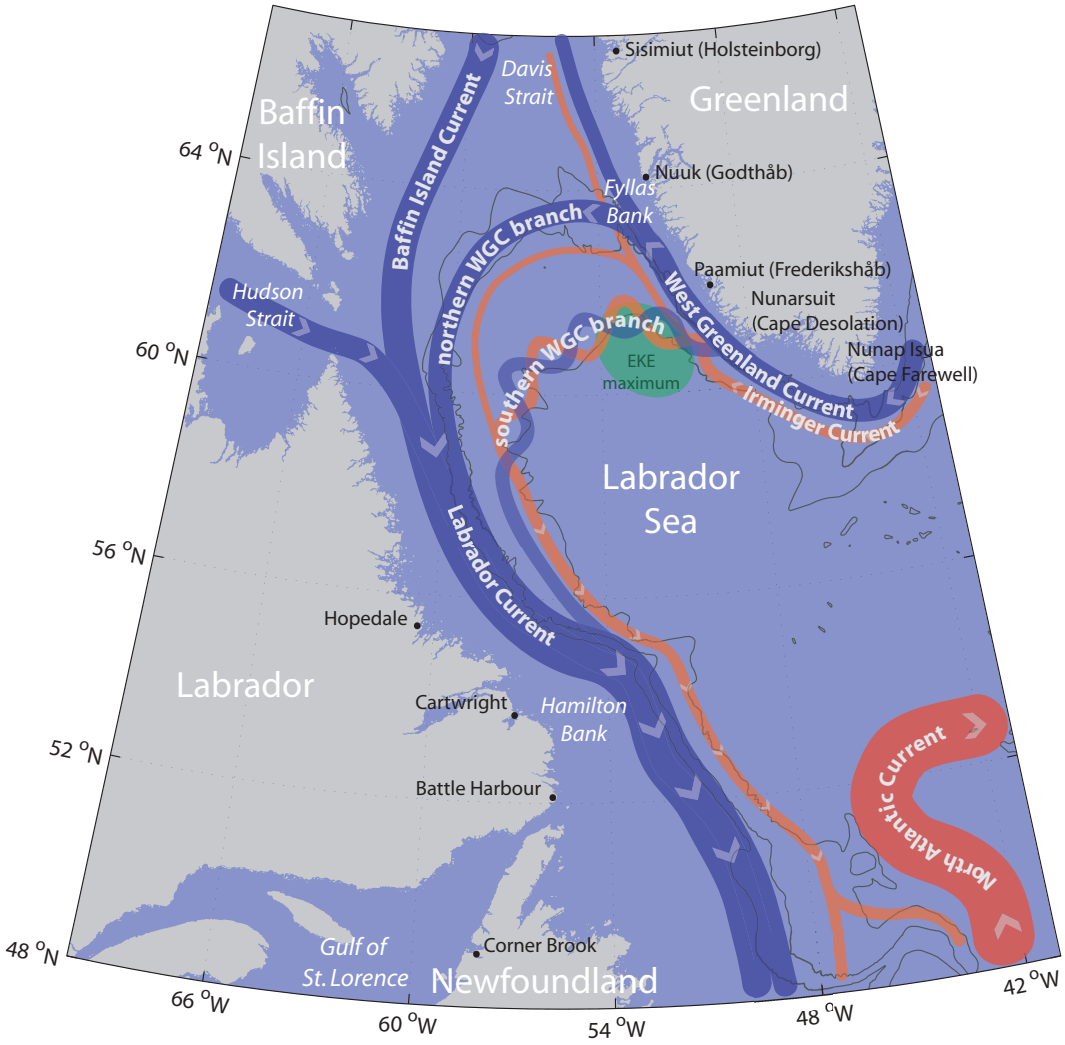

Figure 1.2: Schematic surface currents in the Labrador Sea. Blue are in general cold fresh currents, red warmer saltier ones. The extension of the Irminger Current is mainly beneath the West Greenland and Labrador Current. The width of the currents is not linear correlated to velocities or transports. 1000 m, 2000 m and 3000 m isobath indicated. The location of maximum EKE in the Labrador Sea is marked green. The southern West Greenland Current branch is meandering strongly, indicated by the wiggly line.

continental slope (Lazier and Wright, 1993; Cuny et al., 2002). For this reason the inflow of Irminger Sea Water beneath and offshore of the West Greenland Current is often called the "Irminger Current" (Cuny et al., 2002). The polar waters of both currents includes runoff respectively from Greenland or Canada (Bacon et al., 2002; Straneo and Saucier, 2007), though the amount is expected to be very variable and hard to verify. The 3000 m isobath is in general considered to be the outer limit of the boundary currents. The West Greenland Current bifurcates into several branches past Cape Desolation (figure 1.2), where the 3000 m isobath branches off the continental slope. Corresponding to the naming of Cuny et al. (2002) the two branches entering the Labrador Current are the northern and southern West Greenland Current branch. The strongly meandering southern

branch, often mere regarded as eddy pathway, is drawn in a wiggly line.

The bifurcation of the southern West Greenland Current branch is approximately also the position of the dominant eddy kinetic energy (EKE) signal in the Labrador Sea. This is found directly south of the 3000 m isobath that turns west and finds its origin in the West Greenland Current south of Cape Desolation due to a indentation in the continental slope (e.g. Fratantoni, 2001; Eden and Böning, 2002; Brandt et al., 2004). The location of this EKE maximum of the Labrador Sea will be termed "EKE hot spot" in the following (marked green in figure 1.2). More than a third of the eddies in the central Labrador Sea originated from this area in a census by Lilly et al. (2003). Model analysis suggest that these eddies play an important role in restratifying the Labrador Sea after deep convection (Katsman et al., 2004; Czeschel, 2005).

Open ocean deep convection occurs in the region of strongest atmospheric forcing within the cyclonic gyre. The region may vary but open ocean convection has been observed roughly between $55° - 60°N$ (e.g. Lab-Sea-Group, 1998; Pickart et al., 2002; Kortzinger et al., 2004). Convection down to 1000 m depth within the Labrador Current was also observed (Pickart et al., 2002; Cuny et al., 2004).

Convection depth in the Labrador Sea is first order dependent on late summer stratification and atmospheric forcing. The latter is connected to the North Atlantic Oscillation (NAO), thus a small influence between convection depths and NAO can be found (Dickson et al., 1996). The North Atlantic Oscillation is the dominant mode of atmospheric variability in the north Atlantic and is an index of the meridional gradient in atmospheric sea level pressure. It accounts for more than a third of the total variance in winter sea level pressure. This has direct influence on atmospheric temperature, precipitation and storm track activities (Hurrell, 1995). The strength of this mode is given by the NAO index, generally the sea level pressure difference between Iceland and the Azores. Pickart et al. (2002) show that during high-NAO winters, the intense lows that pass over the southern Labrador Sea draw cold, dry air from the Labrador continent over the relatively warm surface waters of the sea. This causes enhanced airsea buoyancy fluxes, thus favoring convection due to an increase in latent and sensible heat loss. The monthly correlation between NAO index and heat flux is 0.5 (0.45 and 0.56 for the upper and lower 95% confidence bounds). Using only the winter months January to March this correlation increases to 0.71 (0.56 and 0.82 for the upper and lower 95% confidence bounds) and stays around this value for longer time scales. This correlation between Labrador Sea atmospheric heat flux and low pass filtered winter time NAO January to March is shown in figure 1.3. The NAO index has a high monthly variability with a slightly reddish spectrum with barely significant peaks on decadal and inter decadal time scales, though it is not yet clear whether they are significant trends or oscillations (Wunsch, 1999).

Convection during phases of high NAO can reach depths of more than 2000 m (Clarke and Gascard, 1983). Though this shows the importance of the NAO to favor deep convection, it is merely a part of the convective process and cannot explain all variability. For instance the absence of convection deeper than 1400 m since 1995 (Avsic et al., 2006), cannot be explained by the NAO alone (Lazier et al., 2002; Stramma et al., 2004).

One major reason for atmospheric heat flux or NAO index and convection depth not being well correlated is the highly variable interannual stratification of the Labrador Sea (Lab-Sea-Group, 1998), since stratification and duration of the preconditioning phase are

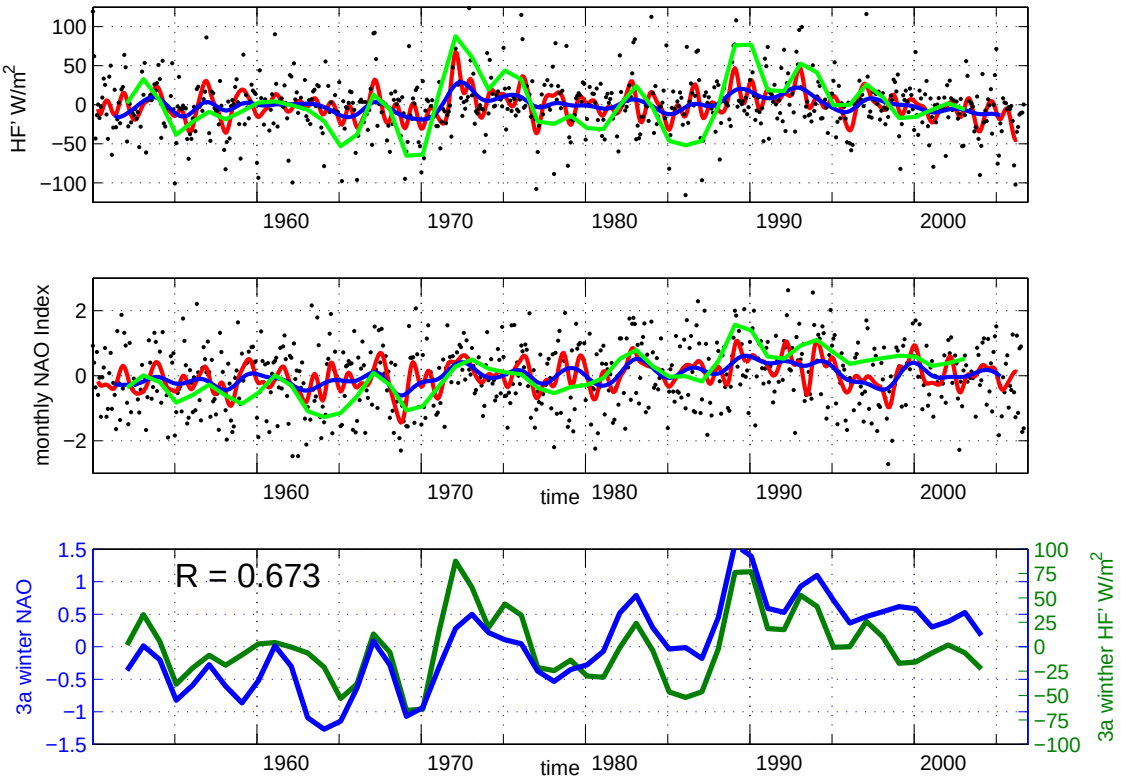

Figure 1.3: Monthly heat flux anomaly, HF' (upper panel) from NCEP and corrected by algorithm from Renfrew et al. (2002) in the central Labrador Sea and NAO index (middle panel). The monthly data is shown in black, 1 year low pass filtered data in blue, 3 years low pass filtered data in red. In Green indicated is the 3 year low pass filtered winter mean (January to March). Lowest panel shows the correlation between the two winter mean data set from the above panels.

correlated. This variability originates to some extent in year-to-year differences of convection activity and depths (Marshall and Schott, 1999; Lu et al., 2007), restratification strength (Dickson et al., 1996; Katsman et al., 2004) as well as summer time heating and freshening of the upper water layers from the boundary currents (Dickson et al., 1996; Straneo, 2006; Schmidt and Send, 2007). All these factors vary (partly independently) strongly on an annual basis. These factors on seasonal and decadal timescales are most pronounced in the upper 200 m (Schmidt and Send (2007)), in which the haline variability extends about twice as deep as the thermal (figure 1.4).

The difference in thermal and haline influence on stratification can be approximated by using the simplified equation for density of seawater:

$$\rho = \rho_0(1 - \alpha(\theta - \theta_0) + \beta(S - S_0)) \tag{1.1}$$

with ρ, θ and S as density, temperature and salinity, and ρ_0, θ_0 and S_0 the reference density, temperature and salinity. β is the haline contraction coefficient and α the thermal expansion coefficient. Since for typical Labrador Sea water properties the haline contraction coefficient, β is in the order of ten times larger than the thermal expansion coefficient α,

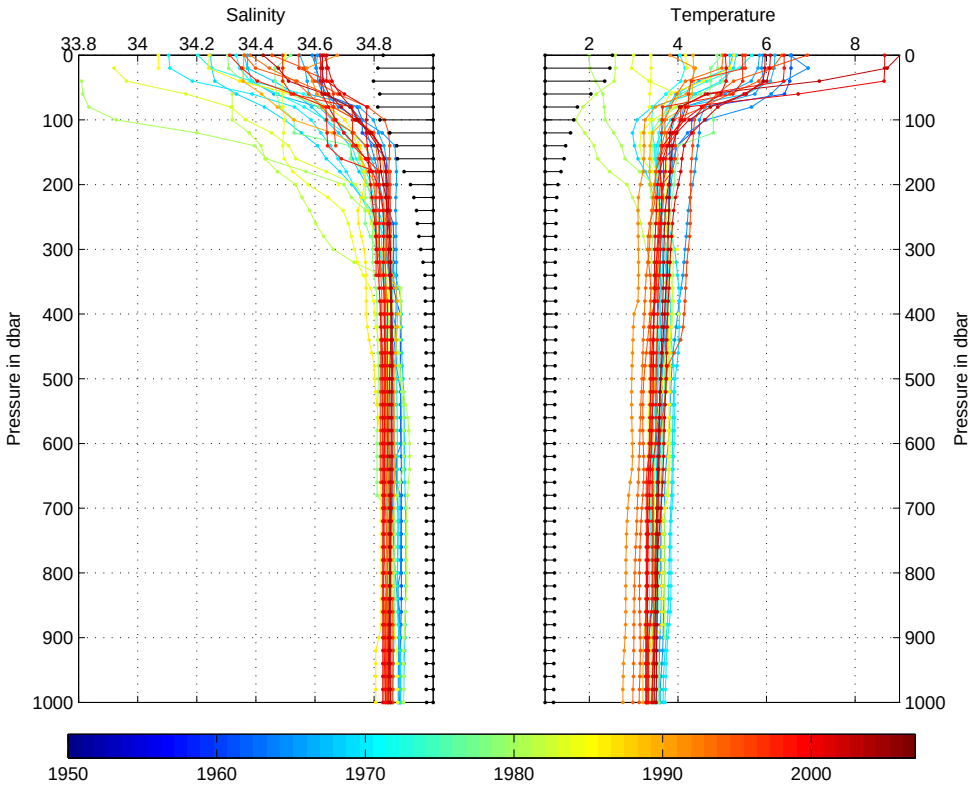

Figure 1.4: Mean October-November salinity and temperature profiles from the central Labrador Sea since 1950. Color indicates the year, the black bars off 35 psu and 1° C give the standard deviation for each depth.

the different variability of temperature and salinity (figure 1.4) in the surface layer reflects directly their role in stratifying the Labrador Sea. This explains why the Labrador Sea in the top 300 m and even the top 800 m has a dominance in haline stratification (figure 1.5). Temperature and salinity have about equal shares in integrated buoyancy content of the top 1800 m. This Labrador Sea stratification sensitivity to salinity emphasizes the importance of understanding the seasonal to decadal variability in upper Labrador Sea freshwater content.

The seasonal variation in stratification is dominated by the effect of restratification after convection. It is the result of salinity as well as temperature stratification that build up after the typical deep mixing or convection period in March and April. The Labrador Sea experiences a net annual heat loss to the atmosphere and due to its special character as a convection region the heat loss is distributed over a larger depth. Loss of heat is balanced by lateral exchanges with warm and salty, modified North Atlantic water (Lilly et al., 2003; Katsman et al., 2004; Straneo, 2006). This water is supplied to the Labrador Sea boundary current regime by the Irminger Current. For the processes involved it is believed that the Irminger Current Eddies, generated by the West Greenland Current off Cape Desolation play a key role (Pickart et al., 1996; Lilly et al., 2000; Prater, 2002; Lilly et al., 2003, e.g.). These eddies consist of a warm and saline body of Irminger Current water origin. Some of these generated eddies propagate southward into the deep Labrador Sea. They release their water properties to this area when dissipating and thus

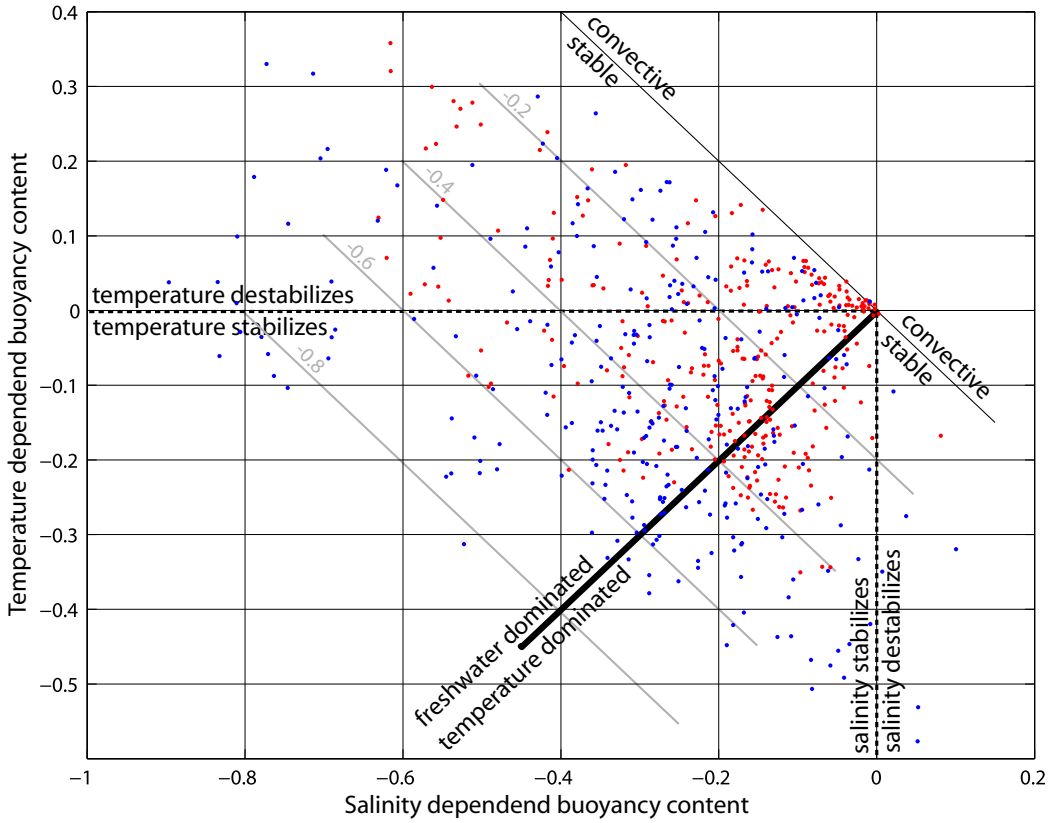

Figure 1.5: Mean monthly buoyancy content integrated from surface to 300 m (red) and top 800 m (blue) since 1950. Data points around (0,0) indicate a completely mixed 300 m (800 m) column. The distance to the "convection-stable" line indicates the strength of stratification (gray lines). The side and distance to the "freshwater-temperature dominated" line is a measure about importance and share in the stratification of temperature and salinity, it represents the difference between integrated haline and thermal buoyancy content.

providing heat and salt to the Labrador Sea. This is especially notable for depths below 300 m in the, after convection, very weakly stratified upper Labrador Sea Water.

After deep convection a pronounced freshening at the surface takes place successively deepening in the course of the year (Straneo, 2006; Schmidt and Send, 2007), forming an approximately 150 m deep very fresh surface layer in November. This freshening cannot be explained by local effects like evaporation and precipitation or ice melt.

Local Salinity Sources and Sinks as Origin of central Labrador Sea freshwater

Possible local sources and sinks of freshwater are precipitation and evaporation, local sea ice melt and vertical mixing. As suggested in Schmidt (2003) and discussed further by Schmidt and Send (2007) these sources and sinks do not play any significant role in the freshening process of the central Labrador Sea, as will be summarized in the following. In the central Labrador Sea vertical mixing is the only major source of salt for the upper water layers above the level of Irminger Sea water ($< 150\,m$). The following can be said about the local fluxes:

Precipitation and evaporation (F_p) has some uncertainties and thus has been stated to be the origin of observed freshening due to the estimated total amount given by precipitation climatologies. The amount of precipitation minus evaporation is in the order of 40 cm per year, with varying strength of seasonal cycle. As this freshwater source is fairly evenly spread over time it can be ruled out as source for sudden freshwater pulses, but could account for roughly 20% of the observed freshening from April to September as described by Schmidt and Send (2007) (e.g. daSilva et al., 1994; Walsh and Portis, 1999; Sathiyamoorthy and Moore, 2002).

Local sea ice melt (F_{ice}) It is known that the central Labrador Sea stays free of sea ice (e.g. Mysak et al., 1990; Wang et al., 1994). Hardly any sea ice drifts into the central Labrador Sea, most of it melts in the boundary current area. The 100 m and 3 000 m isobaths represent approximately the minimum and maximum ice extent between February and May (Peterson et al., 2000). Central Labrador Sea tracer analyses in early summer by Khatiwala et al. (1999) do not show significant influence of local sea ice melt. All this indicates that it is very unlikely that *local* sea ice melt contributes to the first freshwater signal. Further there is no sea ice present in the Labrador Sea area in late summer, during a constant freshening period. Thus it can be assumed that $F_{ice} = 0$ throughout the seasonal freshening period.

Vertical mixing (F_v) Since the surface boundary currents of the Labrador Sea are fresher throughout the year, the only possible pathway for freshwater out of the Labrador Sea is vertical mixing. Autumn and winter heat loss ventilates freshwater to deeper layers and forms an upper part of the North Atlantic Deep Water (NADW). The upward flux of salt restores the central Labrador Sea salinities nearly every year to similar values around 34.7-34.8. This process can be influenced significantly if atmospheric heat loss is not vigourous in winter time and if the upper Labrador Sea buoyancy is anomalously high, as during times of Great Salinity Anomalies.

Since local fluxes cannot explain the freshening phase of the central Labrador Sea salinity cycle it leaves only lateral advection or mixing from the boundary currents as further possible source.

Boundary Currents as Origin of central Labrador Sea freshwater

Freshwater from the boundary currents has to be the source for central Labrador Sea freshening on seasonal and interannual periods. Early works suggested the Labrador Current as the origin of central Labrador Sea freshwater (Lazier, 1973, 1988; Khatiwala et al., 1999, e.g.), while later works see the West Greenland Current as the origin (Cuny et al., 2002; Straneo, 2006; Schmidt and Send, 2007).

Straneo (2006) argues that the density gradient between the interior and the boundary currents triggers the exchange via eddies and small scale features and thus is responsible for the seasonally observed salinities.

In Schmidt and Send (2007) we assume that all sinks and sources for a 0-150 m volume in the interior Labrador Sea balance each other out in a mean state and the sum of anomaly fluxes in and out of the volume explain the interior Labrador Sea seasonal cycle. Thus we

argue that

$$\frac{\Delta v_{ls}}{\Delta t} = F'_{ice} + F'_p + F'_v + F'_{lc} + F'_{wgc} + F'_{ic} \tag{1.2}$$

the temporal change of the Labrador Sea salinity content $\frac{\Delta v_{ls}}{\Delta t}$ can be explained by the sum of local and boundary current anomaly fluxes, the Labrador Current F_{lc}, the West Greenland Current F_{wgc} and the Irminger Current F_{ic}. Since drifter analysis by CUNY ET AL. (2002) show about 1/3 of the West Greenland Current drifters entering the deep Labrador Sea but no Labrador Current drifter doing so, we assume $F_{lc} = 0$. Furthermore F_p was neglected, since it has some influence but can not explain observed cycles. Since no observations about the seasonal variation of F_{ic} existed it was assumed constant, thus reducing the absolute salinity but not contributing to a seasonal cycle. As this thesis will show, this assumption can be quantitatively confirmed by observations. Thus leaving the very straightforward balance:

$$\frac{\Delta v_{ls}}{\Delta t} = F'_v + F'_{wgc} + F'_{ic} \tag{1.3}$$

The equation 1.3 can be sketched for the seasonal cycle and is shown in figure 1.6. This was then further used for a budget calculation using available mean seasonal cycles from the Labrador Sea and the West Greenland Current, showing that the West Greenland Current can explain quantitatively the seasonal Labrador Sea freshening, assuming a constant propagation of 1/3 of the West Greenland Current water into the central Labrador Sea. This volume estimate reflected the number of drifters leaving the West Greenland Current.

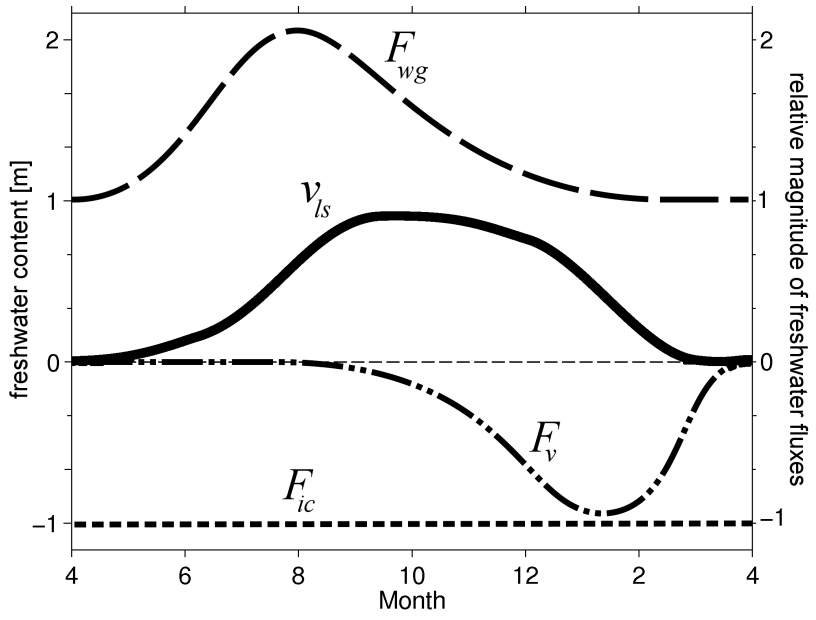

Figure 1.6: Sketch about temporal evolution of freshwater fluxes and freshwater content in central Labrador Sea.

The above calculation applies to the main freshening observed from June to September, but so far the origin and occurrence of an early freshening around May in the seasonal central Labrador Sea salinity cycle is uncertain, next to the main freshening shown in the sketch in figure 1.6. This early freshening was first described by Schmidt (2003) and Schmidt and Send (2007), but could not be found by Straneo (2006) in her later data set covering mainly the years 1997 to 1999.

Addressing more long term variabilities in the Labrador Sea various authors suggest or assume a connection between freshwater export from the Arctic via the East Greenland Current and surface salinities or convection activity in the Labrador Sea (e.g. Aagaard and Carmack, 1989; Dickson et al., 1996; Pickart et al., 2002; Haak et al., 2003; Kwok et al., 2004), for which the Great Salinity Anomaly (GSA) of the 70's is believed to be a pronounced example (Dickson et al., 1988). The GSA of the 70's led to a very fresh surface layer in the central Labrador Sea shutting down convection for three years, as can be seen in figure 1.7 during the years 1969, 1970 and 1971. Since the Labrador Sea has a mean heat loss during the year, the stopped vertical mixing led to significant cooler temperatures during those times (figure 1.8), eventually accompanied by extraordinary atmospheric forcing (compare figure 1.3) starting deep mixing again in 1972.

A smaller salinity anomaly with accompanying lower temperatures can be seen in recent years in 2001 and 2002 in the same figures 1.7 and 1.8, though it was not strong

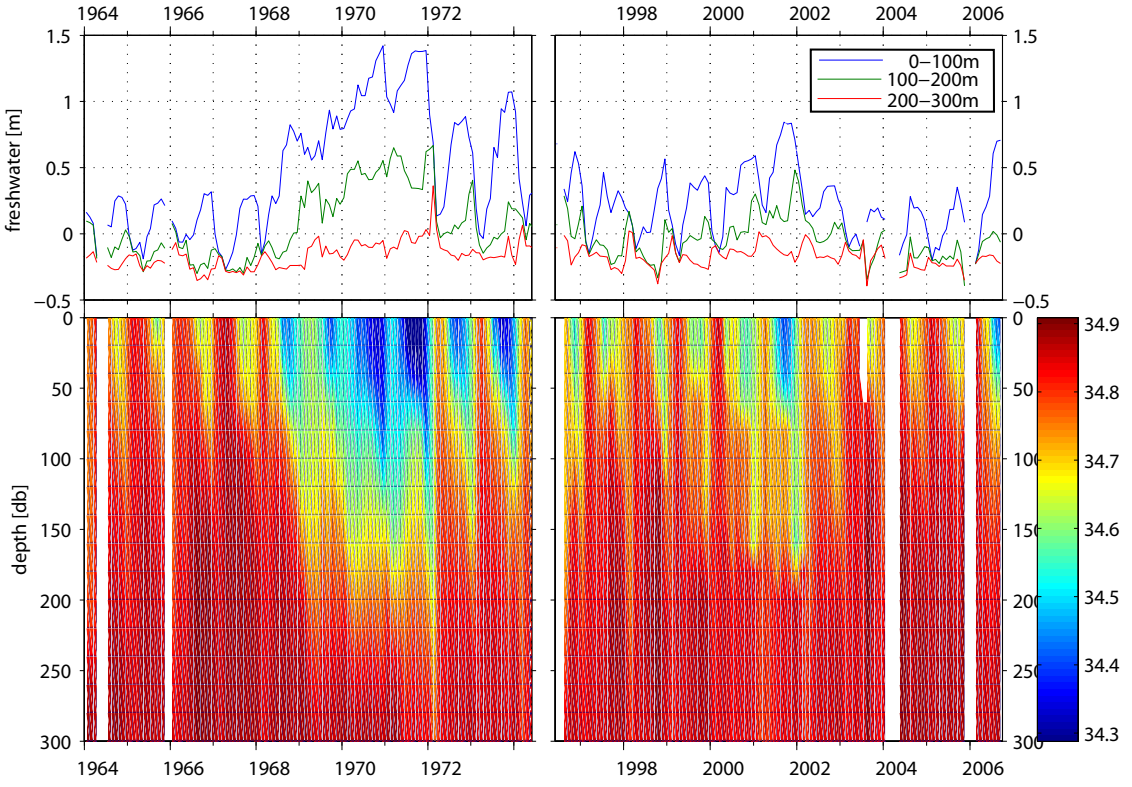

Figure 1.7: Salinity time series from the central Labrador Sea for the two best sampled periods. Upper panel shows the freshwater content for 3 layers to the reference salinity 34.76.

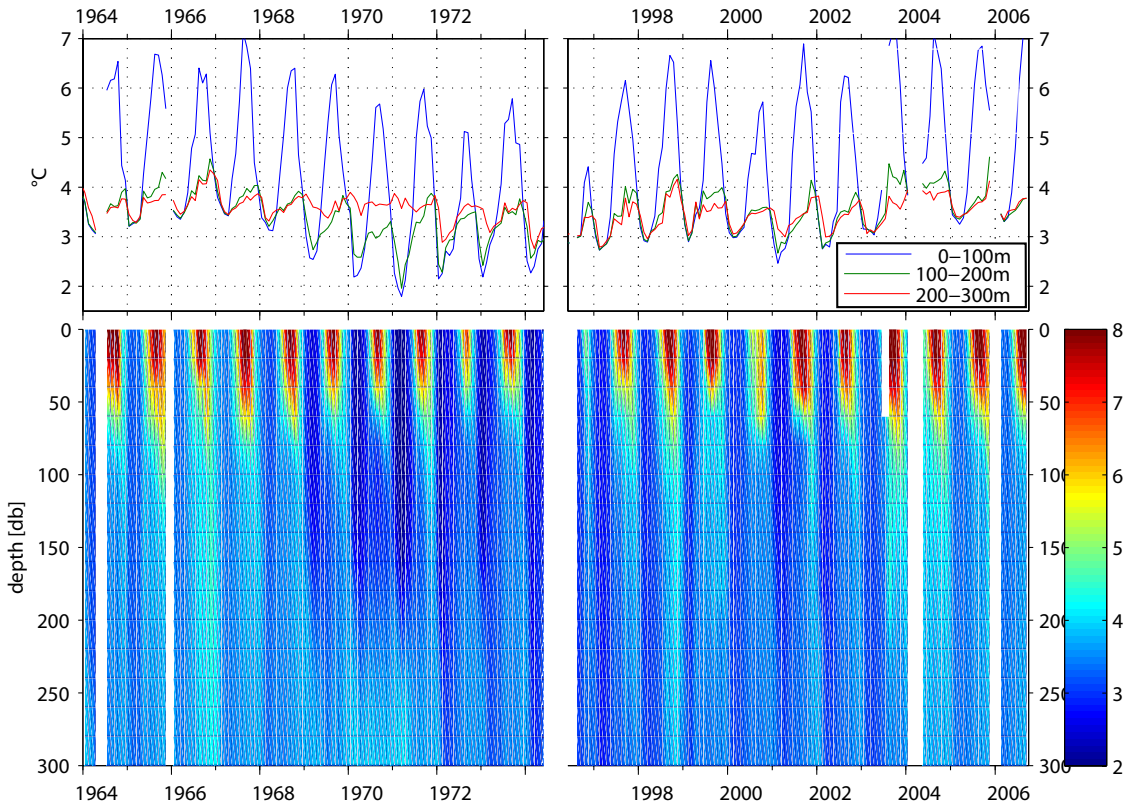

Figure 1.8: Temperature time series from the central Labrador Sea for the two best sampled periods. Upper panel shows the mean temperature for 3 layers.

enough for convection to be suppressed during those years (table 1.1).

Motivation

There are several unanswered questions that are tried to be answered in this thesis.

Schmidt and Send (2007) note two freshening periods for the convection area in the Labrador Sea, but Straneo (2006) sees only one freshening in her data set covering 1997 to 1999. The reason for this is unclear and the thus unsure occurrence needs to be clarified with a much larger data set. If the climatological salinity cycle is well known, a variable occurrence of any signal should result in high variability during months of the passing of this signal. A robust climatological salinity cycle for regions within the Labrador Sea can help to track signals and properties can provide useful information about the origin of water masses. Furthermore adjacent areas need to be analyzed to get more information about the possible origin of this freshening.

Even knowing the climatological cycles of some regions, water properties get influenced by several factors. Therefore it is of major interest to know the impact of modulation from different factors. Especially the influence of the EKE close to the West Greenland boundary current on the central Labrador Sea is still not clear. There is an enhanced salt transport associated with the eddies (Lilly et al., 2003), but the transport estimates are still vague. All previous studies focused mainly on the effect of restratification in the depth of the upper

Year	Convection Depth in db	previous summer top 300m buoyancy (haline percentage)	Heat flux anomaly (Oct-Apr)
1995	2300	-	-13.5
1996	1300	-	37.0
1997	1400	-0.27 (73)	-25.6
1998	1000	-0.30 (29)	3.9
1999	1000	-0.41 (40)	10.5
2000	1100	-	1.7
2001	1100	-0.42 (50)	27.8
2002	1200	-	1.4
2003	1400	-0.36 (51)	3.1
2004	700	-0.45 (15)	26.6
2005	1300	-0.40 (33)	9.2
2006	1000	-0.37 (40)	40.4

Table 1.1: Convection depths and prevailing stratification and surface heat flux. Stratification is from pre-convection late summer (October stratification). Heat flux anomaly is the cumulated monthly anomaly from October to March from the long term mean (1950-2006). 1995-2006 convection depths from Avsic et al. (2006)

Labrador Sea water and the water transported within the eddies. This thesis will analyze the impact of these eddies on the seasonal cycle and check whether times of enhanced EKE in the Labrador Sea vary in further aspects. It is analyzed if the variable occurrence of an early freshening has a connection to the variability in EKE intensity.

A robust climatology further allows to analyze isolated measurements from past decades for anomalies better and thus provides a good long term data set. Looking on these longer time scales it is common believe that the Great Salinity Anomaly of the 70's is advected from the Nordic Seas into the Labrador Sea via the East and West Greenland Current system. Therefore provided with a good data set it should be tried to resemble this pathway within the Labrador Sea and check the origin and propagation of further anomalies described in the Labrador Sea (Belkin et al., 1998). It is of main interest to see if all anomalies have a similar origin, or if different sources can evoke Great Salinity Anomalies in the Labrador Sea.

This motivation is similar to the outline of this thesis:

Since data coverage in temporal and or spatial means is the weakness of most studies from this region, the construction of a database including all free available data from the larger Labrador Sea region was the first task. The data sources used, their thorough quality control and accuracy assumptions are described in chapter 2.

Afterwards regions of interest in the Labrador Sea are defined and climatological salinity cycles are constructed for these regions. The results confirm previous works and give further evidence about the early freshening in the central Labrador Sea. For the West Greenland Current the strong separation between Polar- and Irminger Sea Water at the entrance of the Labrador Sea with very different seasonal cycles get emphasized. This is presented in chapter 3.

The impact of EKE activity is described in chapter 4, by analyzing the eddy kinetic energy in the central Labrador Sea and addressing hydrographic differences during high and low EKE years. Concluding this chapter a pathway hypothesis sketching the differences in

freshwater fluxes from high to low EKE is presented.

Then the Great Salinity Anomalies are analyzed in detail in chapter 5. Due to the large data set and layout of the regions I am able separate the long term anomalies originating from the Nordic Sea and Irminger Sea. The very surprising results contradicting general believe are discussed thoroughly.

Concluding in chapter 6 I give a summary about the results and address future consequences as well as questions that arose from this analysis.

Chapter 2

Data

2.1 Spatial and Temporal Resolution

To get an overall good data coverage many data sources were used. Bathymetry, hydrography and altimetry data are described below. The hydrography data includes float, mooring, CTD and "underway" data.

Combining these different types of hydrography data to one data set can evoke bias, as their spatial and temporal sampling are very different from each other. The float data give good resolution profiles around the year nearly solely for regions deeper then 2000 m. But float data is only available for more recent years with still strong errors on salinity measurements in the first years. Mooring data has the best temporal resolution, but sampling is only one fixed position at a few distinct depths, so local or regional restricted events can be overestimated for a larger region in times of few data. Ship based CTD data is unbeaten in its vertical resolution and accuracy. Unfortunately due to the harsh environmental conditions of the Labrador Sea, few winter profiles exist compared to a large number of summer profiles. This is especially true for some shelf regions, because of a stronger presence of icebergs and sea ice in wintertime. Otherwise the shelf regions are much more densely sampled by CTD than the deep regions of the Labrador Sea. Underway data only gives measurements very close to the surface along ship routes, with a high uncertainty of accuracy. In the Labrador Sea it was mainly available from ships of opportunity sailing to Greenland harbors, thus the sampling on the Greenland shelf is the best (there are much fewer settlements on the Baffin Island and Labrador side that cannot be reached via land or air better).

The specific data sets, and their quality control are described in detail below. Section 2.3.5 notes the few possible procedures taken to minimize bias from sampling and the precaution needed using this combination of data.

2.2 Bathymetry

The bathymetry data used for this thesis were assembled and gridded by Smith and Sandwell (1997). The gridded data ranges from 72° S to 72° N with a resolution of about 1.5×1.5km in the area of the Labrador Sea. Depth of positions used is computed by linear interpolation of the four adjacent points. The depth of a position has strong influence on its weighting when averaging data in one region or for one position close to the shelf break as

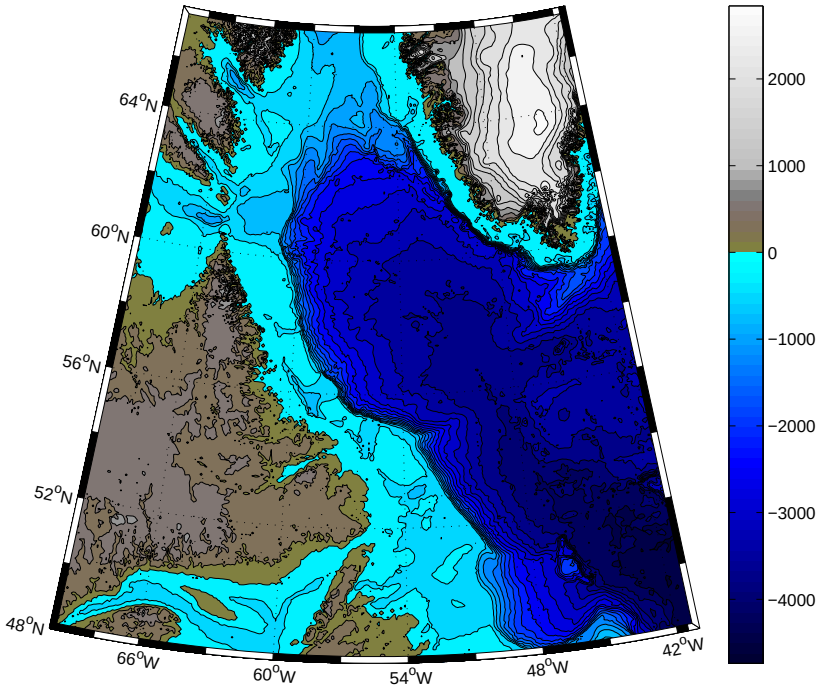

Figure 2.1: Bathymetry of the Labrador Sea. Isobaths are in 100 m intervals. The bathymetry used is assembled and gridded by Smith and Sandwell (1997) and updated 200X.

described in detail in section 3.1. Assuming that the position of a profile is always correct the only uncertainty is the bathymetry data for the weighting. Figure 2.1 shows 100 m isobaths from the seafloor to the top of the ice cap from Greenland. The least steep part of the shelf region in the north of the Labrador Sea is obvious. Leading to the bifurcation of the West Greenland Current into three branches as seen in figure 1.2. The coast line used is in vector format from the GEBCO[1], data set.

2.3 Hydrographic data

Due to the very different temporal, lateral and vertical resolution of the used hydrography data sets they are described separately, before addressing the combined data set.

2.3.1 Floats

The float data used consists of two different data sets. The first float data set is from PALACE[2] floats that were deployed at the Labrador Sea Deep Convection Experiment (1996-1998). A few floats measured until late 1999. Figure 2.2 left hand side red bars shows the number of PALACE float profiles within 3 months. The right hand side shows the distribution of these float profiles in red that passed the validation mentioned below. The blue bars and dots are from the ARGO data set described below. The PALACE

[1] General Bathymetric Chart of the Oceans
[2] **P**rofiling **A**utonomous **LA**grangian **C**irclulation **E**xplorer

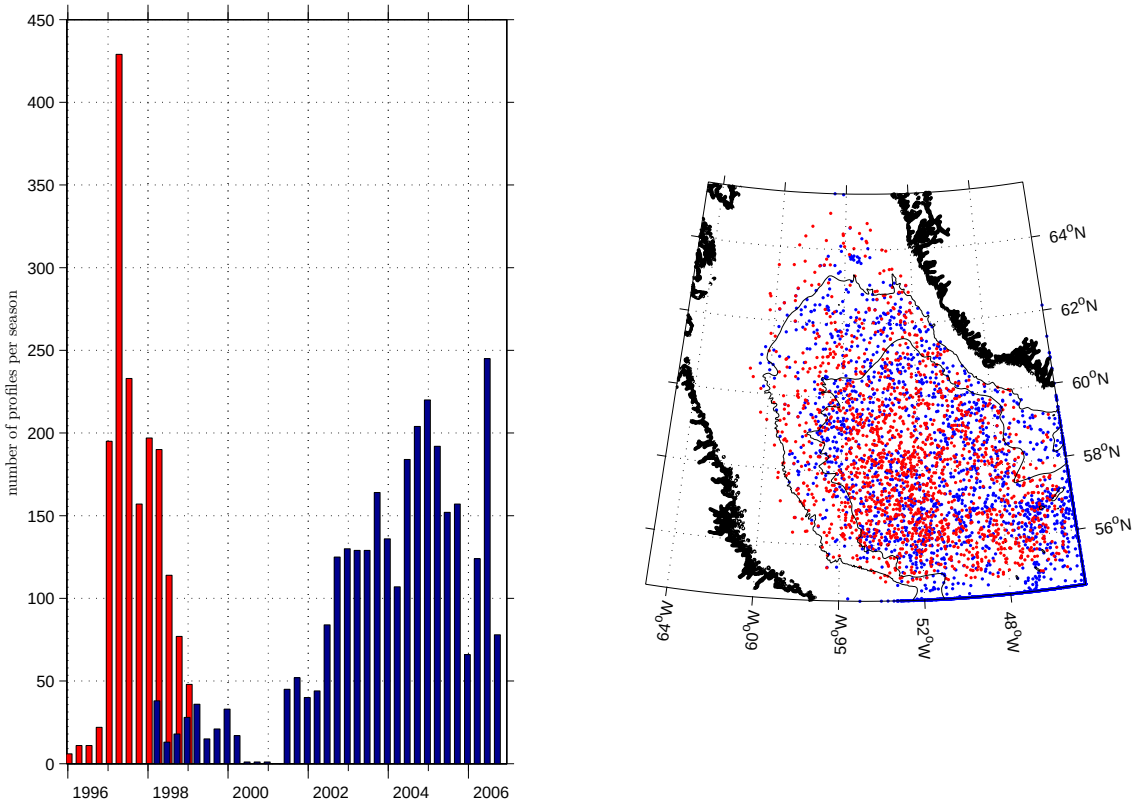

Figure 2.2: Left panel shows the number of profiles in 3 month bins since 1996. The right panel are the central Labrador Sea positions of float profiles. In both panels red are validated PALACE profiles from The Labrador Deep Convection Experiment, the blue validated float profiles from the ARGO project, see text for details.

float data is used and described in detail for instance by Lavender et al. (2002) and Katsman et al. (2004).

During the Labrador Sea Deep Convection Experiment more then 1600 profiles were collected by PALACE floats in the Labrador Sea. These floats took profiles mostly down to 1300 m and some to 1500 m. A lot of these floats had conductivity sensors mounted on them. Both data sets with and without conductivity sensors were used, though in nearly all applications in this thesis whenever next to temperature either density or salinity was needed only the floats with conductivity data were used. These development wise very early conductivity floats are known for their drift in conductivity measurements. The magnitude of conductivity drift becomes obvious looking at the profiles below 1000 m as shown in the left part of figure 2.3. The standard deviation of salinity data in 1300 m was $0.096 psu$. Far out of bounds compared to previous and following observations in the deep Labrador Sea. Though no post deployment calibration is possible another method of correction has to be found. Due to the overall sparse horizontal resolution and with emphasis on the seasonal cycle that has an amplitude in the order of six times that of the uncorrected data, I decided to use the data nonetheless. Because the shapes of all randomly selected profiles seemed very plausible a constant shift of salinity for each profile was applied. Prior to calibrating

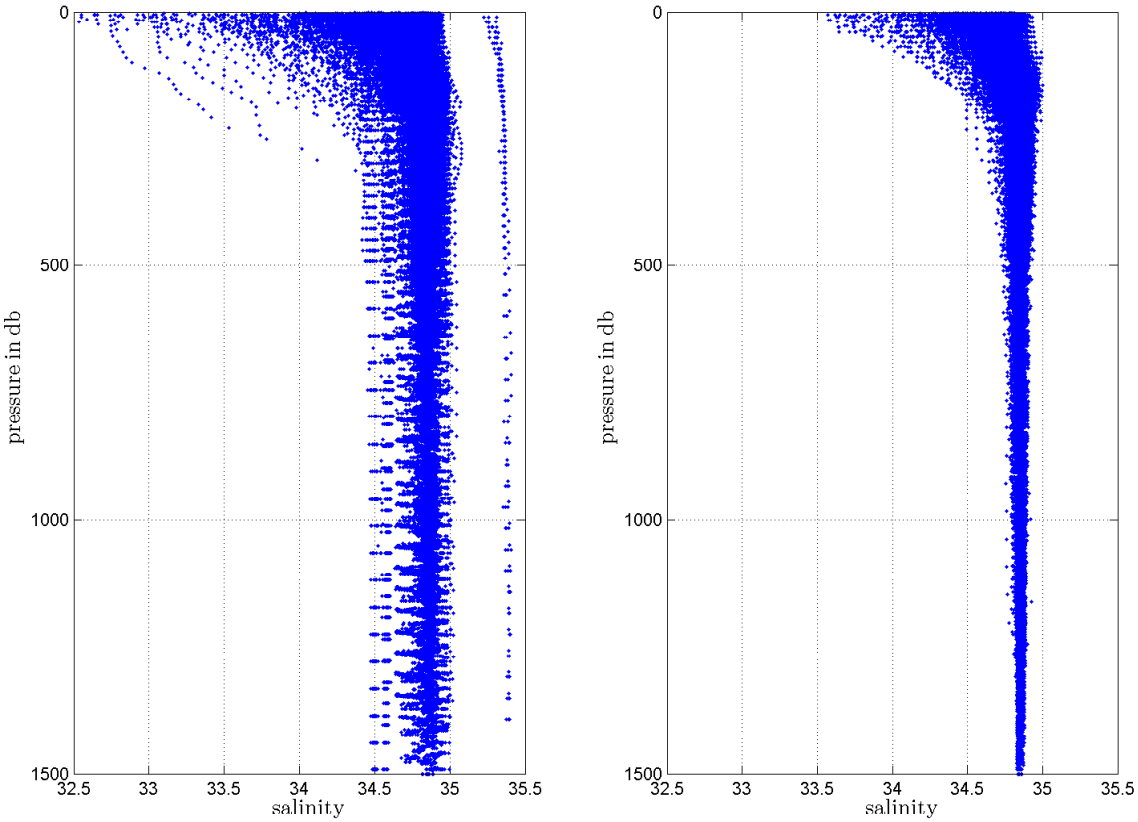

Figure 2.3: P-ALACE float data collected during the Labrador Sea Deep Convection Experiment, before (left part) and after (right part) calibration and validation were applied to data.

salinity all profiles with abnormal temperature behavior were rejected ($-0.8 < \theta < 10.55$ at the surface and θ_{1300db} within $\pm 0.3°C$ of the temperature measured at the mooring Kx1, see section 2.3.4). Further more the shallow profiles that do not extend into depths of low salinity variations (maximum profile depth ≤ 900 m in this case) were rejected, because a determination of the drift was not possible. The signal of main interest at the surface has an order of $0.2psu$ to $0.6psu$, requiring a maximum error of $0.02psu$ in the drift if a signal to noise ratio of 10 is regarded as sufficient.

All profiles extending to depths deeper than 1300 m with a mean 1300 m to 1500 m salinity value larger than $34.87psu$ or smaller than $34.83psu$, were shifted to a $34.84psu$, the observed mean salinity from the mooring for the period of the floats. Profiles exceeding 1100 m but not reaching 1300 m were allowed mean salinity values between $34.89psu$ and $34.82psu$and if necessary shifted to $38.845psu$. For the shallower floats $34.90psu$ and $34.81psu$ were used as boundary and shifted to 34.85. This might allow an error up to $\pm 0.05psu$ for the shallow floats. This error is quite high, but considering that the shallower floats are mainly found close to the boundary current region, where this variability can be well observed, a stricter correction for this depth could produce more errors then removing them. Ignoring the shallow floats on the other hand would result in ignoring some of the already sparse data from the boundary current and shelf brake region. In the end more than 1000 profiles with salinity measurements were regarded as useable. Figure 2.3 shows

on the right hand side the profiles of the shifted data without the rejected profiles.

The second data set was collected and made freely available by the International Argo Project and the national programs that contribute to it. (http://www.argo.ucsd.edu, http://argo.jcommops.org). Argo is a pilot program of the Global Ocean Observing System. The first Argo float profiles from the Labrador Sea are from 1998. Only data that was not flagged as bad was used. Further more profiles had to pass the following criteria. The density profile calculated from raw profile values had to be stable. Salinities measured between 1300 m and 1400 m had to be within the plausible range from 34.80*psu* to 34.90*psu* observed by CTDs. This correction is sufficient, even most recent salinity calibrations of floats calibrate only with a constant offset, because the drift or bias with depth or conductivity is low compared to time (Wong et al., 2003; Oka and Ando, 2004).

2.3.2 surface "underway" data

So called "underway" data increase the sparse data of the low sampled boundary currents significantly, especially in the West Greenland Current. Underway data was, next to research vessels, mainly collected by ships of opportunity, usually supply ships or container freighters, that in most cases were equipped with a conductivity and temperature sensor in the bow of the ship. The data consists nearly solely of temperature and salinity data

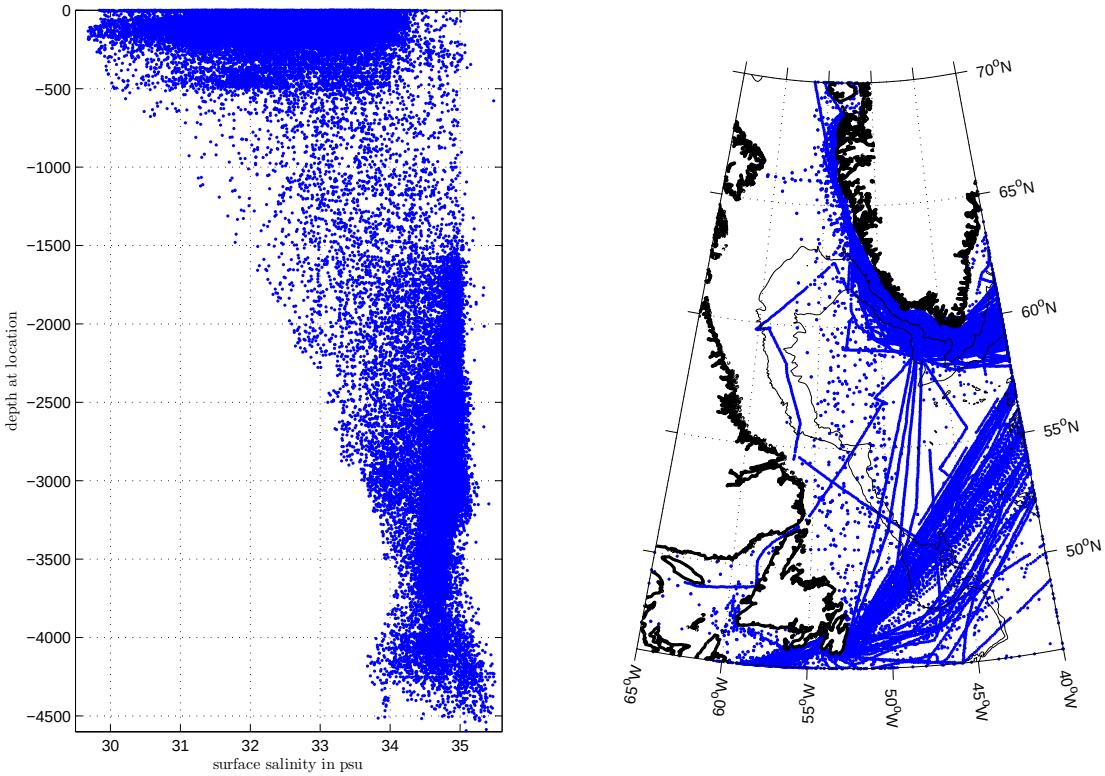

Figure 2.4: Interrelation of surface salinity and depth of the underway data (a). Horizontal distribution of underway data (b). Only data that passed the 99 % criteria is shown.

taken from water in a depth between 2 m and 6 m depending on the type of ship.

The underway data used in this thesis is a freely available data set from ICES[3] at `http://www.ices.dk/ocean/data/underway/underway.htm` . The data set contains data collected since 1891. Data sources for data newer than 1990 in this data set are mainly Alain Dessier (Alain.Dessier@ird.fr), Gilles Reverdin (gilles.reverdin@lodyc.jussieu.fr) and Anthony Walne (ANWA@sahfos.ac.uk).

Newer data is at a very high sample rate. Therefore data taken within 24 hours and closer than 7.5 km to the last data point was combined to one data point. The small radius of 7.5 km was chosen due to the large horizontal variation in the boundary current region.

A validation of the highly variable surface waters is not easy. Data with salinities outside 28.6psu and 35.5psu were ignored. Further more it was decided to apply a 99 % standard deviation filter, meaning only data within 2.6 times the standard deviation was used. Because the deviation of salinity data on the shelf is much larger then in the open ocean (see figure 2.4 (a)), this filter was applied for depth regions in 100 m steps.

Figure 2.4 shows the surface salinities over depth of bathymetry (a) and the horizontal distribution (b). The higher representation on certain ship routes becomes obvious. The fewer data points in water with depths between 500 m and 1500 m has its origin in the lower representation of this depth in the bathymetry, as it represents the typical continental shelf break.

2.3.3 CTD-Measurements

The CTD measurements are mainly taken from two large data sets; the International Council for the Exploration of the Seas (ICES) hydrographic data base and the Department of Fisheries and Oceans Canada (DFO) oceanographic database *climate*. Further more a few CTD profiles used were taken by the Institut für Meeresforschung Kiel[4], during Cruises in the SFB 460.

The ICES data is freely available at `http://www.ices.dk/ocean/`. Else Juul Green from ICES was so kind as to provide me further with ICES data of restricted access. The DFO data is freely available at `http://www.mar.dfo-mpo.gc.ca/science/ocean/database/data_query.html`, this database is described in detail by Gregory (2004). Figure 2.5 shows the number of profiles per year from both data sets. The upper panel shows the data collected in the whole Labrador Sea region including some parts of the Gulf of St. Lawrence, while the lower panel only shows the number of profiles taken in the central Labrador Sea. Red profiles are from the DFO data, blue from ICES data. Figure 2.6 shows the spatial distribution for the different seasons.

To avoid double profiles from both data sets only the DFO profile was taken whenever a double was found. The criteria for being a double profile was: any profile from the opposite data set within a distance of 0.03° latitude and 0.05° longitude - roughly 5 km in the Labrador Sea region - and within 24 hours of the time given. Roughly 2000 double profiles were detected for the central Labrador Sea from 1951 to today. Many profiles from the Gulf of St. Lawrence exist in both databases, but were neither checked nor used here.

[3] International Council for the Exploration of the Seas

[4] now Leibniz Institut für Meereswissenschaften IFM-GEOMAR

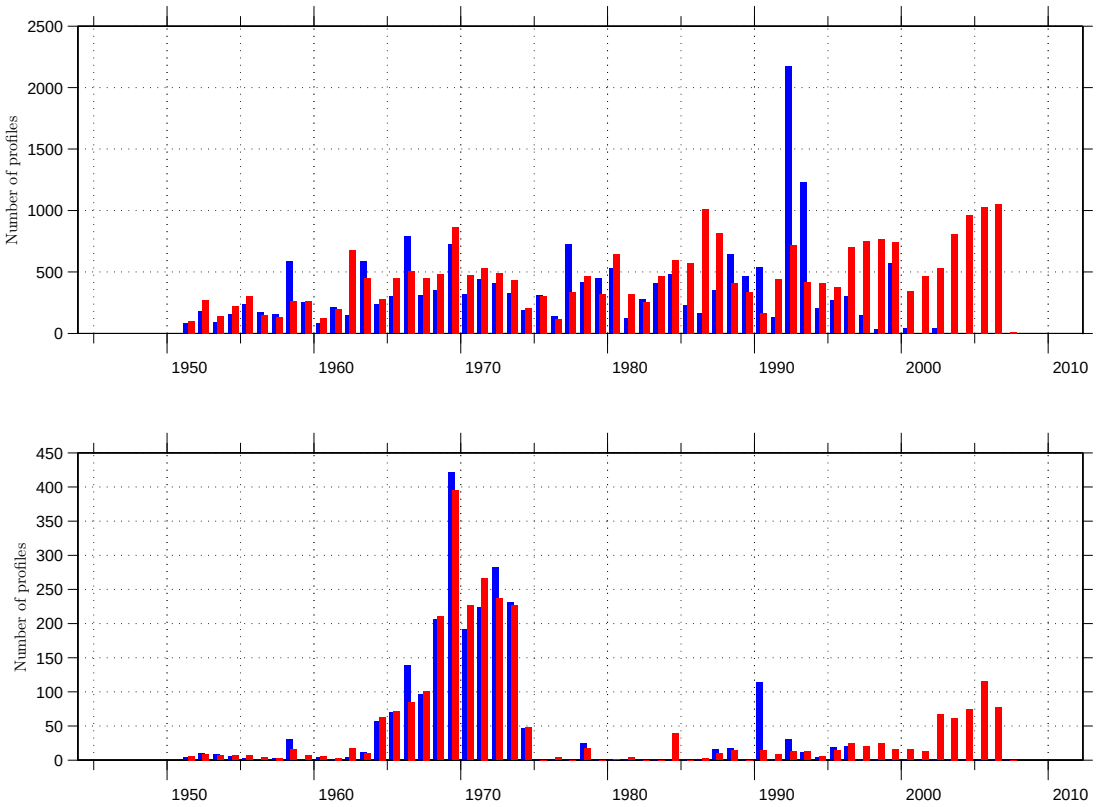

Figure 2.5: The upper panel shows the number of CTD profiles from the ICES (blue) and DFO-Canada (red) data set per year for the whole Labrador Sea region of interest. The lower panel the number of profiles taken in the central Labrador Sea without the boundary currents.

Only profiles taken in a water depth of more then 60 m were used, as a lot of the available profiles in the data set were taken in shallow bays, bights and fjords along the coastline. These mostly do have a connection to the boundary current, though it is not in general obvious how they contribute their waters to the boundary current system, nor if they are the mouth of a river. To reduce this source of bias they were excluded from the calculations.

Data quality was assumed to be good, when no obvious spikes were detected and the profile was stable. Only very few profiles did not match that criteria and were sorted out.

In the lower panel it becomes obvious that very few profiles were taken in the central Labrador Sea from the mid 70's until the 90's. For this reason analysis of the hydrographic conditions of the Labrador Sea during this time is mainly speculation. The implication of this for analyzing the long term variability are addressed in section 5.2.1.

2.3.4 Mooring Data

Mooring data helped to fill the periods when no horizontally spread and vertically high resolution profiles from either CTD or floats were available. Further more the data is the only continuous data that allows the exact timing of events at a fixed position. An exception

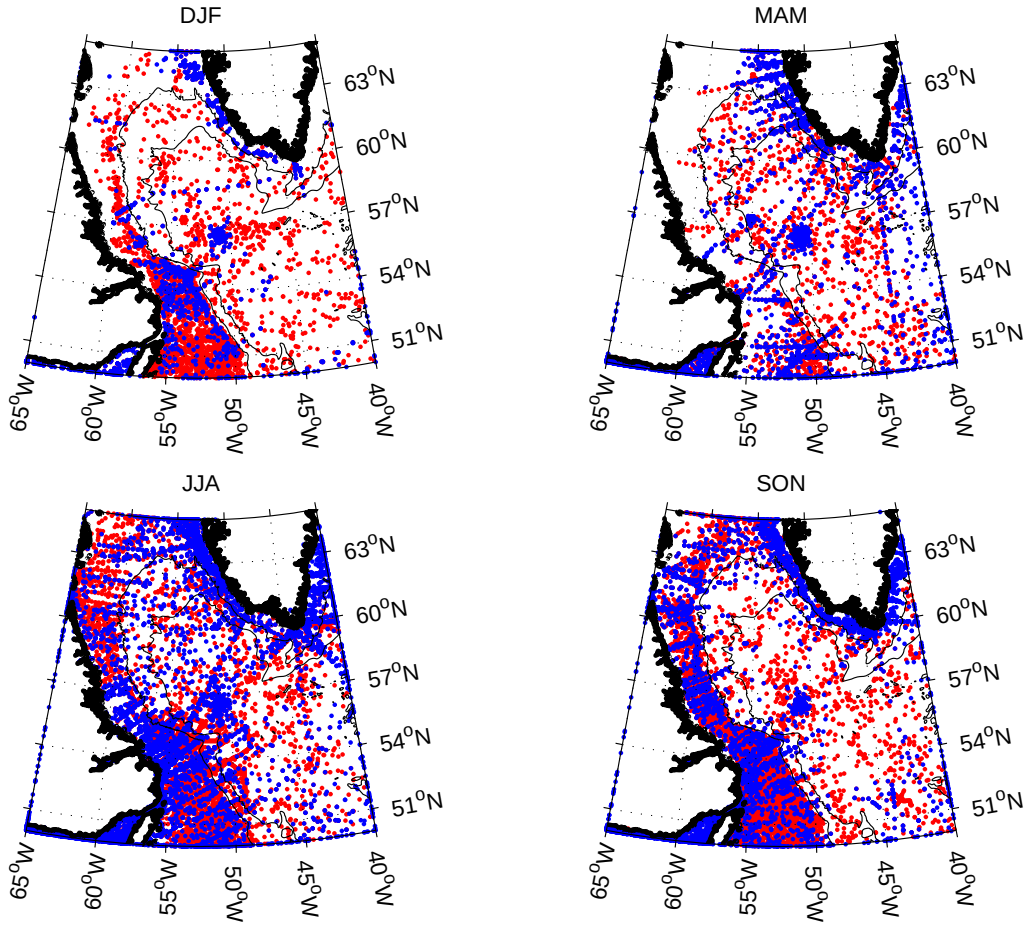

Figure 2.6: Seasonal spatial distribution of CTD profile in the Labrador Sea. ICES (blue) and DFO-Canada (red) data set shown.

is the OWS Bravo, that was moored in the central Labrador Sea for several years until 1974 providing especially in the last 10 years, a nearly continuous vertical high resolution CTD data set from one fixed position as described in section 2.3.3.

Mooring data used in this thesis was collected in the Labrador Sea Deep Convection Experiment and the SFB 460. The mooring from the Labrador Sea Deep Convection Experiment was positioned at the position of the former OWS Bravo. Mooring data from the SFB 460 was collected at several sites. The main source of data is the central Labrador Sea mooring Kx1 some kilometers west of the former OWS Bravo station. K01 was deployed in 1996 and repeatedly in the following years as K11 to K81.

The data used here are only the SeaCat and MicroCat salinity and temperature data calibrated by Tom Avsic and published partly in Avsic et al. (2006).

2.3.5 Processing and mapping of hydrography data

When simple arithmetic averages of data points are constructed, the problem is that profiles with high vertical resolution weighted much more strongly than profiles that are only

available in low vertical resolution, since every measurement from a profile is regarded as one data point.

To overcome this problem, all profiles were linear interpolated on a 10 m vertical grid for the top 140 m, 20 m down to 300 m and 50 m from there on whenever possible. High resolution profiles with steps less than 5 decibar were smoothed with a 15 m running mean filter beforehand. If the upper most value is shallower than 30 m it is assumed that the water column is well mixed down to the first measurement, otherwise no further extrapolation is used.

In a region with distinct boundary currents, like the Labrador Sea region, the current flow is mainly along isobaths. As a result, water properties in general change least along and strongest across isobaths.

This effect is most significant in regions of narrow isobaths like the continental slope. At the shelf break a profile taken in a distance of 40 km along isobaths, is more likely to be representative for the position analyzed, than a profile in a distance of only 10 km but with a difference in water depth of 1000 m. In regions with sparse data the consequence can be that a profile close to the position of interest is not very representative, but another profile further away might be. This is crucial for Labrador Sea boundary current surface data since salinity changes dramatically with water depth as seen for instance in figure 2.4.

To overcome this problem a topography following mapping scheme was used in this

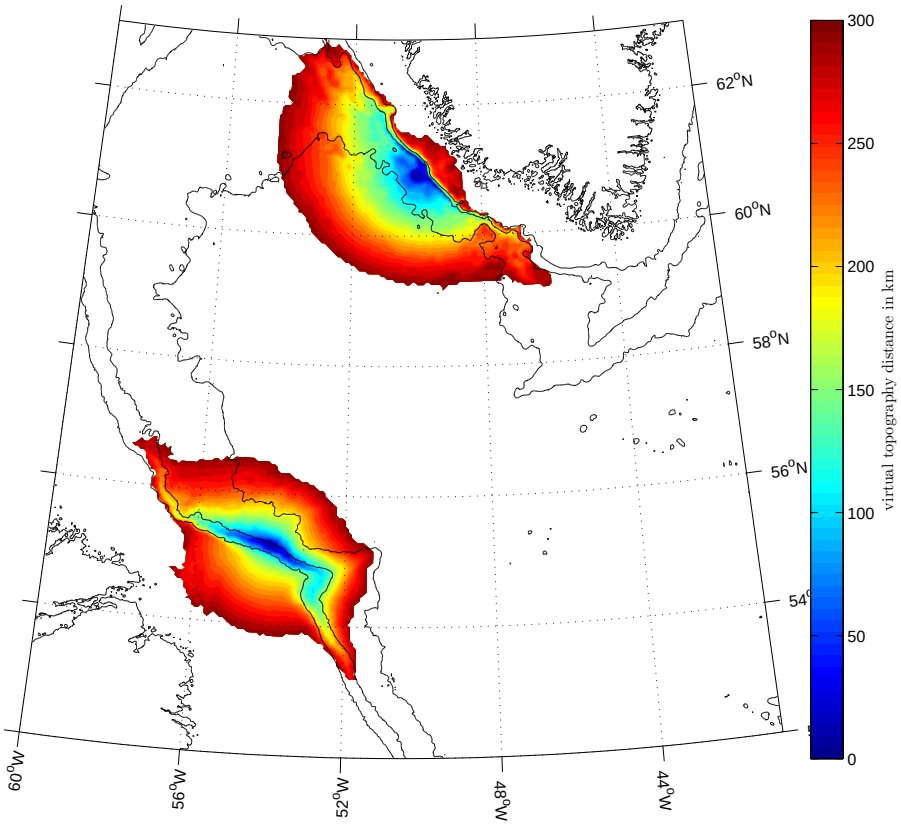

Figure 2.7: Virtual topography distance with a depth to distance ratio of 100 at two example position. The 0 m, 1000 m, 2000 m and 3000 m isobaths are shown as black lines. For explanation see text.

thesis. A height difference of 1 m was regarded as an extra distance of 100 m. Figure 2.7 shows the effect of this virtual topography distance on two exemplar positions. The northern position, $60.9°N 50.1°W$, is based at the bottom of the shelf break in a water depth of 2300 m. The southern one,$55.2°N 54.0°W$, is directly at the shelf brake in a water depth of 1650 m, where the core of the boundary current can be found. The virtual topography distance up to 300 km from the positions are shown for illustration reasons. Data at the bottom of the shelf have a greater virtual topography distance to data on the shelf than to data in the central Labrador Sea, as seen for the northern position. At the southern example you can see that for positions in steep topography, at the shelf break, the virtual distance increases least following the topography. Data from the top shelf as well as from the open ocean have much greater virtual distance. This virtual distance is used for exclusion and weighting of data, when conditions at a certain position are demanded.

For mapping hydrography data no data further away then 133 km of virtual topography distance was used, except if otherwise stated. In addition to the creation of a virtual topography distance a gaussian weighting of the data was used. In this thesis an influence radius, R_{in}, of 50 km and cut off radius, R_cut, of 133 km was used. The distance data, d_i, gets normalized by R_{in} and applied as a Gaussian weighting to the data point x_i. The weight κ_i is then

$$\kappa_i = \frac{e^{-(x_i \frac{d_i}{R_{in}})^2}}{\sqrt{2\pi}}. \tag{2.1}$$

The sum of all weighted x_i is divided by the sum of all weights and the numbers of observations. If n is the number of observations, the best estimate for $< x_i >$, x_{best} is:

$$x_{best} = \frac{1}{n} \cdot \frac{\sum_{i=1}^{n} x_i \, \kappa_i}{\sum_{i=1}^{n} \kappa_i}. \tag{2.2}$$

Data further away than the cutoff radius is discarded beforehand.

2.4 Altimetry data

The altimetry products used in this thesis were produced by Ssalto/Duacs and distributed by Aviso, with support from Cnes. The gridded data for sea surface height anomaly, h, and calculated geostrophic current anomaly, u and v were used. The data available is weekly starting October 1992 and thus covers the complete second well sampled period during the Labrador Sea Deep Convection Experiment and the SFB 460. Naturally no similar data exists during the measurements of the OWS Bravo during the 60's and 70's. The early altimetry data has a lower resolution and larger error then the later one. The lower resolution is interpolated onto the same grid and is thus not obvious in the data, except close to shore. In later years data a few kilometers closer to the shore is available. This matters only for boundary current sections on the shelf.

The eddy kinetic energy (EKE) is calculated for the weekly u and v snapshots.

$$EKE_{xy}(t) = \frac{1}{2}(U_{xy}^2(t) + V_{xy}^2(t)) \tag{2.3}$$

$EKE_{xy}(t)$ is the EKE at position x, y at time t respectively $U_{xy}(t)$ and $V_{xy}(t)$ the geostrophic surface current anomalies.

Chapter 3

Seasonal Salinity Cycle

The variability of salinity and temperature during the course of the year is the dominant signal in the upper Labrador Sea. The meteorological conditions as well as the hydrographic conditions in the boundary currents show a strong seasonal signal. Interactions of these two together with convection strength form the highly variable central upper Labrador Sea water (e.g. Houghton and Visbeck, 2002; Schmidt and Send, 2007). Monthly mean measurements in near surface salinity vary in general from 34.2 psu to 34.8 psu, temperature varies from 2.5° to 6.5° Celsius. During times of pronouncedly different forcing and or advection the seasonal cycle can change dramatically, due to enhanced or stopped convection, mixing, thermal forcing or advection.

Knowing the seasonal cycle of all contributions is important for understanding the resulting variations in a region better, here the convection region in the Labrador Sea. A good estimate of the mean seasonal cycle and removal from sparse data sets also reduces biases in interannual variability calculations. Long-term trends become more obvious and variations with frequencies different to the year can be determined better. Thus a robust climatological seasonal cycle is helpful for determining the variance and presence of other signals that could be masked by the pronounced seasonal cycle.

How to construct a mean least biased seasonal cycle for an area with sparse data? Here, prior to constructing the seasonal cycle, regions with low horizontal variability and sufficient data coverage are chosen. Different approaches for constructing a mean seasonal cycle and their results are explained below and a mean seasonal cycle is then constructed for the different areas. The central Labrador Sea is discussed in detail, the other regions more briefly. A discussion about the results follows.

3.1 Data regions

Which shelf regions and offshelf areas in the Labrador Sea area contain enough data to construct a representative seasonal cycle and which limits of a region should be drawn? To reduce bias due to sampling different water masses within one region, the layout should use regions as homogeneous as possible. This can be achieved by choosing regions as small as possible. Small regions are supported by the fact that larger regions tend to broaden sudden advective signals. Thus the gradient of a signal gets decreased. On the other hand a region should have been sampled as often as possible throughout the year for as many years as possible. For this fact the regions should be made as large as possible, because spatial and temporal sampling is low in most regions of the Labrador

Sea. The third variable that needs to be taken into account is the sampling interval. Since the seasonal cycle needs to be resolved a maximum window width would be 3 months. But as some signals might propagate fast and the different arrival of these signals might reveal information about the state of the Labrador Sea the interval should be considerably smaller. It needs to be balanced with a sufficient number of available sampling years.

For the sampling interval, it was chosen to construct the mean seasonal cycles on a monthly basis. This interval is expected to be large enough to get sufficient data throughout the year and leads to three salinity values per season. But which regions are used?

The layout of the regions has a large impact on the resulting climatological salinity cycles. Thus in the following I discuss the salinity distribution and variation in the course of the year from the raw data. The results are used to decide on regions with similar seasonal cycle within each region.

Figures 3.1 and 3.2 give a first idea of suitable regions. Shown are the Labrador Sea surface to 100 m and 200 m to 300 m mean salinities for intervals of two months. For every grid point on a $\frac{1}{3}^{\circ}$-grid a monthly Gaussian mean of all available profiles within one month since 1990 and a maximum topography distance of 150 km were used (see section 2.3.5). For taking the possible variability within one month into account without applying a two dimensional filter, a difference of 15 days to the middle of the month was treated as a virtual distance of an additional 30 km. There was no differentiation between upstream and downstream or mean current velocities. This constructed monthly salinity map was averaged over 2 months for the shown figures. The salinities for 200 m to 300 m (figure 3.2) are shown as well, because vertical mixing due to winter mixed layer deepening, isopycnal mixing and other processes may evoke an interaction of this layer with the surface layer. Color limits were chosen to resolve changes in the Labrador Sea; salinities below 34.5, thus all boundary currents, are not resolved with this color axis. These maps can further be enhanced through objective weighting of data by using the results of this and the following chapter, but the purpose here is mainly to decide on the regions of interest and give a first overview of the seasonal development of Labrador Sea salinities.

What can be seen from the raw data maps that is useful for deciding on regions? Figure 3.1 illustrates the strong but very different seasonal cycles in the various parts of the Labrador Sea. At first glance salty Irminger Current water enters the Labrador Sea around Cape Farewell along the West Greenland Current and spreads west into the Labrador Sea in the course of a year. Taking also figure 3.2 (different color axis) into account, the seasonal cycle of the Irminger Current seems to be inverted. The reason for this can be revealed in an analysis of the mixed layer depth. During times of strong vertical exchange mainly due to pronounced atmospheric heat flux, the surface waters get saltier and the Irminger Current waters become fresher. If the water masses are completely mixed it results in a salinity minimum in the 200 m - 300 m layer and a maximum in the surface layer as is the case from January to March (upper panels in figure 3.1 and 3.2). Thus the 0-100 m salinity maximum in the major part of the Labrador Sea originates in previous year inflow of salty water and winter mixing with deeper layers. Salty waters enter the Labrador Sea along the West Greenland Current and spread especially into the northern Labrador Sea. The export along the Labrador Current is deeper than the 200 m - 300 m layer but can still be seen in

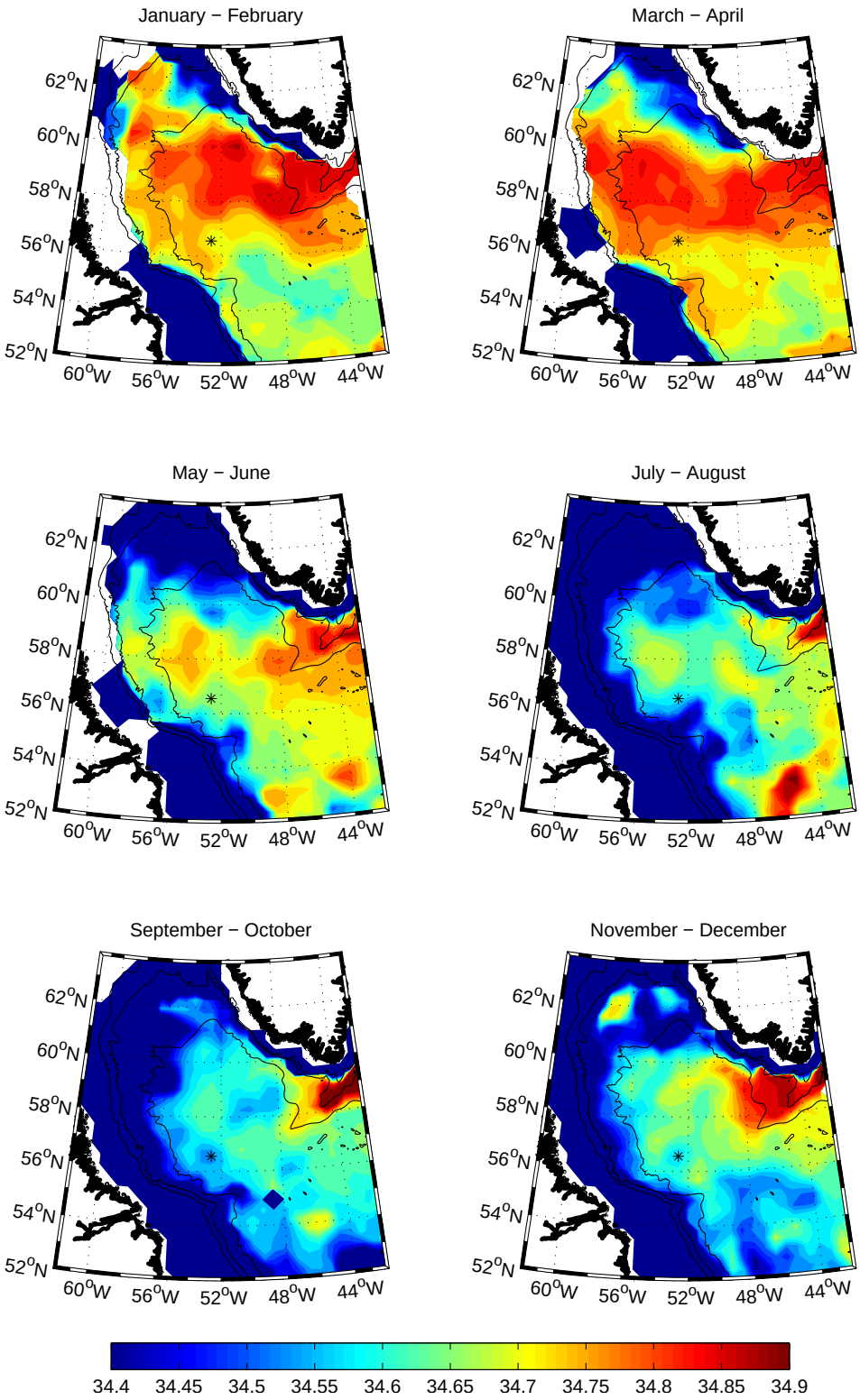

Figure 3.1: Top 100 m mean salinities in the Labrador Sea and its boundary currents. Each panel describes the mean of 2 months. Annual weighting was not performed for creating the 1-monthly maps, thus the bias to higher sampled years is not removed. The star marks the position of the Labrador Sea moorings K01 to K81.

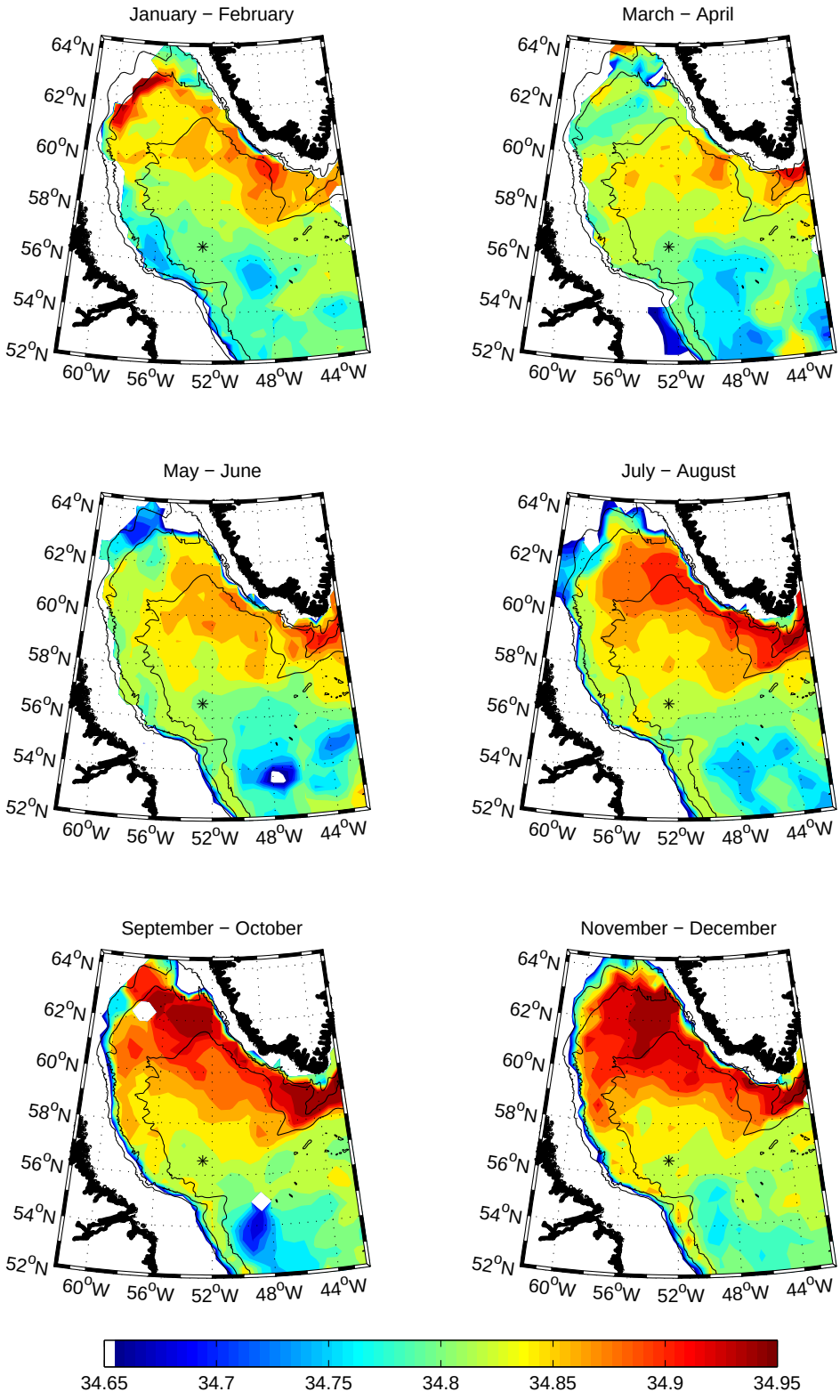

Figure 3.2: Mean 200 m-300 m salinities in the Labrador Sea and its boundary currents. Each panel describes the mean of 2 months. Annual weighting was not performed for creating the 1-monthly maps, thus the bias to higher sampled years is not removed. The star marks the position of the Labrador Sea moorings K01 to K81.

the November-December mean in figure 3.2.

The interesting feature along the West Greenland shelf is the change of surface freshwater distribution past Cape Desolation. The fresh surface boundary current waters cover the underlying salty waters even in winter. There is no visible change at Cape Desolation in the Irminger Current waters in the layer 200 m - 300 m. This eminent freshening of the surface waters past Cape Desolation leads to a sectioning of the West Greenland Current into a northern (downstream) and a southern (upstream) part for following analysis.

For what region to decide in the central Labrador Sea? In the central Labrador Sea data coverage is best around the former OWS Bravo and the Kiel moorings Kx1 (marked as black star in figures 3.1, 3.2 and following ones). This area has smaller changes in the seasonal development than the northeast or northwest Labrador Sea. Furthermore the central Labrador Sea west of the mooring position close to the 3000 m isobath is believed to be repeatedly the region of deepest convection in the Labrador Sea (e.g. Lab-Sea-Group, 1998; Lilly et al., 1999). Pickart et al. (2002) found the deepest mixed layer around $56.7°N$ close to the 3000 m isobath, with rapidly decreasing mixed layer depths towards the shelf. The convection site extended mainly east from this deepest mixed spot towards the mooring site. These reasons make it an ideal region for a central Labrador Sea data area. The central Labrador Sea region analyzed is chosen to represent the salinity cycle from this region of deep convection.

A further area in the deep Labrador Sea chosen for the analysis is the northwestern part. This area has strong Irminger Current water influence and an early freshening as indicated by figure 3.1. The western part of this area has the strongest winter heat loss in the Labrador Sea and mixed layer depths down to 1400 m have been observed there (Kortzinger et al., 2004).

What are the limits for the boundary current regions? Since the color axis of figures 3.1 and 3.2 do not resolve the boundary currents. Figure 3.3 illustrates the maximum horizontal gradient in salinity on the above described $\frac{1}{3}^\circ$-grid for a more revealing view of the changes in the vicinity of the boundary currents. Throughout the year the maximum gradient exists between the 1000 m and 2000 m isobaths. The gradient varies slightly between summer and winter. It is a sharp gradient in winter and extends down to the 3000 m isobath in summer on the Labrador shelf. Because of this gradient the boundary current areas for the West Greenland (north and south) and Labrador Current are split into a shelf and an offshelf area to minimize data from regions with strong gradients. The shelf regions are limited from the shelf up to the 900 m isobath. The offshelf regions are defined from the 2100 m to the 3000 m isobath. In the northwestern Labrador Sea at the location of the two West Greenland Current branches (compare figure 1.2) a broader gradient can be observed, with a minimum between the branches. This is the area of the southern West Greenland Current branch and since several floats from recent years cover this area, it is suitable for an analysis, though only the offshelf region (2100 m to the 3000 m isobath) has enough data here.

Using the above findings it was decided to use nine non-overlapping regions. The regions with all available data positions from 1950 to 2006 are plotted in figure 3.4 in different colors. For referencing these regions in the following it was decided on the following naming. The West Greenland Current areas are named WGC with an appendix addressing the position: **n** (north) for past Cape Desolation and **-ic** for offshelf (covering the Irminger Current waters).

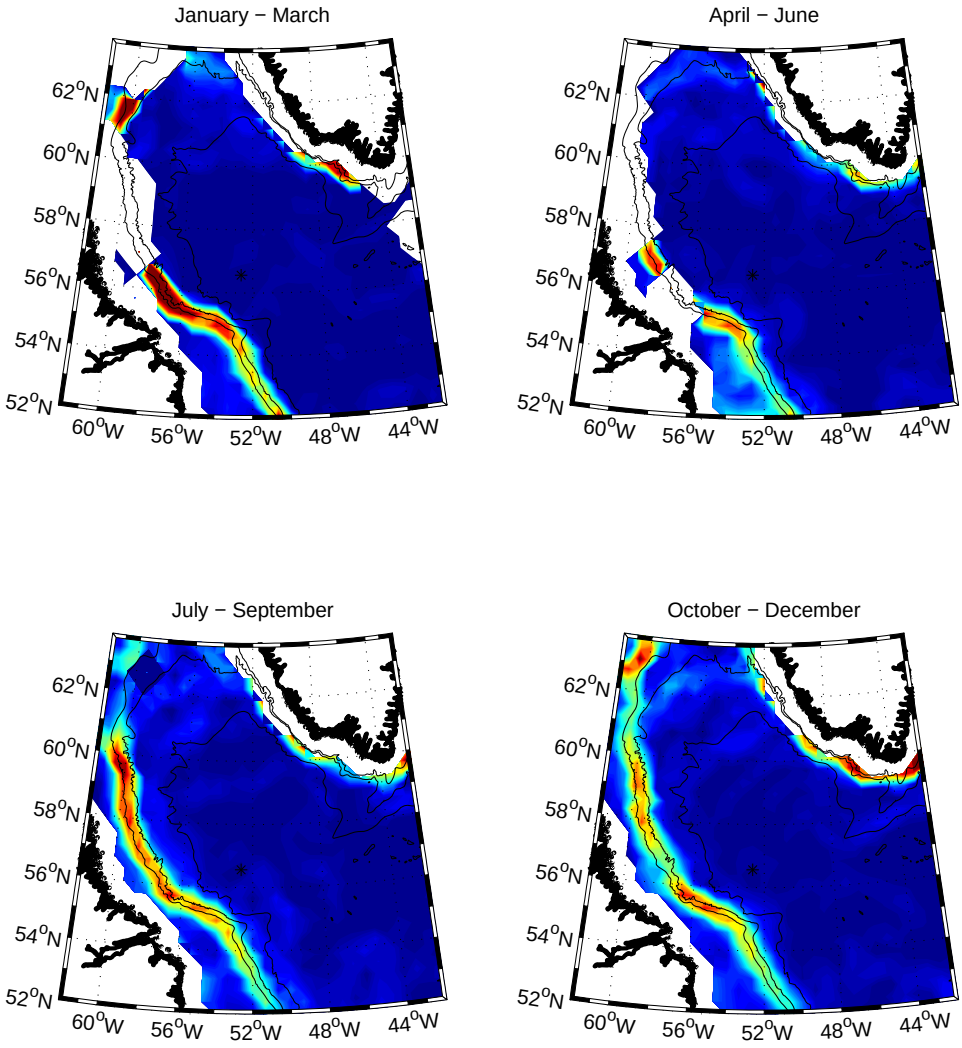

Figure 3.3: Top 100 m salinity gradient on a $\frac{1}{3}^{\circ}$-grid. Each panel describes the mean of 3 months. Annual weighting was not performed for creating the monthly map, thus the bias to higher sampled years is not removed.

The area of the southern West Greenland Current branch is named sWGCb, the northern West Greenland Current branch has not enough data to perform the analysis as stated above. For clarity reasons the Labrador Current (LC) region that is situated offshore was also given the appendix **-ic**. Inside the Labrador Sea the area around the central Labrador Sea mooring is named cLS. LSn is the abbreviation for the northern Labrador Sea region. Each region has a different data quantity and quality coverage as will be explored in the following.

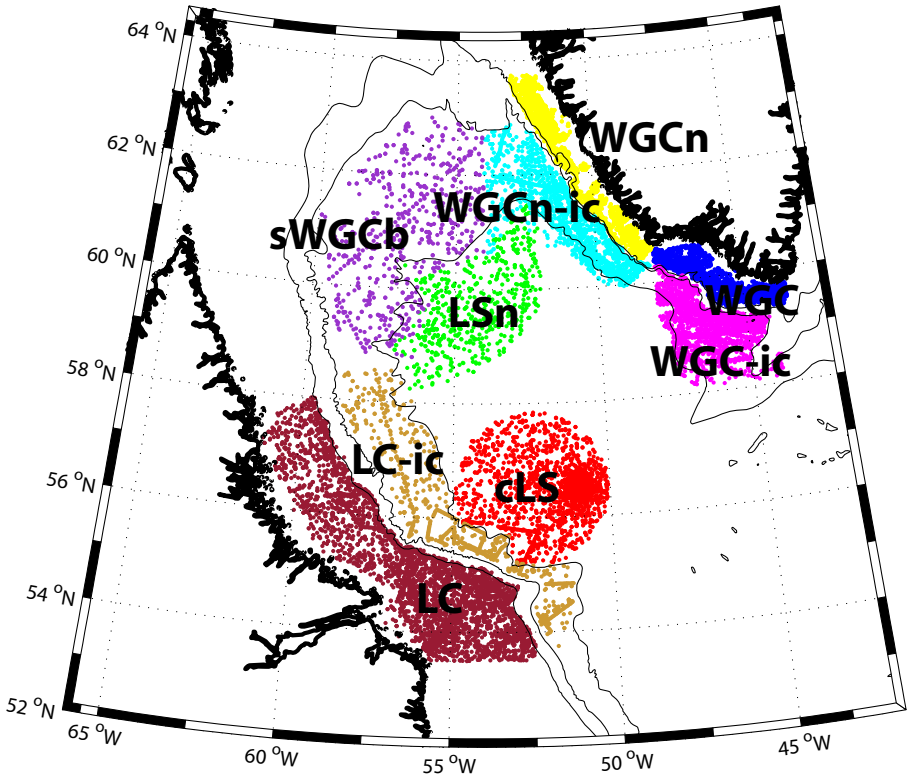

Figure 3.4: Labrador Sea and boundary current areas used for analysis. Every dot indicates an available profile.

3.1.1 Robust Seasonal Cycle

There are many ways to statistically analyze a function similar to the seasonal cycle. But most methods require a close to evenly spread data set in time to produce confident results, thus the methods are required to be robust do data gaps as large as decades. Further more good sampling during some months and no or very few samples in others throughout the data is common for the Labrador Sea and needs to be taken into account. Thus often used methods like empirical orthogonal functions or harmonic analysis are not suitable (TAYLOR AND STEPHENS, 1980; DESSIER AND DONGUY, 1994). Therefore simple straightforward procedures will get used.

Four methods are used for each region and the results will be analyzed. The most trusted cycle is then further used for analyzing the interannual trends. For some regions all methods return a very similar cycle, in other regions every method describes a diverse seasonal cycle. Since no method can be used for all regions due to different data basis a selection of method needs to be made individually. Which are the four methods used?

The first and most straight-forward method is using the mean for every month from the monthly mean data set. The advantage is that the standard deviations for each month can be determined easily and the sum of the residuals is zero. The main disadvantage is the fact that a few extreme low or extreme high measurements during a low sampled period can modulate the seasonal cycle, creating a fictional cycle that is unlikely to occur in reality. For a region with a sufficient number of years of data for each month and a removal of the

long-term trends from the data set (see chapter 5), this method can produce reliable results.

The second method used here is the monthly median. The median is more robust to the influence of occasional extreme events, thus it follows the observed value that is found in the middle if all measurements are lined up. For an even number of measurements the mean of the two middle values is taken. If there exists for instance two states of a seasonal cycle with a 1/3 vs 2/3 distribution, it mainly represents the state of the majority.

A completely different approach is used for the last two methods. The monthly salinity change of consecutive months of data are determined, this result is afterwards shifted to the month best sampled with least variations. The advantage of this approach is the stronger independence to long term trends and variability.

The monthly differences are calculated for the whole data set. These differences are sorted into twelve pairs describing the monthly salinity change. For every month the mean and the median of the monthly salinity change are corrected by subtracting a twelfth of the sum of the mean/median cycle. This correction is necessary to prevent a long trend in the seasonal cycle as will be illustrated exemplary for the first region in section 3.2.1. The cumulative sum of these changes represents the seasonal cycle starting with zero. The resulting seasonal cycle is shifted to the best-sampled month with low standard deviation. This method has some advantages and disadvantages. Long-term trends have hardly an influence or none at all since the monthly change is not effected. The actual shape of the seasonal cycle is preserved and strong variations in the monthly change indicate either a time shift or an amplitude shift in the seasonal cycle. The disadvantage is the necessity of data in at least two successive months for every value, thus an already low sampled data set has even less data describing it. Measurements performed without leading or trailing measurements are not used in this method, therefore critically reducing the data set for some regions. Another systematic bias of this method, not so obvious at first, is that research cruises and floats collecting data in one region in two consecutive months mostly underestimate the monthly change. As both spend in general only a limited amount of time in a region the measurements do not represent the middle of the months. It is more likely that they represent one month and the beginning of the second, or worse the end of the first and the beginning of the second month. The same is the case for any amount of successive sampling months, in most cases the first and last changes are underestimated. To try to reduce this bias data from the beginning and the end of a month were weighted less while constructing the time series as described in section 2.3.5. This underestimate of the seasonal cycle is balanced by stretching the cycle to a degree that it has about the same amplitude as the median or mean. This implements the assumption that pronounced monthly change is more strongly underestimated than small change, as it would be the case for a similar amount of measurements for every monthly change.

The fourth method is another possibility to reduce the underestimate of the cycle. This method is similar to the previous one, but instead taking the bimonthly change. This bimonthly change is regarded as robust change between the first two and last two months of the triplet, thus the cumulative half of every bimonthly change describes the seasonal cycle. As this cycle does not describe the monthly change but the inter monthly change, it is shifted to the mean of the best two adjacent months. This method is very robust and would be the method of choice in a slowly varying region but broadens sudden changes in the seasonal cycle as can be seen for several regions in the following. This broadening makes it unsuitable for many of the regions discussed below, due to rapid changes in salinity.

These four methods are used for every region with a decision on the most reliable one, afterwards. Spectral analysis and other methods did not provide any useful results since the data is very unevenly distributed within the year for all regions. Still there might be other methods providing similar robust seasonal cycles.

For demonstration of the procedure deriving the climatological salinity cycle the central Labrador Sea region is discussed in detail in the following. After a short introduction of the region the procedure is explained. Since the procedure is similar for all other regions only the results and specialties are discussed for them.

3.2 Labrador Sea salinity cycle

A hydrographic overview about the region analyzed is given first in the following before discussing the procedure of constructing the salinity climatology. In both Labrador Sea areas (cLS and LSn) mixed layer depths deeper than 1000 m have been observed. This was observed regularly for the central Labrador Sea area, but also for the LSn area, for instance by a float described by Kortzinger et al. (2004). The convection itself makes it a highly variable region. The different strength of convection in winter give a different starting condition for the seasonal cycle in every year, thus making the development of freshwater input in individual years less comparable.

The different influence of winter-time deep mixing on surface salinities can be seen as exemplary for the cLS area in figure 3.5. Displayed is the frequency of occurrence of maximum winter salinities between February and April. The width of each bin is 0.0333 psu and data for 24 winters are available in the monthly mean data set for the cLS area. The three years with maximum winter salinities below 34.6 belong to the Great Salinity

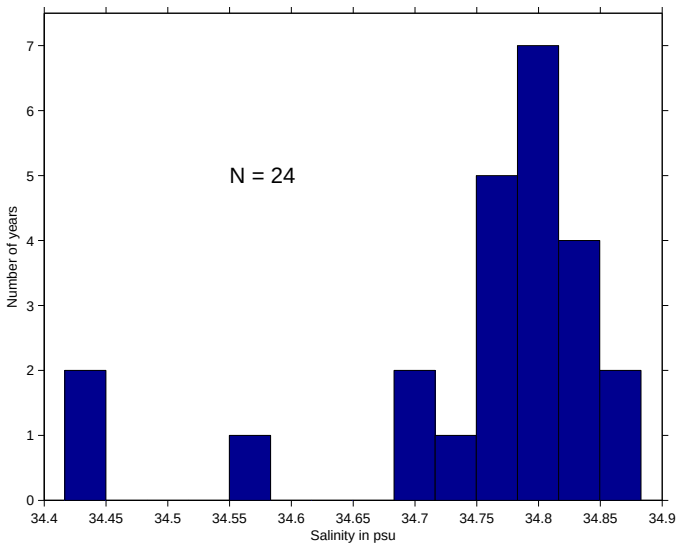

Figure 3.5: Winter maximum salinities from monthly mean data since 1950. The window width is 0.0333 psu. Winter maximum salinities below 34.6 belong to the years of the Great Salinity Anomaly, 1969-1971.

Anomaly from 1969-1971 described by Dickson et al. (1988). Even if excluding the Great Salinity Anomaly of the 1970s, winter maximum salinities still vary by more than 0.15 psu. The reasons can be found in long term variations and different convection strengths, though it is not always possible to differentiate them as will be discussed in section 5.2.1.

Since convection and thus deep ocean ventilation has been the variable of highest interest for a long time and was first observed close to OWS Bravo in the central Labrador Sea, a lot of data exists in area cLS. The more remote region LSn is sampled much less frequently, without recent years of continuous float data an analysis here would hardly be possible.

3.2.1 Central Labrador Sea (area cLS)

This central Labrador Sea area cLS is sampled most frequently of all the offshelf regions. Because of several years of mooring data, weather ship data and WOCE hydrographic section data, the sampling is good for some periods but has gaps of several years to decades. Due to the position of the OWS Bravo the data set during the 1960s and 1970s is biased towards the east of this region as can be seen in figure 3.4. This is especially the case in winter months, since they are sampled very infrequently afterwards.

The upper panel figure 3.6 shows the two methods using monthly change, ΔS and the lower panel shows the methods via salinity itself. The blue dots in the upper panel of figure 3.6 demonstrate the availability of data for the monthly change method. The salinity change between January and February is shown between month 1 and 2 on the x-axis, the other changes are displayed respectively. Since the data basis is good throughout the year all values more than two times the standard deviation of the mean are discarded for each month to reduce the impact of extraordinary events. The red dashed line shows two times the standard deviation of the remaining monthly change data. The black line is the median and the red the mean of each change. The green line is the corrected monthly change to exclude a trend from bias in mean monthly change. The numbers inside the plot indicate the available number of individual changes for each mean change.

The monthly salinities observed are displayed in the lower panel, the colors are assigned similarly to the upper panel. The numbers inside the plot indicate the available number of years with measurements during that month.

The mean monthly change cycle (upper panel 3.6) shows surface salinification from November to March with a maximum between December and February due to vertical mixing. March to May illustrates a short strong freshening with very low freshening in the following month. The low freshening in June is accompanied by low variation. The freshening continues in June with decreasing intensity until November. The partitioning of Labrador Sea freshening into a short and a long period has been discovered and described before by Schmidt (2003) and Schmidt and Send (2007). The short freshening period from April to May will be called the first freshening and the long period from June to November the second or main freshening hereinafter. The much less pronounced or absence of the separation in two freshenings in the lower panel is addressed further below.

The monthly change data is spread evenly with 15 to 26 years of observations, but the variability of the monthly change differs significantly. Local variability minimums can be found from May to June and October to November, local variability maximums in summer and between December and January. The local variability maximum in December to January is likely due to the maximum high variable salinification of surface waters by

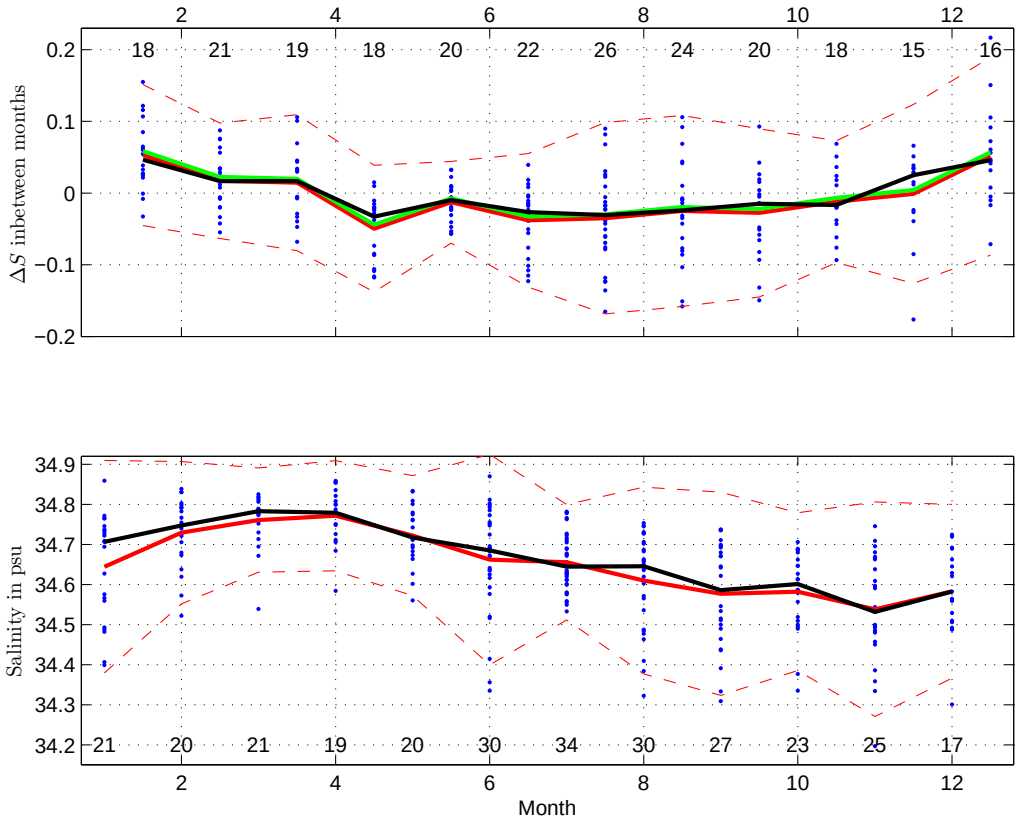

Figure 3.6: Central Labrador Sea salinity change between monthly data (upper panel). Further shown are the median (black curve) and the mean (red curve) and the corrected mean (green curve). The red dashed line indicates two times the standard deviation of the data. The numbers in the axes the amount of years of available data. The lower panel shows all individual months with data, median (black), mean (red) and standard deviation (dashed red) are shown.

mixing with deeper layers. This continues in the following observations from January to February but especially changes in the onset will have a major effect on the gradient in December to January. The maximum variability in summer with higher individual salinifications than in autumn might be connected to salty boundary current eddies in area cLS as observed and described by Lilly and Rhines (2002). Summertime data that might be sampled inside such an eddy for one month will show strong salinification at first and strong freshening afterwards when no eddy water masses are sampled again. But how can the minima be explained? The minimum between October and November can just be the result of the two explained maxima. Timewise the likelihood of eddies is reduced again (see also section 4.1) and the emphasized deepening of the thermocline has not set in yet. The first minimum in variability from May to June is less clear. The monthly change has strong freshening before and after. Having a close look at the previous change, the first freshening reveals an arrangement into two groups. The first group of four visible data points around -0.1 psu consists of seven years (each of the lower 3 years consists of two years), the other group spreads around -0.02 psu with two outsiders showing low salinification. Assuming two states of the Labrador Sea, with and without the first freshening, only the larger

group would represent the one state. April to May would have a freshening as low as May to June, thus the main freshening would set in in March and strengthen until June. This view is supported by STRANEO (2006) who finds only one freshening. Thus without the first freshening the variability of April to May would be very low, as vertical mixing stopped and significant freshening has not set in yet. In May the optional first freshening has already occurred. This could explain the low variability of May to June salinity changes.

The construction of the bimonthly change is not plotted, but the results resemble the variability and shape of the monthly change data to a large degree. Due to the 2 month window sudden changes like the first freshening are broadened and can no longer be distinguished clearly. The whole cycle is damped as will be shown in the comparison of the possible climatological cycles below.

The monthly mean (red curve) and median (black curve) salinity are illustrated in the lower panel of figure 3.6. The red dashed lines mark the area of twice the standard deviation around the mean and the numbers inside the plot represent the available years of data for each month. The mean and the median are very similar since the data basis is good throughout the year. January to March mean salinities are lower than the median because of the Great Salinity Anomaly. The generally large variations in each month originate in interannual variability as opposed to temporal and spatial variability within a month and an area in a given year and is discussed below. Variations in the raw data including long term trends are lower in winter and higher in summer, indicating that the maximum freshening is more variable than the winter maximum salinity.

The local maximum in high standard deviation in June is surprising. The high variabilities in January and September to November have more obvious possible reasons all related to vertical mixing and mixed layer depth reaching the sampling depth of 100 m. The reasons for this variability maximum in June may be the arrival of eddies or waters from dissipating eddies north of area cLS or the first freshening that has occurred in several years and thus spreading the possible June values. Eddies in the Labrador Sea are discussed in detail in section 4.1. The first freshening pulse cannot be seen in the mean and median salinity cycle in the bottom panel, but looking at the individual observations in June and July a first freshening between May and June even with erosion afterwards from June to July is likely. These two mechanisms have opposite effects on the central Labrador salinity and can therefore explain the large variance in observed June salinities.

Comparison of the seasonal cycles

In the following it is decided on a seasonal cycle for detrending the data set and afterwards recalculating the seasonal cycle. Due to sparse measurements in several years a most accurate mean seasonal cycle is needed for detrending the data.

How do these seasonal cycles compare? The climatological cycle of the mean, as seen in the lower panel of figure 3.6, is also plotted in figure 3.7. In both figures it is represented by the red curve. The same applies to the black curve for the median. The cycles derived from monthly change are marked with triangles. For the climatological cycle the monthly change cycles shifted to the April mean salinity and the bi-monthly change cycle to the March-April

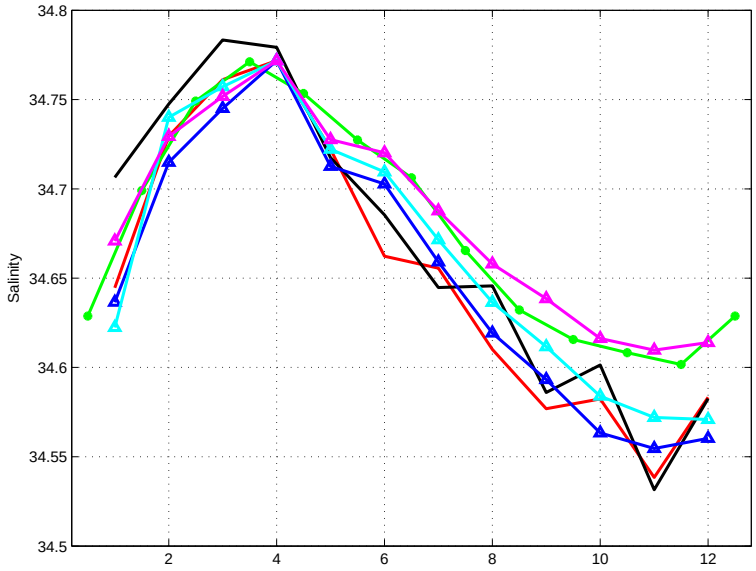

Figure 3.7: Central Labrador Sea climatological salinity cycles. The mean is shown in red, the median in black, green with circles is the climatology derived from bimonthly change. The cycles derived from monthly change are marked with triangles, uncorrected in cyan, corrected for seasonal trend in magenta and in final form in dark blue. See text for details.

mean salinity respectively, since they only include the variation and no absolute salinity. The uncorrected cycle is plotted in cyan and has similar amplitudes as the mean. For the reasons described in section 3.1.1 this cycle is subtracted by a twelfth of the sum of the individual elements so the sum and cumulative sum does not show a trend. This corrected cycle is represented by the magenta curve. For a better representation of the climatological cycle the corrected cycle is stretched to a degree that the standard deviation and the sum of the difference between the stretched cycle and the mean curve are at a minimum. The bimonthly change climatological cycle is corrected but not stretched.

All four methods provide a similar salinity climatology for the central Labrador Sea region cLS. The difference can mainly be seen in the fluctuation and the first freshening (slope from May to June). The median has the highest fluctuations in late summer salinities and does not show the first freshening. A reason for this is the fact that in just more than half of the years sampled the first freshening is low or non-existent (compare individual observations upper panel figure 3.6). The fluctuations in late summer for the median result from long term trends as will be seen below. The bimonthly change climatology does broaden out events that last only one month thus the first freshening cannot be seen by matter of computation. This leaves the monthly change and the mean climatological cycle if the first freshening should be represented.

The mean cycle does have a first freshening over two months and a low salinification from September to October. This low salinification can be seen in the median and mean. Since it neither shows up in the monthly change nor in higher variability from the monthly change as seen in the upper panel of figure 3.6, it is not expected to be significant. This view is supported with the detrended data set as described below. Thus for a smoother climatological cycle the monthly change climatological salinity cycle is chosen to represent the salinity in area cLS. It should be kept in mind that the first freshening from April to

May is the low estimate of the majority of the observed first freshenings. The upper panel of figure 3.6 indicates that this freshening could be much higher. As this monthly change data set is not biased by long-term trends, long-term variations are not the reason for the variability spreading of data in the change between April and May.

The monthly change climatological salinity cycle is used in the following to detrend the data. The same procedure as described of finding the climatological salinity cycle is repeated afterwards with the detrended data set.

Detrended data set

Can the seasonal mean and median cycle be improved if the data set was not be biased by long term variations? The seasonal cycle is removed from the monthly data set and the residuals are smoothed by a two year running mean filter. A detailed discussion about the interannual variations can be found in chapter 5 and in particular for the central Labrador Sea in section 5.2.1 and will not be discussed here. The smoothed residuals are then subtracted from the original monthly data set. Thus the data does not have any long-term variations extending two years. Short-term fluctuations are only changed a little. Since the main interest here is on the seasonal development and its representation a short 2 year filter was favored over a longer filter removing only very long term trends. There are better methods of preserving short-term fluctuations and removing long-term trends than a running mean filter, but for the purpose here this method is sufficient.

The climatological mean cycle from this new detrended data set, including the standard deviation and all data points, is compared with the data from the original data set in figure 3.8. The detrended mean cycle and data are plotted in red, the original data in gray. For a better visualization of the change the old data points were shifted by 0.2 months. For

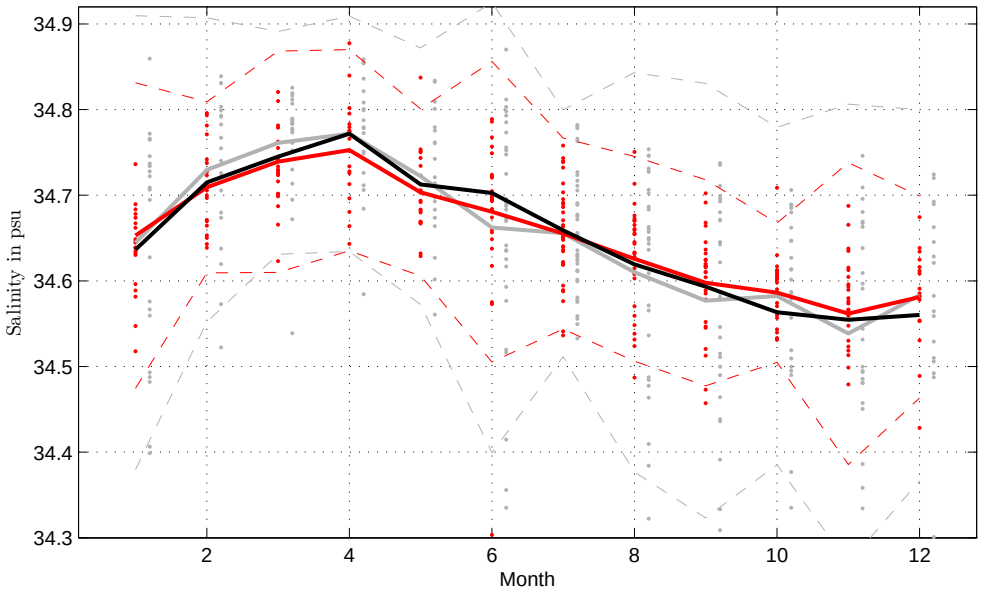

Figure 3.8: cLS mean climatological salinity cycles with data points and twice the standard deviation. Red is indicating the detrended data set while gray is the original data as already shown lower panel figure 3.6. The black curve is the cycle derived from monthly change. The black curve is the median from the detrended data set.

reference purposes the black line indicates the climatological salinity from monthly change.

There are a couple of remarkable differences and similarities between the two data sets. The mean cycle does not change significantly by detrending the data set. The main difference is the reduced variability for some months. The summer standard deviation is cut in half but the winter standard deviation only shows a slight reduction. The whole cycle is smoothed significantly indicating the removal of bias induced in the mean by irregularly sampled data from different periods. The first freshening is still purely represented in the detrended mean cycle (red curve), but the previously unexpected strong variability in June addressed to this first freshening is still present. The nearly unchanged remaining high variability in June and November indicate that those events (first freshening and onset of destabilizing the upper water layer) are mainly interannual while the other variability is either short term variability or long term trends and sampling errors.

What are the conclusions that can be drawn from this? Long-term and short-term variations both make up about half of the variance found in the cLS area in summer for the periods covered by the data. Salinities during the convection season have very little long-term influence. Nearly the whole variance belongs to short-term fluctuations thus mainly the mixed layer depth, since mixed layer depth can be seen as a function of previous late summer stratification, atmospheric forcing and possibly advection. The strong variance maximum in June indicates the high variability of the beginning of the freshening. This again is an indicator for a strong altering first freshening. The monthly change derived climatological salinity cycle represents the area well, as expected and explained above it does not change significantly recalculating it from the detrended data set. Thus the monthly change salinity cycle is used as the climatological salinity cycle for the central Labrador Sea area cLS.

The similar procedure is used for the following eight regions. Only major differences and specialties of the regions will be addressed and only the final cycles compared the the raw data are shown. A discussion of each region is necessary to understand the uncertainties of the presented climatological cycles below in the discussion (section 3.4)

3.2.2 Northern Labrador Sea (LSn)

The data basis in area LSn is much lower than for the central Labrador Sea. Only very sparse summer and hardly any winter data exist prior to 1995. More data is available since 1996, because since then this area is sampled reasonable well by floats. The seasonal and interannual variability of this region has not been described in detail so far. Deep mixed layers have been observed in the western part of this region by Kortzinger et al. (2004). Figure 3.1 and 3.2 show that eroding of the surface layer takes place earlier than in the central Labrador Sea, but also does the surface freshwater layer build up very rapidly early in the freshening season. How are these observations reflected in a climatological salinity cycle?

The bimonthly-derived climatological salinity cycle is used to remove the seasonal variations from the data set, since it seemed to be most robust. The derived climatological cycle from the detrended data is shown in figure 3.9 a. The red curve represents the monthly mean from the detrended data, black the median. In gray the original data is given. Looking at

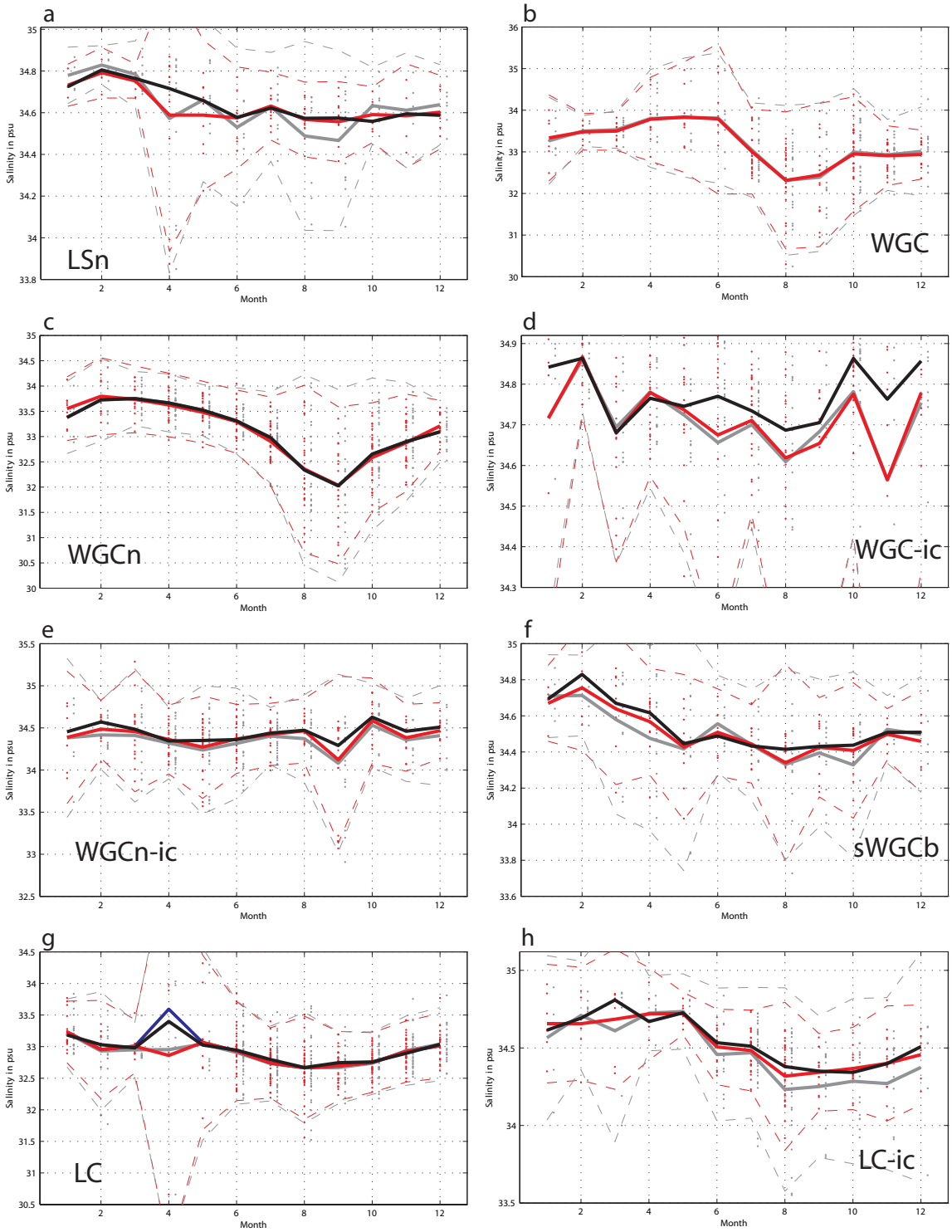

Figure 3.9: Mean climatological salinity cycles for eight regions with data points and twice the standard deviation. Red is indicating the detrended data set while gray is the original data, thus the gray line the best guess before detrending the data.

the monthly mean (red curve figure 3.9 a) there is a strong freshening from April to May and a similar strong salinification from December to February. During the rest of the year no significant variation can be found with low alternating salinification and freshening. The median (black curve figure 3.9 a) shows a slower freshening in the beginning of the year, but is similar to the monthly mean cycle for the rest of the year.

The reason for this can be seen by looking at the standard deviation, it can be seen that the variability is low throughout the year except from March to June. Resulting in the different cycles from mean and median. This variance was not reduced by detrending the data, thus it originates in year to year variability and short term fluxes. This signal looks very similar to the pronounced variance originating from the first freshening in the central Labrador Sea. Thus the first freshening also effects the northern Labrador Sea.

To represent the early freshening the monthly mean cycle (red curve in figure 3.9 a) is used as the best guess for area LSn and used in the following, since the median does not show this freshening.

3.3 Boundary Currents

One aspect of trying to construct climatological salinity cycles for boundary currents is sea ice and its variability. The northern Labrador Current is covered by land-fast first year sea ice for some time of the year (Mysak et al., 1990; Deser et al., 2002). The West Greenland Current sea ice is accompanied by many small icebergs (e.g. Buch, 2000). The interannual variability of sea ice and icebergs is high, but since the sea ice and icebergs stay in general on the shelf (e.g. Mysak et al., 1990, 1996; Peterson et al., 2000), freshwater is not exported as ice in offshelf regions. Thus it was chosen to not explicitly calculate the freshwater transported in the sea ice and icebergs, since it would effect the boundary current salinities before available for fluxes into the central Labrador Sea. Though it has to be remembered that forming and melting of sea ice can modulate the salinity signal along the flow of the boundary currents and thus influence interannual variability significantly for all boundary currents on the shelf in the Labrador Sea.

The boundary currents will be discussed along the boundary flow counterclockwise around the Labrador Sea.

3.3.1 West Greenland Current shelf areas (WGC and WGCn)

The West Greenland Current is the extension of the East Greenland Current. The freshwater sources of them are multiple, including Fram Strait freshwater export (Aagaard and Carmack, 1989), Greenland Sea Ice melt (Martin and Wadhams, 1999), Greenland ice shield meltwater (Bacon et al., 2002) as well as arctic multi-year ice and icebergs (Wadhams, 2000). Since all of these sources have a significant interannual and decadal variability this is also expected for the part of the West Greenland Current flowing on the shelf, representing these origins.

The data basis is much better in this northern part since profitable fishing grounds are found at Fyllas Bank. Thus the northern area WGCn has been sampled regularly by the Northwest Atlantic Fisheries Organization (NAFO).

Figure 3.9 b+c show the salinity cycles of the two shelf regions of the West Greenland Current before and after Cape Desolation. The monthly mean cycle was used to detrend the data for area WGC and similar for area WGCn.

Area WGC shows a strong freshening from June to August and a continuous slow increase of salinities from August to June thus reminding of a sawtooth signal (figure 3.9 b). The very salty individual observations in April and May might originate spatial sampling bias, since in April and May more data is sampled close to the adjacent Irminger Current Waters on the shelfbreak (compare figure 3.1), since the shelf area contains many small icebergs and loose sea ice during these months.

Though area WGC feeds area WGCn the strong freshening from June to August is broadened in area WGCn (figure 3.9 c). The minimum salinity is shifted by one month to September, representing well the mean flow observed by Cuny et al. (2002). Still the freshening sets in earlier in area WGCn than it does further south. Though the monthly freshening is low between March and July it sums up to about 0.5 psu, nearly a third of the seasonal amplitude. What are the reasons of this earlier onset of freshening?

There are three plausible reasons for this low but constant early freshening. Most likely responsible are sea ice and iceberg that melt along the current and West Greenland runoff, but also bias of data cannot be ruled out. All tries to specify one of these origins failed, since no reliable seasonal runoff data exist and the data variability in the more southern WGC area is too high to find this possible small early freshening. The reason for bias in sampling might be the positioning of data samples on the shelf. The majority positions of data samples spreads differently within the areas in ice-free and ice months. As sea ice conditions are more severe in area WGC this early freshening might have easily been missed. Further north with decreasing ice probability the positions of sampling data in area WGCn move closer to the shore. Thus an influence of data bias is likely but it cannot be ruled out that this freshening is a signal in area WGCn that does not exist in area WGC. The data basis for the mean climatological cycle is good for the northern area WGCn and all constructions of the salinity cycle show the same result.

The variability is similar in both regions and as large as expected from the numbers and type of sources mentioned above. The double standard deviation exceeds 2 psu in the summer months. Despite the high variability detrending the data set did not have any visible influence on the variability nor on the mean cycle. Nearly the complete variability must originate in short-term fluxes and year to year variability. The origins of these fluxes are either imported East Greenland Current fluxes combined with possible highly variable mixing around Cape Farewell with saltier Irminger Current Waters or the data bias of using data from the whole shelf and not like Lazier (1982) and Houghton and Visbeck (2002) in bands of distance to shore. The last point might induce some of the variance but since the four constructed salinity cycles are very pronounced and very similar this influence seems to be limited.

Due to better data coverage the monthly mean climatological salinity cycles compared to monthly change data and otherwise similar cycles, the monthly mean is used for both areas in the following.

3.3.2 West Greenland Current offshelf areas (WGC-ic and WGCn-ic)

After discussing the shelf parts of the West Greenland Current, the offshelf parts of the same currents are analyzed in the following (figure 3.9 d+e). Concluding from figure 3.1 the offshelf waters from the West Greenland Current are dominated by Irminger Current Waters, gradually freshening along the current. In some studies the offshelf West Greenland Current is called Irminger Current (Cuny et al., 2002). Since this inflow of Irminger Sea Water is the main freshwater sink or salt supply for the upper Labrador Sea it has a key role for the upper Labrador Sea salinity and Labrador Sea stratification.

Figure 3.9 d+e show the data from the offshelf areas along the West Greenland Current. For detrending the data set from area WGCn-ic the median salinity cycle was used, since its variation is small and has a good data basis. The mean cycle was used for area WGC-ic. The same as for the on shelf West Greenland Current applies for the offshelf part, the northern area WGCn-ic past Cape Desolation is much better sampled than the southern area WGC-ic. In both areas no pronounced seasonal cycle can be found, thus supporting direct the assumption of Schmidt and Send (2007) who calculated a freshwater budget with an assumed constant climatological Irminger Sea Water inflow. But especially the northern area WGCn-ic shows a freshening in September followed by the saltiest values one month later.

What are the reasons for this strong variation from fresh to salty in an otherwise low varying seasonal cycle? The fresh peak in September coincides with minimum salinities on the shelf and figure 3.1 suggests that the fresh part of the boundary current is extending in late summer covering the offshelf part. Furthermore since these very low salinity observations show up irregularly and mainly during the period of minimum salinities in the shelf current (compare figure 3.9 b+c), it is assumed that they are due to bias in the data. Since the median is hardly influenced by them, the median-derived cycle is used for this region in the following.

No matter which cycle represents this area best, it can be stated that the variations are small with an amplitude depending on the method of 0.15 psu to 0.25 psu. This surprises when comparing this range to the shelf part of the West Greenland Current with an amplitude of 1.2 psu in the climatological salinity cycle. Still a constant along-stream mixing with shelf waters must take place since the area WGCn-ic is about 0.35 psu fresher in the mean than area WGC-ic. Mixing with central Labrador Sea water can not explain this freshening since it has higher salinities than this region for every month.

The detrended mean and median cycles (red and black curves) only show a small difference to the original data. The monthly variance does not change significantly by detrending the data, but month to month variations of the median reduced significantly for area WGC-ic. Knowing about the decadal variations of this region as discussed later in chapter 5 this is surprising. The reason is very likely the monthly fluctuations, that seem to dominate the seasonal climatological cycle or an insufficient data base. The interannual variability is discussed in detail in section 5.3.2.

The climatological salinity cycles for the offshelf areas WGC-ic and WGCn-ic are varying hardly in the course of the year, no strong seasonal signal if any seems to be present in the water originating from the Irminger Sea. This does not surprise seeing these areas

as extension of the Irminger Current that inherits its properties from the North Atlantic Current, but it does surprise seeing the very strong seasonal cycle a few kilometers further on the shelf. Monthly variations dominate these regions of Irminger Current Water inflow into the Labrador Sea.

3.3.3 Southern West Greenland Current branch (sWGCb)

The southern West Greenland Current branch bifurcates off the West Greenland Current halfway between Cape Desolation and Nuuk (figure 1.2). It is expected that the water properties are mainly inherited from the origin.

The data basis does not contain many sampling years. Since the number monthly change data points is significantly lower than the monthly data for this region, the monthly median is used for detrending the data from this region. The original and detrended cycles are shown in figure 3.9 f. Since also in the detrended data set some far outlying data points influence the mean as can be seen especially for August in figure 3.9 f only the median is used. The seasonal cycle shows a strong freshening in the beginning of the year and again in beginning of summer with lower variations in the summer months. From December to January strong salinification is observed.

The region sWGCb shows a different seasonal cycle compared to its sources WGCn or WGCn-ic, thus seasonal change in advection, mixing or forcing must play a role for explaining this climatological cycle. This is plausible since the area branches of at the area of maximum EKE in the Labrador Sea. This will be further addressed below in the discussion, section 3.4.

3.3.4 Labrador Current shelf area (LC)

The last two areas are the shelf and offshelf Labrador Current. Analogous to the West Greenland Current first the shelf area LC will be analyzed, followed by the offshelf area LC-ic.

The Labrador Current originates in the merging from several currents. In first order the Labrador Current can be seen as the continuation of the Baffin Island Current and is joined by the Hudson Strait Current and the West Greenland Current branches (e.g. Lazier and Wright, 1993). Due to rich fishing grounds the Labrador and Newfoundland shelves are very well sampled during ice-free times. Lazier (1982) and Houghton and Visbeck (2002) describe a cross-shelf salinity variability. This cross-shelf variability is not taken into account for this analysis on the shelf. To address this bias to a certain degree data close to the shore is not used. Since the cross-shelf variability is strongest near the shore and at the shelf break (Houghton and Visbeck, 2002) the bias is reduced in this study by removing data close to the shore and from the shelf break, but not removed.

The Labrador shelf has 41 years of July observations in the data set and still 34 years consecutive observations in July and August. The opposite is the case for the monthly change between April and May with only one monthly change observation or four available observations in April. Apart from April the Labrador shelf is sampled at a high frequency since 1950, resulting in the best quantity of data of all areas in summer. The effect of this can be seen in figure 3.9 g in April, the median and mean show very different behavior.

Three of the four April observations were hardly changed by detrending the data and the extreme spread in April persist. Looking at the corresponding years it reveals that the very low April measurement was taken 1970, thus during the Great Salinity Anomaly. Therefore I decided to remove this 1970 April observation and use the mean of the remaining three observations for April (figure 3.9 g blue curve). This is supported by the seasonal cycles recorded by an Aanderaa current meter with a conductivity cell in two years on the Labrador shelf (Lazier, 1982). The current meter shows a very similar cycle in salinity to the here shown climatological mean salinity cycle from the detrended data. This cycle is used in the following for area LC.

3.3.5 Labrador Current offshelf area (LC-ic)

The area LC-ic is the offshelf Labrador Current part and mainly the continuation of the West Greenland Current branches. Therefore a shifted similar seasonal cycle to area sWGCb is expected.

Observations in the offshelf Labrador Current area LC-ic are spread throughout the year, but similar to the shelf part the winter months are sparsely sampled compared to the summer months. Variability is lower in winter increasing successively in the course of the year. Continuous freshening is seen from April to September and salinification from September to March. The seasonal cycle is very similar to the cycle from the central Labrador Sea, even the separation of the freshening in two pulses, mainly May to June and July to August, is represented.

The detrended data set has a reduced amplitude in the seasonal cycle compared to the original data and can be seen in figure 3.9 h. The variance is reduced significantly by detrending the data. The detrended median climatological salinity cycle is used for this area.

3.4 Discussion

The best estimate for the seasonal salinity cycle was established for every region. These cycles will be used in the following for all further analyzes, especially constructing the decadal variations in chapter 5. All climatological salinity cycles with corresponding freshwater change are displayed in figure 3.10. The upper panels in all sub-figures show the monthly freshwater flux in meters, derived from the salinity cycle shown in the lower panels. For reference purposes the gray horizontal lines in the lower panels indicate the maximum and minimum climatological monthly salinity from the central Labrador Sea area cLS. Monthly freshwater change is represented by blue bars for positive freshwater flux and by red bars for salinification. Please note the inverted y-axis so that the freshwater is correlated to the derivative of the salinity cycle. Thus a blue bar facing down is in-phase with decreasing salinities. The freshwater flux shown is calculated as column of water with no salinity that is added or subtracted from the 100 m water column to describe the observed monthly change in salinity. The gray lines give the minimum and maximum salinity from the central Labrador Sea region (area cLS) and provide a reference for the salinity values and variability in each region.

The salinity cycles are obvious very different in shape and amplitude for the different

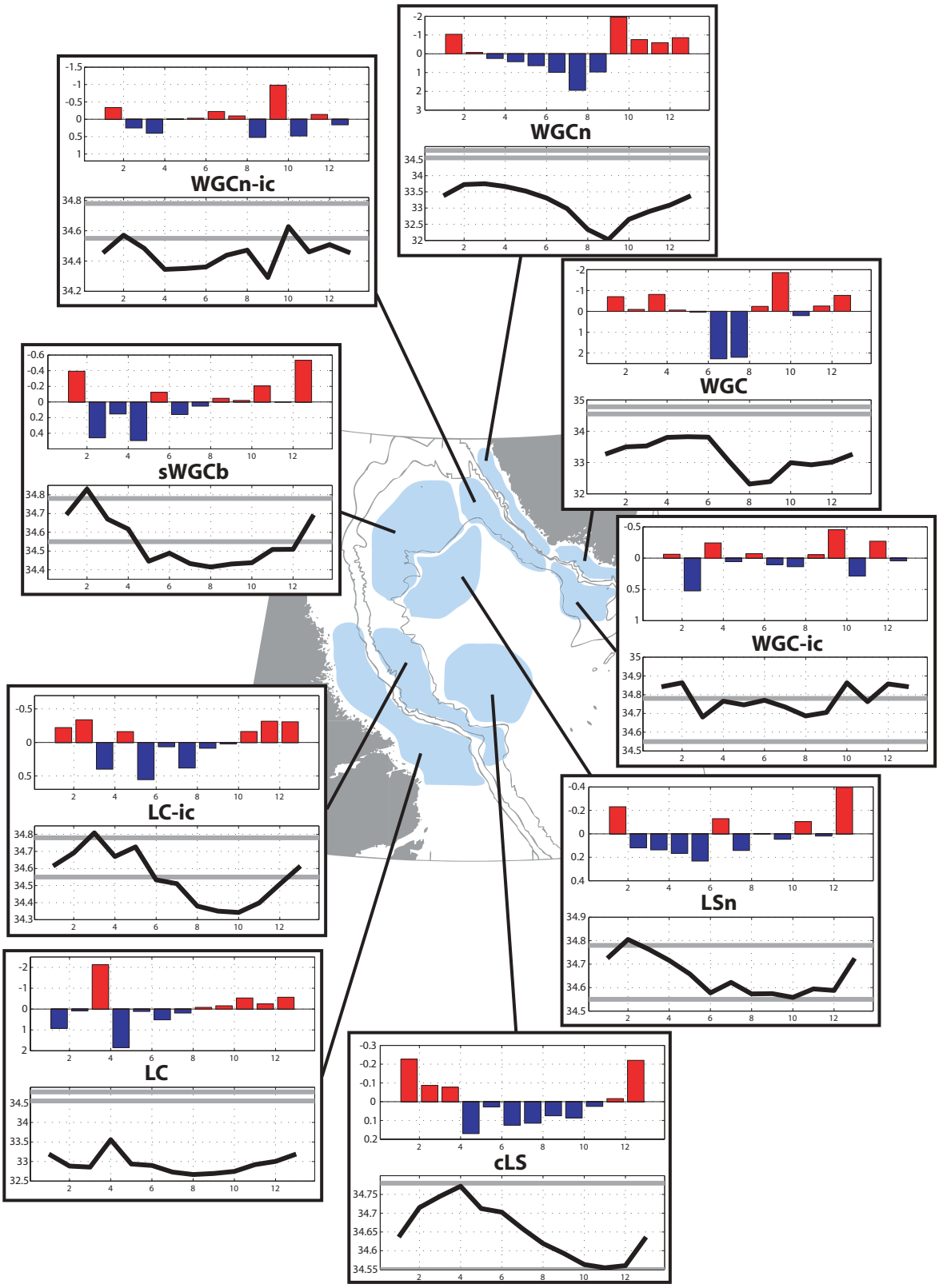

Figure 3.10: Top 100 m climatological salinity and freshwater flux in Labrador Sea areas. The upper panels illustrate the monthly freshwater flux in m, please note the inverted y-axis. The lower panels are the best estimate for the seasonal salinity cycle, the gray bars indicate the maximum and minimum from the central Labrador Sea Salinity cycle. Regions of origin are sketched.

areas in the Labrador Sea. At the inflow in the Labrador Sea the shelf and offshelf current have a difference of up to 2.5 psu this is about 10 times the amplitude of the central Labrador Sea salinity cycle. At the exit of the Labrador Sea in the Labrador Current the shelf and offshelf salinity gradient is still 1.8 psu.

With the knowledge of the mean currents (figure 1.2) and since the offshelf currents insulate the shelf currents from the interior Labrador Sea, the offshelf currents will be discussed in detail counter-clockwise around the Labrador Sea along the flow. Afterwards the northern Labrador Sea area LSn and the central Labrador Sea area cLS will be examined. Salinity cycles from the shelf currents can help to understand offshelf current changes but will not be discussed individually. This has already been done to a certain degree for the West Greenland shelf for instance by Mineral Resource Administration for Greenland (1998); Buch (2000) and in detail for the Labrador Sea shelf by Lazier (1982); Lazier and Wright (1993); Houghton and Visbeck (2002) and others.

Next to using the salinity climatologies for constructing and analyzing the long trends and variabilities from the regions, it allows to draw further conclusions from these results. No other work known to me has constructed and discussed the seasonal cycles from so many adjacent regions in the Labrador Sea or even separated the boundary currents in a way discussed and presented here. The layout of these nine areas covers all relevant areas for the central Labrador Sea and the areas are small enough to be sure that bias from different water masses with different seasonal salinity cycles is minimized. The clear differentiation between offshelf Irminger waters and on shelf polar waters shows unmistakeably the origin of water from these regions. Further these nine regions allow me to analyze the propagation of seasonal signals throughout the Labrador Sea.

Therefore I will discuss in the following some possible conclusions that can be drawn from figure 3.10 with emphasize on the offshelf boundary currents and the central Labrador Sea.

The area WGC-ic is the saltiest of all areas analyzed. It represents the characteristics of the Irminger Current Waters entering the Labrador Sea around Cape Farewell. No other place in the Labrador Sea found during the analysis has a larger horizontal salinity gradient as area WGC-ic compared to the shelf. Along-current the salty Irminger Current Waters mix with fresh shelf waters and waters from the interior. The salinity is reduced by 0.3 psu from area WGC-ic south of Cape Desolation to area WGCn-ic past Cape Desolation. As a rough guess the distance between the average area positions is 350 km and less than 400 km along isobaths. This corresponds to a decrease of 0.075 psu-0.1 psu per 100 km. While area WGC-ic at the surface is saltier than the central Labrador Sea, this is reversed further north in area WGCn-ic before the bifurcation of the southern West Greenland Current branch that flows along the 3000 m isobath. This is only true for top 100 m column analyzed here. The core of Irminger Current Waters has a depth around 200 m to 300 m and salinities in that depth do not change as much. This can be seen in the salt map for the 200 m to 300 m water layer in figure 3.2.

Even though it was mentioned in section 3.3.2 that the derived seasonal cycle is doubtful and monthly variations dominate, the shape of the independent climatological cycles of area WGC-ic and WGCn-ic are similar with a lag of one month. Thus it can be expected that they do represent the main features of their seasonal cycles well. This lag is similar to the mean advection velocity (Cuny et al., 2002). Even the so far unexplained

salinification from September to October in area WGCn-ic is found one month prior at the entrance of the Labrador Sea and thus might have an advective origin. A signal found downstream in area WGCn-ic but not beforehand is the freshening in September directly before the salinification. Since the salinity reaches the minimum on the shelf as well in September this is the only plausible source.

While the summer values stay in the same order between area WGCn-ic and the southern West Greenland Current branch, the winter values in area sWGCb decrease. Since the southern West Greenland Current is much slower than the West Greenland Current along the Greenland shelf (Cuny et al., 2002), surface heat flux and thus buoyancy increase the mixed layer depth along the current significantly. This becomes obvious when comparing the November to December surface salinities from figure 3.1 with the position of the branches in figure 1.2. The very low flow area between the northern and southern branch shows a mixed water column reaching higher salinities earlier than the southern branch. In the following months the western part of area sWGCb continuously has higher salinities than the eastern part, though as seen in figure 3.2 the underlying waters are saltier in the east. As soon as atmospheric heat loss eases, surface salinities in area sWGCb decrease to values similar to area WGCn-ic. The onset of this freshening seems to vary, since salinity variability is low in February and June and high in between (figure 3.9 f). February and March have similar strong atmospheric heat loss, thus only the later part of the freshening after March can be explained this way. The reason for the variable freshwater flux from February to March (5 out of 10 years in figure 3.9 f) cannot be found at the source, since enhanced variations are not found in the areas WGCn-ic or WGCn. This variable first freshwater flux (area sWGCb in figure 3.10) is believed to originate from different strength in EKE as will be discussed in detail in section 4.5.

Can the properties of area sWGCb still be found in the offshore Labrador Current (area LC-ic), though further freshwater sources like the northern West Greenland Current branch, Baffin Island Current and Hudson Strait waters join the Labrador Current further north? Since waters of the West Greenland Current branches are expected to be furthest offshore from the above mentioned other sources, mixing with those West Greenland Current waters will dominate. It is assumed that the northern West Greenland Current branch has the same shape in salinity cycle like area WGCn. Thus the similar, one month shifted, shape of area LC-ic to area sWGCb from February to July and further freshening in late summer can be explained well. This shift corresponds to the mean velocity (Cuny et al., 2002). Since area LC-ic is much better sampled in summer than area sWGCb the small differences in summer might also originate in a different basis of sampling years.

The first sudden freshening in area sWGCb from February to March is also found here in area LC-ic one month later. The variability is similar with three out of five available years showing a fresh April (figure 3.9 h).

The Labrador Sea seasonal salinity cycle is mainly formed by interaction of the boundary currents with the interior as has been described in the literature. Though doubts still exist about the importance of the different currents for the central Labrador Sea. In preliminary work to this thesis Schmidt and Send (2007) claim by budget analysis the major responsibility of the West Greenland Current for the central Labrador Sea but leave the first variable freshening as well as the pathway unaddressed. What can be seen in the

significantly enlarged data set and also more objective construction of the seasonal cycle?

Focussing first on area LSn a long slow decrease of salinities can be seen. A closer look at figure 3.9 a reveals that this constant freshwater flux has a very high variability in April with four out of 11 years with fresh events, as if representing two states. Thus the freshwater flux would have a maximum peak between March and April. This is analogous with a shift by one month earlier in area sWGCb. The high variability in March can be tracked back to area sWGCb. The summer salinities in the northern Labrador Sea are similar to the southern West Greenland Current branch, delayed by one month. The minimum salinity in area LSn is 0.15 psu higher than in area sWGCb likely due to mixing with central Labrador Sea waters. The decrease from December to February is, as mentioned above, caused by deepening of the mixed layer depth. By looking at the seasonal cycle it can be summarized that area LSn is similar to area sWGCb mixed with a water mass of constant winter salinity value. The difference in freshwater fluxes in the beginning of the year can be found in different sampling years with and without the variable early freshening and is thus not seen in 3.10 since four out of 11 years do not effect the median used to represent this region and thus are not represented in the climatological cycle.

In the central Labrador Sea the determined seasonal cycle is similar to the one described in Schmidt and Send (2007). Since the data base is significantly enlarged and the construction of the climatological cycle is more robust here, summer variability was reduced significantly. Area cLS has a sudden strong freshening from April to May. Freshening continues from June through October. Those two periods were called the first and the second freshening by Schmidt and Send (2007). Roughly half of the available years show the first freshening (figure 3.7), the other years show a lower but constant freshening from May to October with no significant decrease of the freshening from April to May. The second freshening is one month early compared to Schmidt and Send (2007), but their cycle has a higher variability. Comparing the central Labrador Sea with the adjacent regions area LSn and LC-ic the origin is not obvious at once (keeping the first freshening for area LSn in mind which does not show up in figure 3.10) since both regions adapt there properties from area sWGCb. The first freshening occurs in area LSn and area LC-ic one month prior to area cLS. The amplitude of the cycle is similar to area LSn and the shape is more similar to area LC-ic. The similar amplitude makes area LSn as only source unlikely since mixing with more haline waters along the propagation pathway is likely. Thus it is likely that the central Labrador Sea acquires its freshwater from the outer parts of the offshore Labrador Current and the northern Labrador Sea. This does not contradict the results from Schmidt and Send (2007), since the seasonal properties of these areas originate in the West Greenland Current. Looking at the timing argument from Schmidt and Send (2007), it can be seen in figure 3.10 that the lowest salinities, thus analogous to Schmidt and Send (2007) the largest freshwater anomaly compared to a constant reference salinity is in August in area WGC, September in area WGCn and between October and December in the central Labrador Sea. Schmidt and Send (2007) see the freshening in the central Labrador Sea even earlier due to a less robust seasonal cycle.

Thus the timing qualitatively supports the work from Schmidt and Send (2007) further with a more confident timing. This compared to Schmidt and Send (2007) later central Labrador Sea maximum freshening can better explain the freshwater pathway along the West Greenland Current and from the north into the central Labrador Sea. The short timing suggested by the data of Schmidt and Send (2007) could not have explained this longer pathway.

3.5 Conclusion

With four statistical methods it was possible to describe the climatological cycle for several independent Labrador Sea areas. The emphasize of the layout proved to be crucial for several results. Despite the fact of timewise and spatially spread different data sets for each region the cycles were shown to be robust and it was possible to track along-stream features and explain their variability.

The boundary currents show significantly different salinity cycles between the shelf and offshelf, that do not only differ in amplitude as suggested in previous works. Around the Labrador Sea shelf currents and offshelf currents originate from different water masses and not only differ by a constant shift in salinities. Thus for tracking long-term changes a mixture of them would provide very different likely misinterpreted results.

The assumption of a constant salinity for Irminger Current Waters compared to the polar waters of West Greenland Current entering the Labrador Sea by Schmidt and Send (2007) could be approved in first order, finding a seasonal salinity cycle of less than 0.2 psu for Irminger Current Waters compared to a larger than 1.5 psu cycle for the fresher shelf waters.

The two freshenings of the Labrador Sea as described by Schmidt and Send (2007) were confirmed as well as the timing of the lowest salinities (strongest freshwater anomaly compared to a constant reference salinity in Schmidt and Send (2007)) for the main freshening. The fact of Straneo (2006) not seeing two pulses in the mid-90's must be addressed to the high variability of the first pulse and its absence in several years and will be discussed in the following chapter in section 4.5.

The central Labrador Sea salinity cycle has high similarities with two adjacent regions that both originate in the southern West Greenland Current branch. Thus it is undoubted that the central Labrador Sea acquires its seasonal salinity cycle from the West Greenland Current. This confirms the work of Schmidt and Send (2007) who showed the West Greenland Current to be the origin by calculating a freshwater budget, but gives clarity about the freshwater pathway that travels further along the West Greenland Current before moving south again into the central Labrador Sea.

Chapter 4

Phases of EKE

The seasonal freshwater in the central Labrador Sea has its origin in the freshwater signal in the West Greenland Current. The analysis by Schmidt and Send (2007) explains the main freshening of the seasonal cycle. These findings were qualitatively confirmed in the previous chapter 3. But the reason why some years do not show a first intense freshening as described by Straneo (2006) is still unexplained. The seasonal cycles suggest the southern West Greenland Current branch as the origin of these. The region of highest EKE in the Labrador Sea is found at the bifurcation of this branch.

For a better understanding of these variations I explore now the influence of the pronounced and well discussed seasonal EKE maximum of Cape Desolation on the upper Labrador Sea freshwater. Up to now the eddies from this region are known to be responsible for a reasonable salt flux into the central Labrador Sea (e.g. Lilly et al., 2003) by dissipating and releasing there interior waters. In the following, the years with reliable EKE data are sorted into phases of high and low EKE. The differences of these phases are analyzed in terms of surface geostrophic currents and hydrography changes.

4.1 Spreading EKE in the Labrador Sea

Before going into detail I want to give a general overview about the EKE in the Labrador Sea and decide on regions of special interest.

EKE derived from SSH anomalies in the Labrador Sea has a strong interannual and seasonal variability. The literature focuses especially on the area with enhanced EKE north west of Cape Desolation (amongst others: Eden and Böning, 2002; Brandt et al., 2004; Funk and Brandt, 2007). Its influence on Labrador Sea convection variability has also been described (e.g. Czeschel, 2005). The pronounced seasonal cycle in the Labrador Sea is visible in figure 4.1 as discussed in detail by Brandt et al. (2004) and Funk and Brandt (2007). The most obvious feature throughout all seasons is the maximum EKE intensity from the North Atlantic Current in the south east corner of all plots. The EKE of the North Atlantic Drift is well above the shown upper limit of 140 $\frac{cm^2}{s^2}$ in the graph. I will not go into further details of that maximum as no drifter or float known to me within the upper 300 m has made its way from there to the central Labrador Sea without circulating around the Irminger Sea basin thus there seems to be no direct water or salt exchange with that region. Furthermore no propagation of EKE from that region into the central Labrador

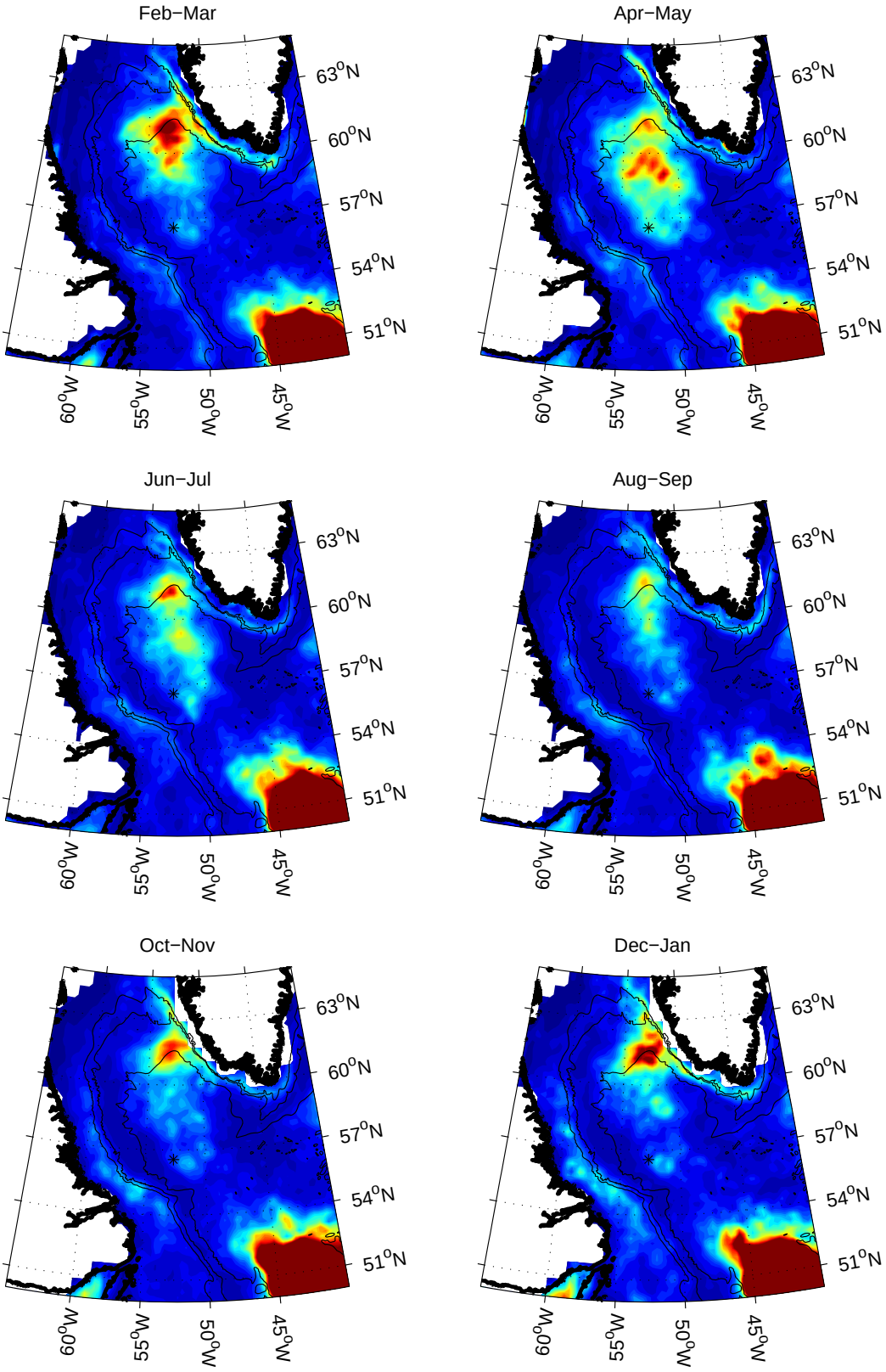

Figure 4.1: The six panels show the mean EKE for different 2 months periods, calculated from the weekly grided data since 1993 available from AVISO. Black lines indicate the coast (thick) and 1000 m, 2000 m and 3000 m isobaths. The color scheme is the same in all panels $0 - 140\ \frac{cm^2}{s^2}$.

Sea can be seen in a weekly snapshot animation of Labrador Sea EKE[1].

The seasonal cycle has a local EKE maximum north west of Cape Desolation throughout the whole year (figure 4.1 all panels). The maximum is most developed between December and March. The seasonal southward propagation of that maximum is already very obvious in February-March (upper most left panel) and continuing until June-July (middle left panel). From August till January only the remainders of the southward propagation can be seen in the mean, decreasing in intensity while dissipating. This is also described for instance by Funk and Brandt (2007), who find a southward propagating EKE signal arriving in the area around the central Labrador Sea mooring in May-June (black star figure 4.1 all panels). Minimum EKE activity north west of Cape Desolation is found in the mean in August-September (middle right panel same figure).

Further areas of EKE intensity that are not so obvious areas are the West Greenland Current at the shelf break upstream and downstream of the EKE hot spot northwest of Cape Desolation and the Labrador Current on the shelf.

The described regions and the convection area were used for a more objective analysis of the Labrador Sea states due to EKE. The regions chosen are shown in a map of mean EKE in figure 4.2. The black circle marks the position of the central Labrador Sea mooring Kx1 (see section 2.3.4 for details). The areas A to E were chosen to cover all areas of enhanced EKE activity separately, area F is used in the following to classify each year as high or low EKE-phase for the Labrador Sea region. Though an exception is made as discussed below. Using only main EKE area B for selection into high and low years proved to be insufficient. For example when considering only area B, a long lived stational eddy would have a much larger impact than justified. Nevertheless since area F includes area B, and even more area B is the origin of nearly all EKE in area F, the correlation of 100 day low pass filtered data between area B and area F is $R = 0.73$ with upper and lower bounds of 95% confidence at $R = 0.76$ and $R = 0.69$. Unless otherwise stated 100 day low pass filtered data of the areas refers to EKE data in regions A through F (Butterworth filter with cut off frequency of 100 days).

Another remarkable region not selected as individual region here is the distinct EKE minimum between the 2000 m and 3000 m isobaths at the Labrador shelf break between $54^\circ W$ and $58^\circ W$. This minimum, like the maximum, is present without exceptions in all seasons as seen in figure 4.1. Any eddy mixing in this zone between the boundary current and the interior is therefore very unlikely. The same conclusion applies for strong seasonal current variation. This is necessary to keep in mind when discussing water propagation or mixing from boundary currents into the central Labrador Sea and vice versa.

Figure 4.3 shows the time series of EKE data in the areas defined in figure 4.2. The thin blue line is the weekly available data averaged over the region, the red line is the same data filtered with a 100 day butterworth low pass filter. Areas A to F are shown from top to bottom, please note the different scales on the y-axis. The highest EKE and EKE variance is found in area B as expected. The boundary currents, area A, area C (West Greenland Current) and area E (Labrador Current) show a similar magnitude with slightly stronger variations in the West Greenland Current. Area D has generally low EKE and low variability with the exception of three events. The first event will be ignored due to

[1] see section 2.4 and `https://ftp.ifm-geomar.de/users/sschmidt/eke_movie.avi`

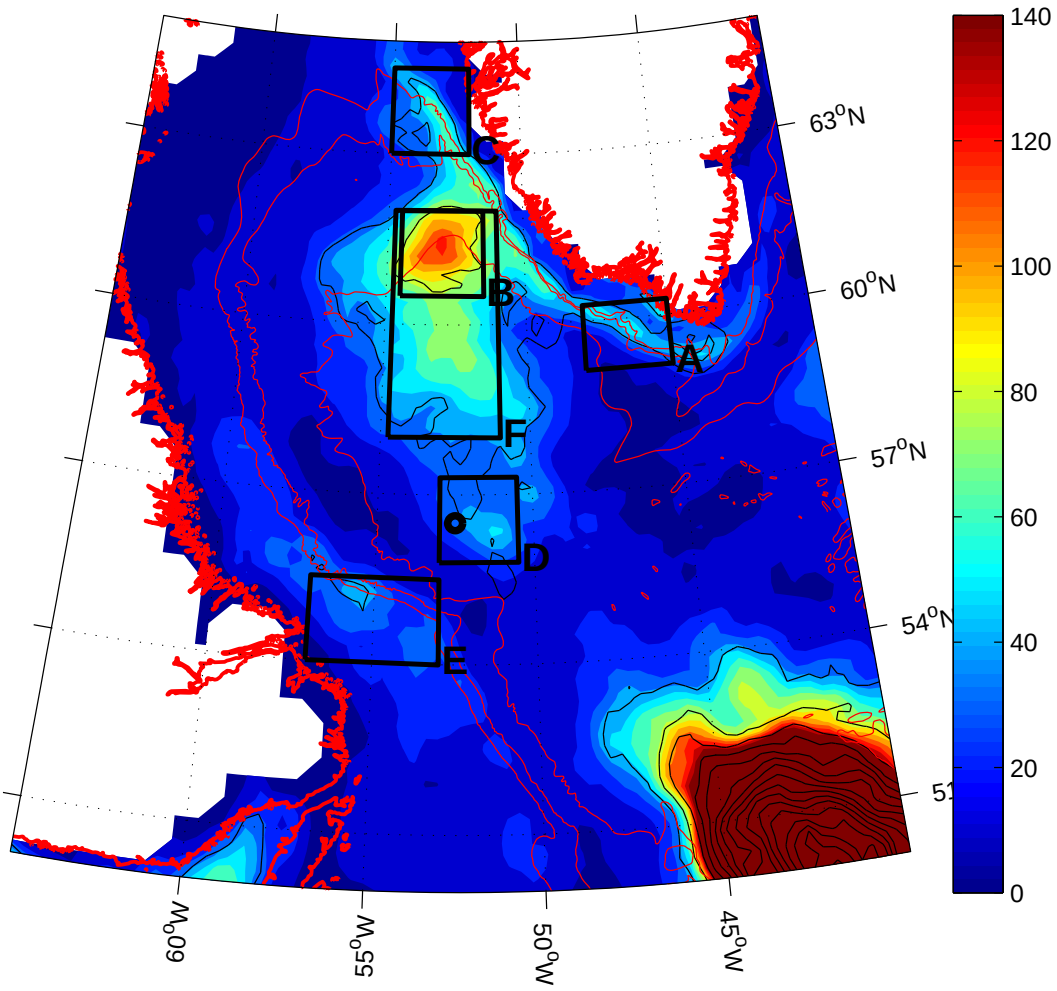

Figure 4.2: Mean EKE in $\frac{cm^2}{s^2}$ and its standard deviation in steps of 50 $\frac{cm^2}{s^2}$ (black thin line). In red is the shore (thick), 1000m, 2000m and 3000m isobaths. The labeled boxes indicate the areas used for averaging, see text for details.

the absence of hydrography data. Further the data was sampled at the beginning of the TOPEX/Poseidon mission resulting in limited trustworthiness of the EKE data.

Another analysis of these time series in figure 4.4 shows the corresponding autocorrelation functions of each area. A seasonal signal can be found with varying strength for all areas. Areas D and E are probably seasonally influenced, but in those cases other variabilities seem to mask the low seasonal signal. In areas A, C and E short term fluctuations are a dominant feature, as can be inferred from the fast descending curve. No explanations were found for the maximums in the autocorrelations of 210 days and around 400 days for area C. The minimum at 210 days can be explained by a short summer and long winter season in high latitudes, though this does not explain the 400 day lag in the low pass filtered data. As a short summary, the EKE regions on the Greenland side show a considerably higher seasonality than on the Labrador side. Due to the lower seasonal signal and high short term variability on the Labrador side, tracing the propagation of an EKE in a mean seasonal cycle is not promising.

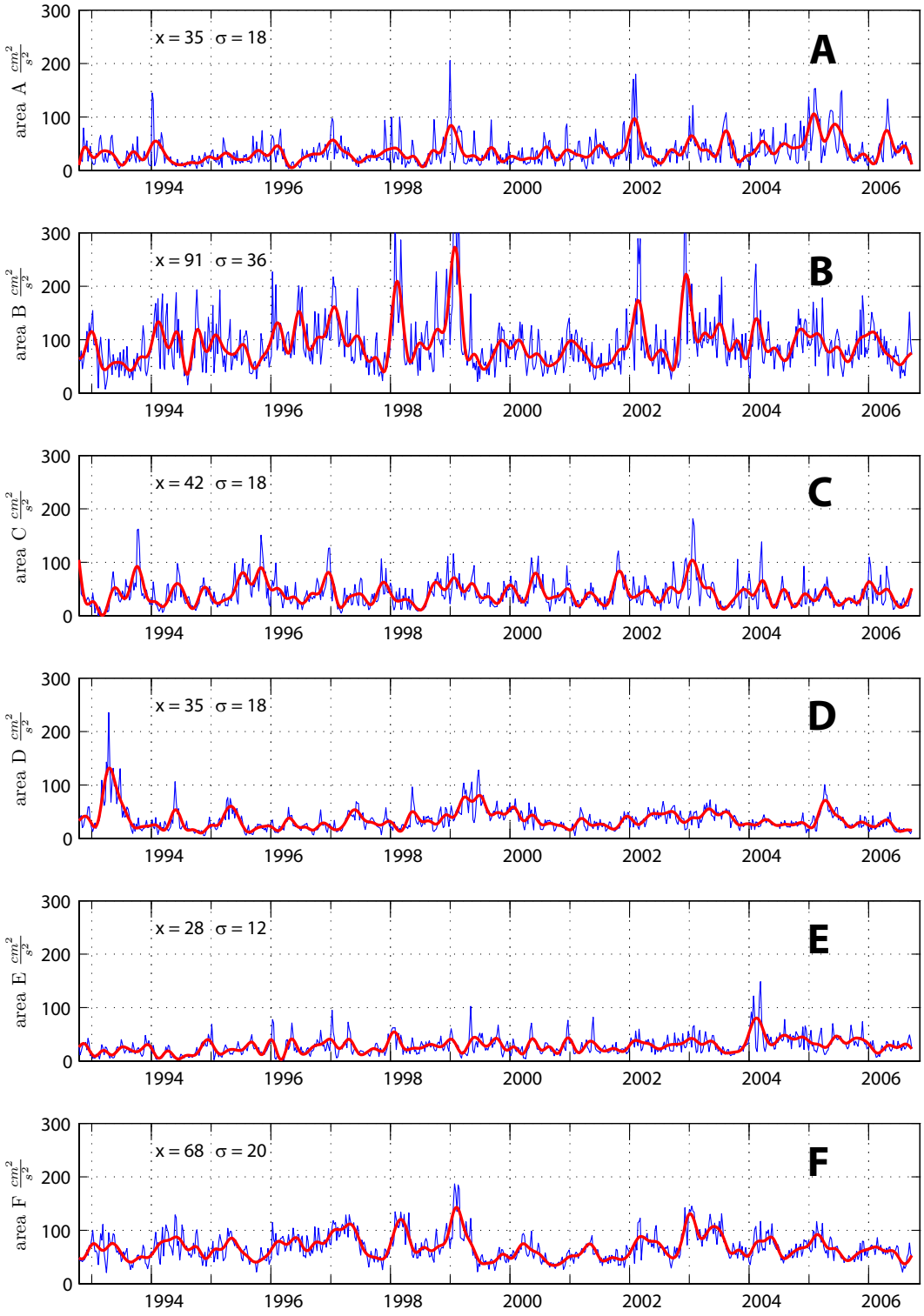

Figure 4.3: Spatial average EKE data for the regions A to F, weekly data in blue and 100 day butterworth low pass filtered data in red. Y-axis is similar in all panels.

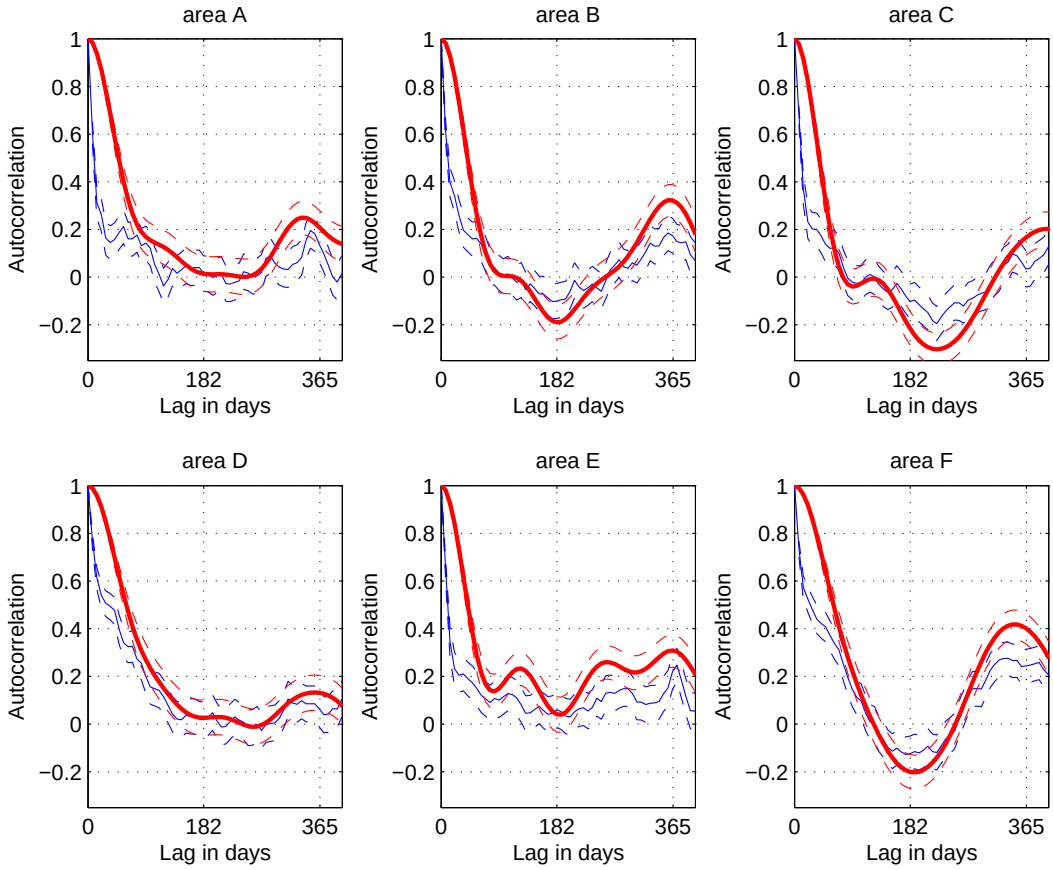

Figure 4.4: The autocorrelation functions for the regions A to F. Auto correlation (solid) and 95% confidence intervals (dashed) shown for weekly data in blue and 100 day butterworth low pass filtered data in red.

In the following I show that area F inherits most EKE from area B and derive propagation speeds through the Labrador Sea (after Funk and Brandt (2007)).

A trace of high EKE events is not possible for all events in figure 4.3. The well-known fact that some high EKE events in region B have their origin in enhanced EKE in area A is timewise apparent. Though area A has much less EKE than area B, baroclinic instabilities in the boundary current region increase the propagating EKE signal from SSH anomalies. For the other non adjacent areas, especially area D, a trace of an EKE signal from this figure is only speculation. For a better analysis of the southward propagation of EKE from area B the EKE intensity is plotted in a time and latitude domain (figure 4.5). Similar figures can be found for instance in Funk and Brandt (2007). The dashed red line indicates the central Labrador Sea mooring position in the convection area. The figureshows a southward propagation of nearly all strong EKE events from area B. The average southward propagation of the yearly EKE maximum seen in figure 4.5 is 5° in 5 months, which corresponds to an average southward velocity of 4.3 $\frac{cm}{s}$; it is probably sufficient to assume a speed between 3.5 $\frac{cm}{s}$ and 5 $\frac{cm}{s}$. Funk and Brandt (2007) find a southward speed of 4.7 $\frac{cm}{s}$ in their constructed mean EKE field based on the raw data of the gridded product I used here. Some

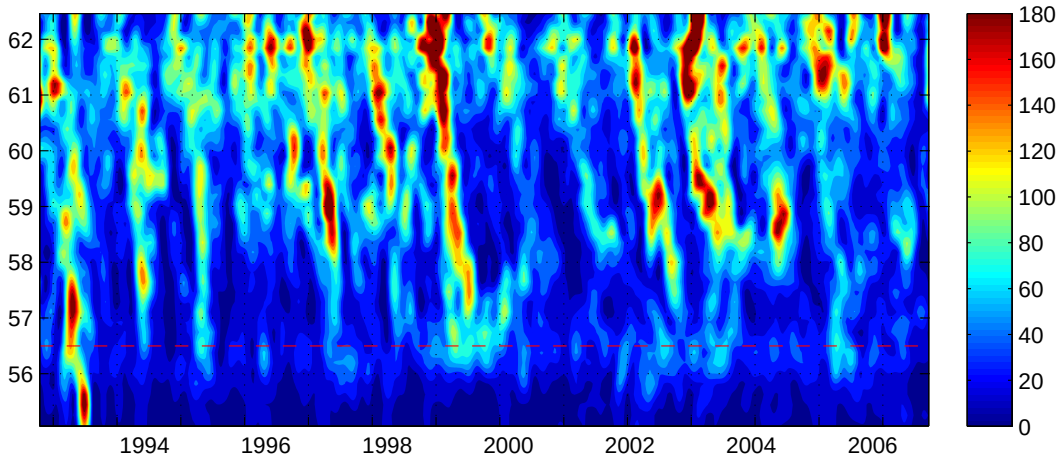

Figure 4.5: Zonal averaged EKE in $\frac{cm^2}{s^2}$ 100 day low pass filtered in the Labrador Sea between $53° W$ and $51° W$. The red dashed line marks the central Labrador Sea mooring position, similar to OWS Bravo. Area B is between $60.5° N$ and $62° N$, respectively area F $58° N$ and $62.5° N$, area D $55.8° N$ and $57.3° N$. No meridional interpolation is applied here.

maxima reach the latitude of area D, while most EKE (mainly boundary current eddies, Prater (2002); Lilly et al. (2003)) dissipates north of $57.5° N$, thus eddies from the boundary current release their salty interior water into the Labrador Sea.

There is a noticeable absence of any larger EKE for some years.

Comparing all areas and propagations of EKE in figure 4.5, area F represents best long lived EKE in the Labrador Sea and is not as strongly influenced by short term events like area B. Thus area F will be used in the following to classify individual years as high or low EKE years.

4.2 EKE phases

Which years have high or low EKE and what are the main features? How do they affect the Labrador Sea surface circulation and mixing of water masses?

In figure 4.6 the EKE from area F (compare figure 4.3) is analyzed; the blue lines represent the mean EKE for the period December till October. Due to the fact that the dissipation of eddies are assumed to provide an additional salt flux to the central Labrador Sea (Lilly et al., 2003) the decrease of EKE between the winter maximum and summer minimum is also plotted (red triangle). For the winter maxima the annual maximum of 100 day low pass filtered EKE data from area F between December and March was taken, for the summer minima respectively the annual minimum between July and October. This shown dissipation value also includes EKE that moves out of the area and is not dissipated and thus has to be interpreted with caution.

Using the annual mean EKE from figure 4.6 I will select in the following years to

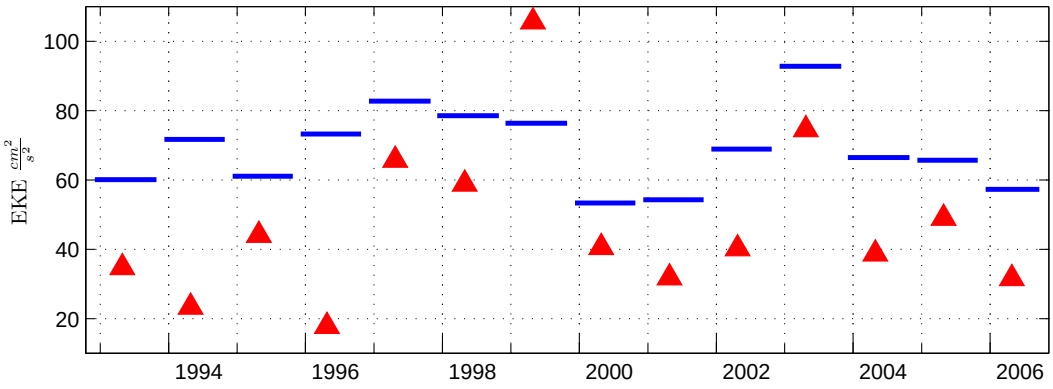

Figure 4.6: Mean December to October EKE in area F in blue bars and the difference between winter maximum and summer minimum EKE for the same area. Weekly data from figure 4.3, area F, used.

represent the high and low EKE. To clearly separate high and low EKE years I decided to not classify years with medium EKE.

As a criteria for a year of low EKE, an upper limit of mean EKE of area F of about 60 $\frac{cm^2}{s^2}$ was chosen (blue bars figure 4.6). This leads to the low EKE years of 1993, 1995, 2000, 2001 and 2006. 1993 was removed from this set, as it was one of the first TOPEX/Poseidon years with data not covering the complete Labrador Sea and boundary currents. Using 1993 data could lead to a regional bias in the mean. Another fact that makes 1993 probably unsuitable for constructing a low EKE mean is the unexplained highest satellite recorded EKE in area D, that might have an unrecorded origin in area B.

Deciding on high EKE years a lower limit of 75 $\frac{cm^2}{s^2}$ leads to the high EKE years of 1997, 1998, 1999 and 2003. 2002 was also declared a high EKE year as it has the 4th highest recorded EKE in area B (figure 4.3) and also a well defined southward propagating EKE maximum (figure 4.5). As the previous two years had very low EKE it seems that the background EKE was very low in 2002. Therefore the EKE signal does not show up as strongly in the spatial mean as expected from the other figures.

Though 1994 and 1996 had higher mean EKE than 2002, both years had an extremely low EKE dissipation (red triangles in figure 4.6). Since this is not the case for 2002 and together with the above arguments it is justified to take 2002 as a high EKE year into account.

For a comparison of high and low EKE times, average EKE and current maps derived from SSH anomaly are plotted for the Labrador Sea in figures 4.7 and 4.8. With the definition of the EKE at time t (equation 2.3) and t_{high}, the years of high EKE as defined above, the following definition of high EKE are shown (respectively for low EKE years):

$$EKE_{xy,high} = \overline{EKE_{xy}(t_{high})} - \overline{EKE_{xy}(t_{all})}. \tag{4.1}$$

The overbar represents the temporal mean $EKE_{xy}(t)$, the EKE at position (x,y) during the times t. Thus $EKE_{xy,high}$ is the average EKE anomaly at position (x,y) during phases of high EKE (t_{high}). EKE_{low} is defined with t_{low}. The currents plotted are

$$\overrightarrow{U}_{xy,high} = \overline{\overrightarrow{U}_{xy}(t_{high})} - \overline{\overrightarrow{U}_{xy}(t_{all})}. \tag{4.2}$$

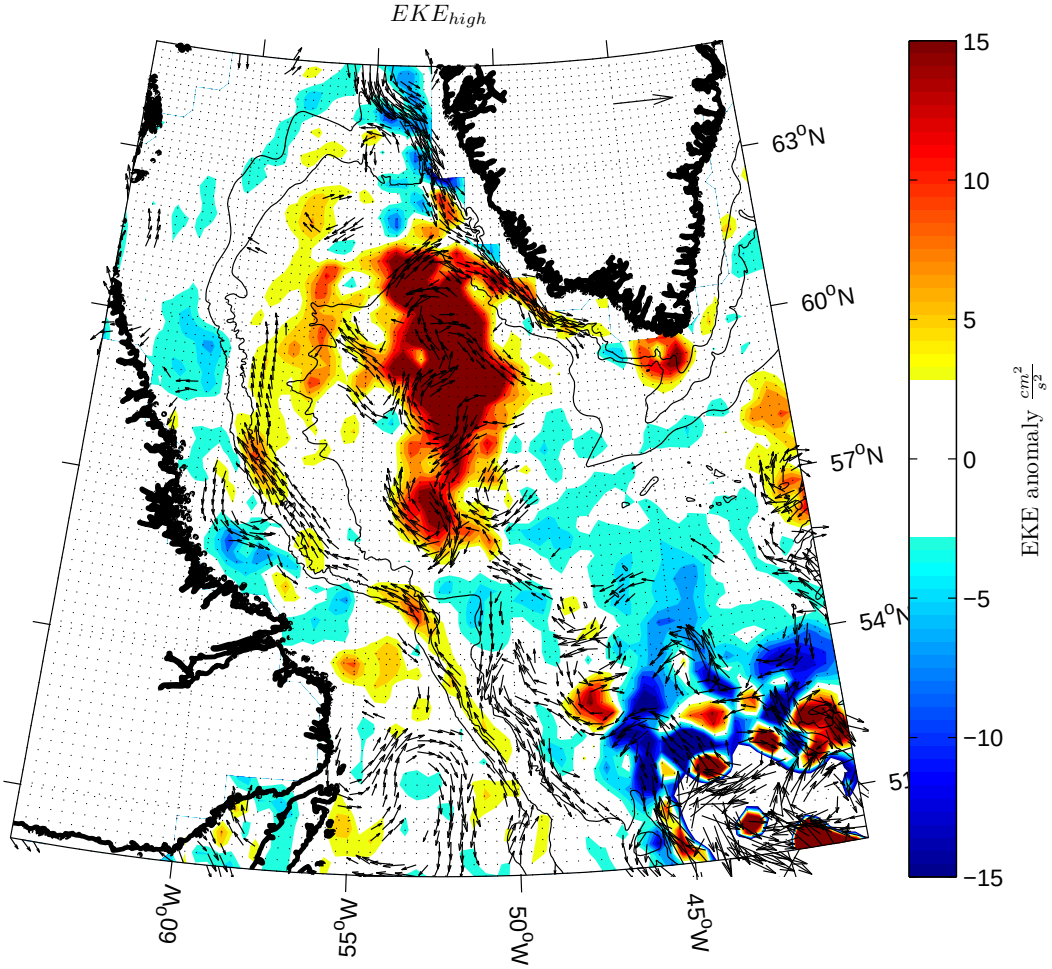

Figure 4.7: EKE anomaly and mean SSH anomaly derived geostrophic current anomalies during phases of high EKE. EKE anomaly is capped at $\pm 15\,\frac{cm^2}{s^2}$. Current vectors have an upper limit of $5\frac{cm}{s}$, shown inside Greenland as reference. 1997-1999 and 2002-2003 were regarded as high EKE phases. Isobaths shown are 1000 m, 2000 m and 3000 m (black lines). See text for details.

Therefore $\overrightarrow{U}_{xy,high}$ is the average SSH anomaly-based geostrophic current anomaly at position (x,y) during phases of high EKE (t_{high}). $\overrightarrow{U}_{xy,low}$ is defined respectively with t_{low}. Please note that regions of high/low mean EKE anomaly do not necessarily have a high geostrophic current anomaly because

$$\frac{1}{2}(\overline{U_{xy}}^2 + \overline{V_{xy}}^2) \neq \overline{\frac{1}{2}({U_{xy}}^2 + {V_{xy}}^2)}. \tag{4.3}$$

As an example, a strong alternating current with no mean current speed has a high EKE at each of those time steps. At each time step the EKE corresponds to the currents, but the mean EKE is high, while the mean current speed is zero. Due to this the currents plotted here include further information about the state during high/low phases.

Back to figure 4.7, the maximum EKE anomaly shown is $\pm 15\,\frac{cm^2}{s^2}$. In core regions this

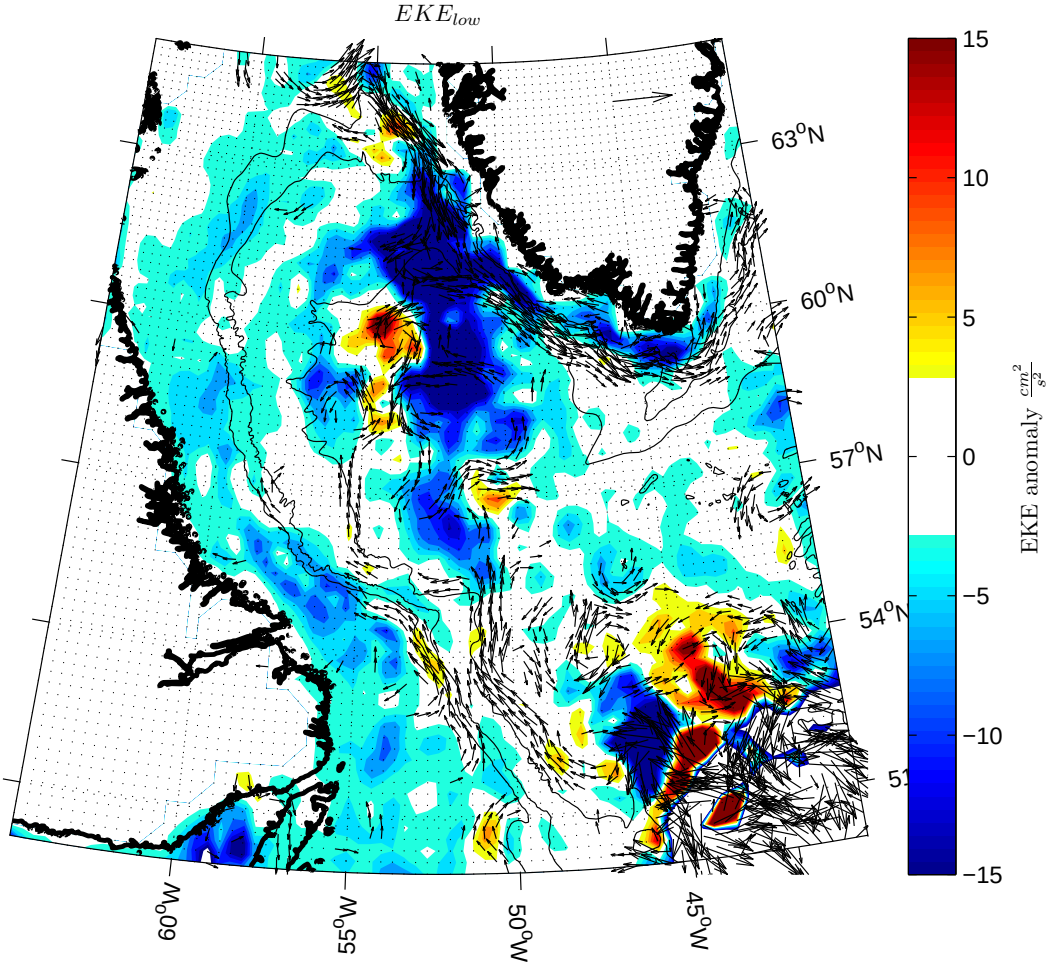

Figure 4.8: EKE anomaly and mean SSH anomaly derived geostrophic current anomalies during phases of low EKE. EKE anomaly is capped at $\pm 15\,\frac{cm^2}{s^2}$. Current vectors have an upper limit of $5\frac{cm}{s}$, shown inside Greenland as reference. 1995, 2000-2001 and 2006 were regarded as low EKE phases. Isobaths shown are 1000 m, 2000 m and 3000 m (black lines). See text for details.

value is exceeded. Values between $\pm 3\,\frac{cm^2}{s^2}$ are not shown for clarity reasons. The current vector inside Greenland shows the maximum shown current speed of $5\frac{cm}{s}$. Per definition the EKE anomaly is high in area F. The boundary currents appear to show high EKE anomalies as well during these times. Surprisingly the stronger EKE in the boundary currents is very closely associated with the region between the 1000 m and 2000 m isobaths and is present around the basin in the West Greenland and Labrador Current. In the northern Labrador Sea. Off Cape Desolation some EKE leaves this depth-region and moves deeper to about 2000 m and 3000 m, but moves closer to the 2000 m isobath again in the course of the Labrador shelf.

Looking at the mean current anomaly shown in figure 4.7 two features are noteable. The geostrophic SSH-current component on all shelf breaks between the 1000 m and 2000 m isobath (moving further to the 2000 m isobath south of $55°\,N$) seems to be reduced by

$1.5 - 2.5\frac{cm}{s}$. A reduced current of up to $3\frac{cm}{s}$ can be recognized in the West Greenland Current north of the bifurcation. A southward component of $1.5 - 2.5\frac{cm}{s}$ can be seen at the exit of the Labrador Sea offshore of the shelf deeper than 3000 m and south of $54° N$.

Current and EKE anomalies in the region of the North Atlantic Drift have a much higher variability (compare figure 4.2 black lines), but will not be discussed here in further detail, as no direct link exists.

While discussing these features one has to keep in mind that the overall mean is based on only 13 years of data, including the five years regarded as high EKE years. The same is true for the low EKE that is explained in the following. Afterwards the discussion will concentrate on the differences of the mean high and low EKE years.

Figure 4.8 of low EKE phases is constructed similar to the above described figure 4.7 for high EKE. The selected phases of low EKE seem to be representative for a low EKE state of the whole region, since the EKE anomaly shown is negative in all areas. Area F has a strong negative EKE anomaly again due to the definition of phases. But more details can be recognized. On the Greenland side the negative EKE anomaly is above the shelf unlike the positive anomaly during high EKE (trapped between the 1000 m and 2000 m isobath). The same can be said about a large part of the Labrador shelf break. Some increased negative EKE anomaly is found on the Labrador shelf upstream of Hamilton Bank. During low phases the EKE anomaly on the Greenland shelf is about three times as strong as on the Labrador shelf, while it was on the same order of magnitude during high phases. The positive EKE anomaly spot in the northern basin of the Labrador Sea is very likely due to variations in the pathway of eddies and the limited amount of years with data. Four years of data out of an overall mean of 13 years were used for the EKE low phase.

The mean current anomaly during low EKE years is much more pronounced than during high EKE times. Especially the currents at the bottom of the Greenland shelf break at depths deeper than 2000 m have a strong negative anomaly. It increases along the current from around $2\frac{cm}{s}$ on the east side of Greenland, to about $3.5\frac{cm}{s}$ off Cape Desolation and even up to $4.5\frac{cm}{s}$ north of the West Greenland Current bifurcation close to Davis Strait. Contrary to these off-shelf currents, the currents on the Greenland shelf very close to the shore have a positive along-current anomaly of the order of around $1.5 - 2\frac{cm}{s}$ from the region around Cape Farewell up to the bifurcation. On the Labrador side two current anomalies stand out. One stays close to the 3000 m isobath extending from south of the Labrador Sea at $51° N$ up to past the convective region around $58° N$, with anomalies of up to $1.5\frac{cm}{s}$ west of the convective region and around $2.5\frac{cm}{s}$ south of the convective region. The other anomaly is on the Labrador shelf break directly above the 1000 m isobath with current anomalies of around $2\frac{cm}{s}$.

The in-phase EKE link between the West Greenland Current and area F is plausible and discussed in detail in the literature as well as mentioned above. The EKE in area F (figure 4.2) originates in water property changes of the West Greenland Current (Eden and Böning, 2002) and higher boundary current kinetic energy (Funk and Brandt, 2007). Notable is the down slope shift of the current anomalies at Cape Desolation. During the EKE high time the anomaly is situated above the 1000 m and 2000 m isobath, while it is between the 2000 m and 3000 m isobath during low times. This down slope shift of the negative current anomaly from high to low EKE phases could indicate a change in

the position of the West Greenland Current. This has to be kept in mind, since it can be important for the overall freshwater transported in the whole West Greenland Current, on the shelf and offshelf.

Low and high EKE phases have a distinct EKE anomaly and current anomaly pattern. It is helpful to check the differences between EKE_{high} and EKE_{low}. Figure 4.9 shows the difference between figure 4.7 and figure 4.8. The EKE difference between high and low phases is shown up to $\pm 20\,\frac{cm^2}{s^2}$. The EKE between $\pm 5\,\frac{cm^2}{s^2}$ was regarded as uncertain and is not shown. The current vectors are shown up to $5\frac{cm}{s}$, as plotted inside Greenland for reference purposes. The central Labrador Sea EKE differences show a correlation to the EKE on the Labrador shelf.

A correlation analysis of the signal on the Labrador shelf, area B versus area E, have maximum correlation of $R = 0.34$ at lag of 4 to 5 weeks, with upper and lower bounds of

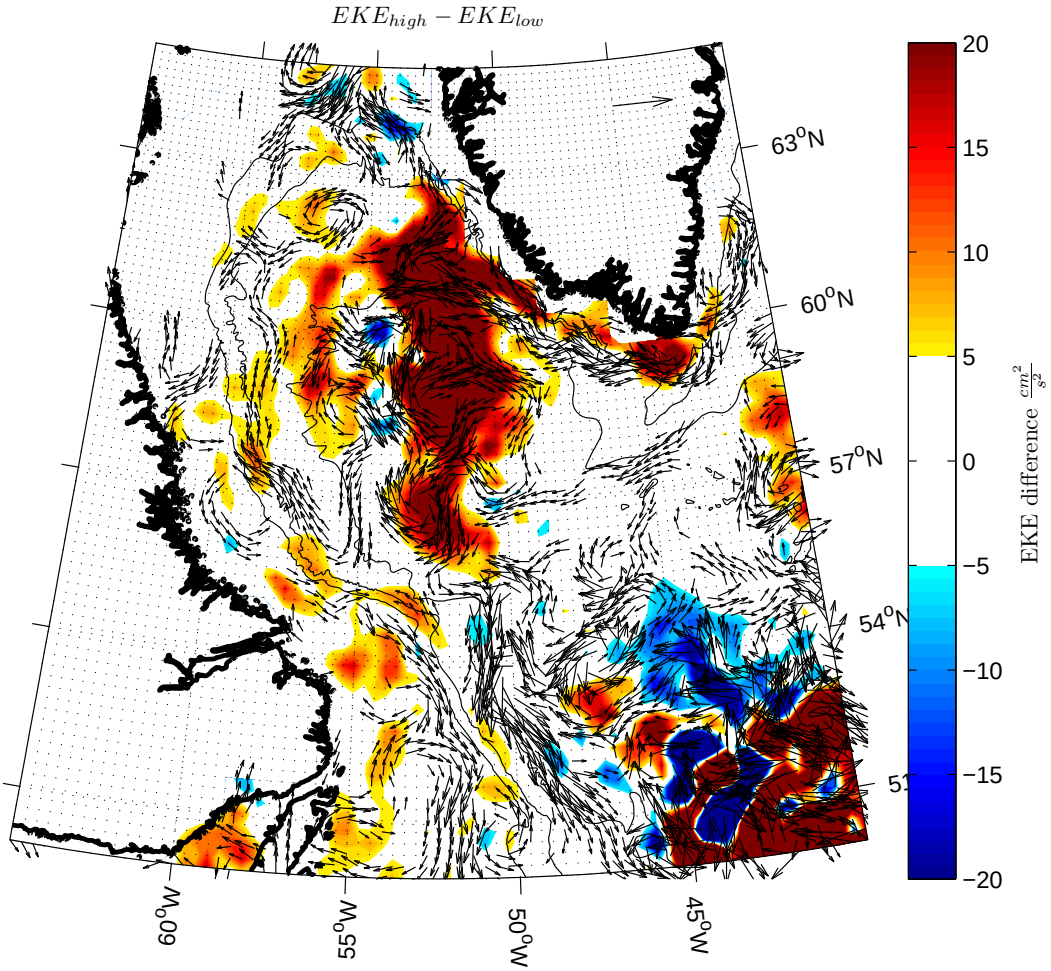

Figure 4.9: Difference in EKE pattern from phases of low EKE and high EKE. EKE difference is capped at $\pm 20\,\frac{cm^2}{s^2}$. Current vectors have an upper limit of $5\frac{cm}{s}$, shown inside Greenland as reference. Isobaths shown are 1000 m, 2000 m and 3000 m (black lines). See text for details.

the 95% confidence interval of $R = 0.40$ and $R = 0.27$. This would correspond to a velocity of $33\frac{cm}{s}$ to $41\frac{cm}{s}$, at an assumed track length of 1000 km. This is a low distance estimate as no EKE signal can be found in any here given analysis in the EKE minimum zone north of area E. A pathway around area E it would be more than 100 km longer. Resulting currents would be about $10\frac{cm}{s}$ faster, thus $43\frac{cm}{s}$ to $51\frac{cm}{s}$. This represents the core current speeds detected by surface drifters from CUNY ET AL. (2002) well.

What can be found in the differences of geostrophic surface velocity anomalies in figure 4.9?

Compared to low EKE times the West Greenland Boundary Current is accelerated by about $3\frac{cm}{s}$ in water depths deeper than 2000 m and decreased by $1.5\frac{cm}{s}$ on the shelf during high EKE phases. The boundary current circulation at the exit of the Labrador Sea is strengthened by $4 - 5\frac{cm}{s}$ seaward of the 3000 m isobath and by about $2.5\frac{cm}{s}$ on the shelf. Also there seems to be an anticyclonic circulation difference between phases in the Labrador Sea with rim speeds around $2\frac{cm}{s}$. The increased cyclonic circulation on the boundary currents in high phases could be a sampling bias due to the slowing of the North Atlantic subpolar gyre (HÄKKINEN AND RHINES, 2004). This is because the high EKE years used (1997-1999 and 2002-2003) are on average slightly earlier then the low EKE years (1995, 2000-2001 and 2006). It is questionable though if this on average half year difference does have an effect. Nevertheless it will be discussed what effect the observed intensification during high EKE phases or the decrease during low phases can evoke in the Labrador Sea.

For relevance of the found anomalies the strength of the anomalies compared to the mean flow needs to be analyzed. Further this will have to answer what the impact on the central Labrador Sea salinities is from these observations.

4.3 Changes in Pathways and Transport

What is the relevance of the analyzed EKE for the upper Labrador Sea freshwater so far? The theory of no or hardly any freshwater exchange between the central Labrador Sea and the adjacent Labrador boundary current is supported by the large persistent EKE minimum along the Labrador shelf. The boundary current system responsible for the freshwater in the Labrador Sea shows several geostrophic surface current anomalies, though their relevance compared to the mean flow needs to be examined.

Before going into detail of hydrographic differences the relevance of the velocity anomalies found is checked for relevance to associated transport changes, thus the strength of the mean flow. This will be done for all boundary currents. Figure 4.10 shows the above found current anomalies (colored background) above $1\frac{cm}{s}$. Anomalies below $1\frac{cm}{s}$ are omitted. For direction of these currents please refer to figure 4.9. These anomalies are overlayed with the mean geostrophic surface currents (black arrows).

The high anomalies on low mean flow in the central Labrador Sea are the result of only a few years of data used and no spatial averaging. They originate from the limited amount of eddies present in the years analyzed and would reduce to a large degree or vanish over an extended amount of sampling years. Unfortunately this EKE activity masks any possible small central Labrador Sea current changes. Looking at figure 4.10 the regions with high

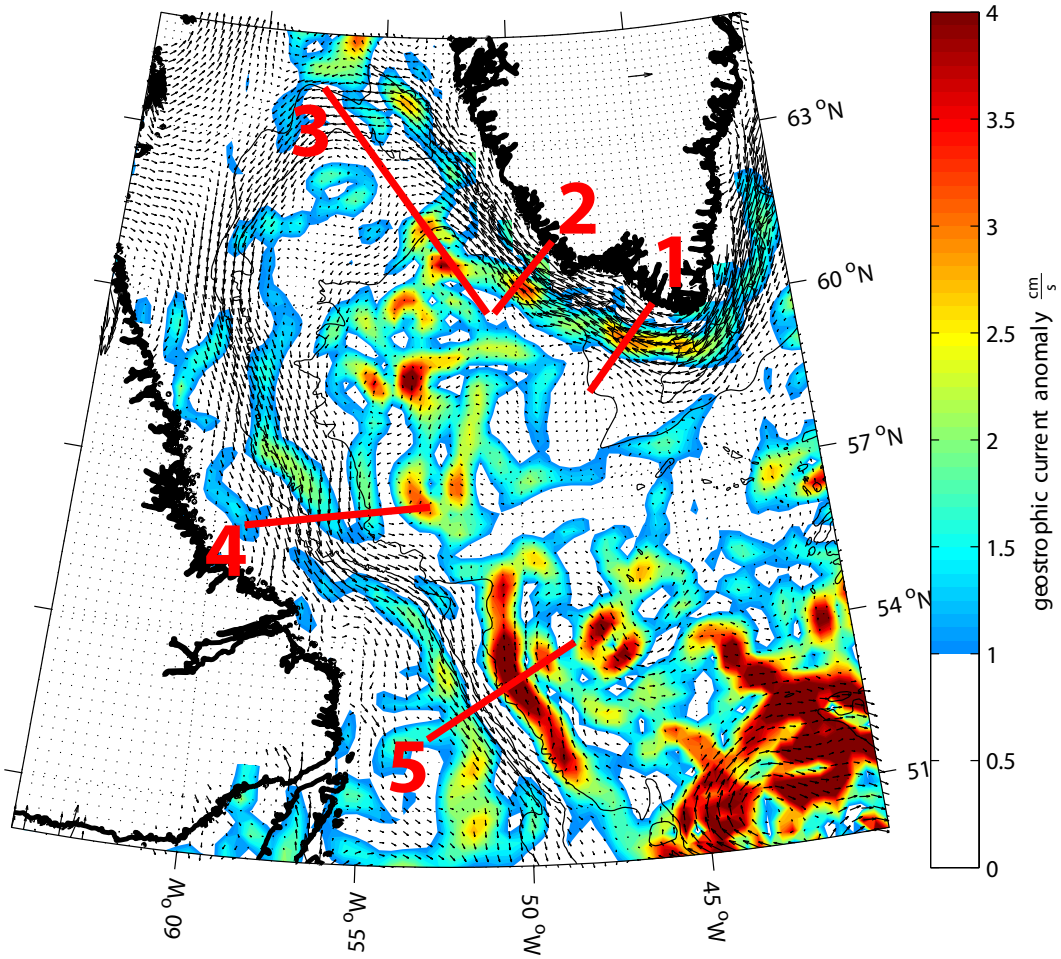

Figure 4.10: Mean geostrophic surface currents in the Labrador Sea as arrows, a reference arrow in Greenland indicates a speed of 30 $\frac{cm}{s}$. The color indicates the velocity of mean geostrophic current anomaly during EKE high phases compared to EKE low phases. Five sections that are analyzed in more detail are marked.

geostrophic current anomaly, that could play a role for the freshening of the Labrador Sea are the above mentioned enhanced velocities of the West Greenland Current and the decreased currents on the Labrador shelf break and at the exit of the Labrador Sea. These currents are analyzed counter-clockwise around the Labrador Sea at the sections drawn in red in figure 4.10. First for the shelf part, afterwards offshelf parts.

There are two sections in the West Greenland Current, because the intensification anomaly seems to shift from the 2000 m isobath after Cape Farewell to around 3000 m and even further offshelf north after the topographic feature that is made responsible for baroclinic instabilities causing the EKE hot spot. The first section is positioned well before the second and well behind Cape Desolation. Further downstream past Cape Desolation the topographic gradient of the shelf increases significantly. A significant influence of the EKE phases is expected here at the second West Greenland Current section from figure 4.9. This is because of the anomaly moving to greater depths into slower current regions as seen

in figure 4.9.

The third section is situated close to the bifurcation and is as only section exemplarily displayed in a Hoffmüller-diagram in figure 4.11. The northern and southern West Greenland Current branch surround the low velocity region as can be seen in figure 4.9 and in more detail as well in figure 4.11. This low current area extents from the 2400 m isobath to the 2500 m isobath, which are about 70 km apart on this section. The northern branch has its core on the shelf break with maximum velocities between the 1000 m and 1600 m isobath. The southern branch meanders strongly in the area between the 2600 m and 3000 m isobath, thus could be interpreted as an eddy pathway more than a constant current.

The fourth section is situated west of the central Labrador Sea area and the fifth at the exit of the Labrador Sea capturing the recirculation cell in that region.

4.3.1 on-shelf geostrophic surface velocities

The core speeds of geostrophic surface currents around the Labrador Sea are displayed for five sections in figure 4.12. Shown is the 30-day low pass filtered geostrophic surface velocity. Years of high EKE are displayed in red and years of low EKE in blue. Black crosses indicate the corresponding annually averages from December to October. The data prior to 1996 is not discussed, since the data quality is poor.

Obvious are higher boundary current core speeds in high EKE years compared to low EKE years in December/January, but this cannot be seen in the mean (black cross). The velocity peaks in winter that are timewise correlated to the seasonal maximum in the cycle of the EKE off Cape Desolation (Brandt et al., 2004) are more pronounced in high EKE phases. These peaks increase the 30 day low pass filtered velocities by a third, from typically

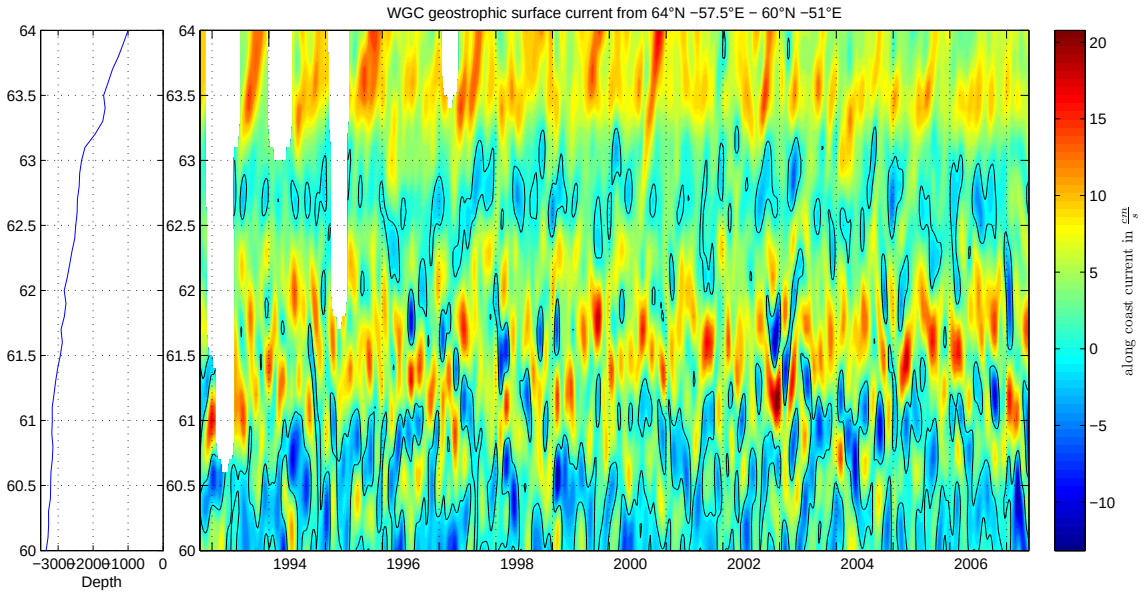

Figure 4.11: 30-day low pass filtered geostrophic surface velocity in the northern and southern West Greenland Current branch section (see figure 4.10). Along current orthogonal to section velocities are positive. The left panel shows the water depths.

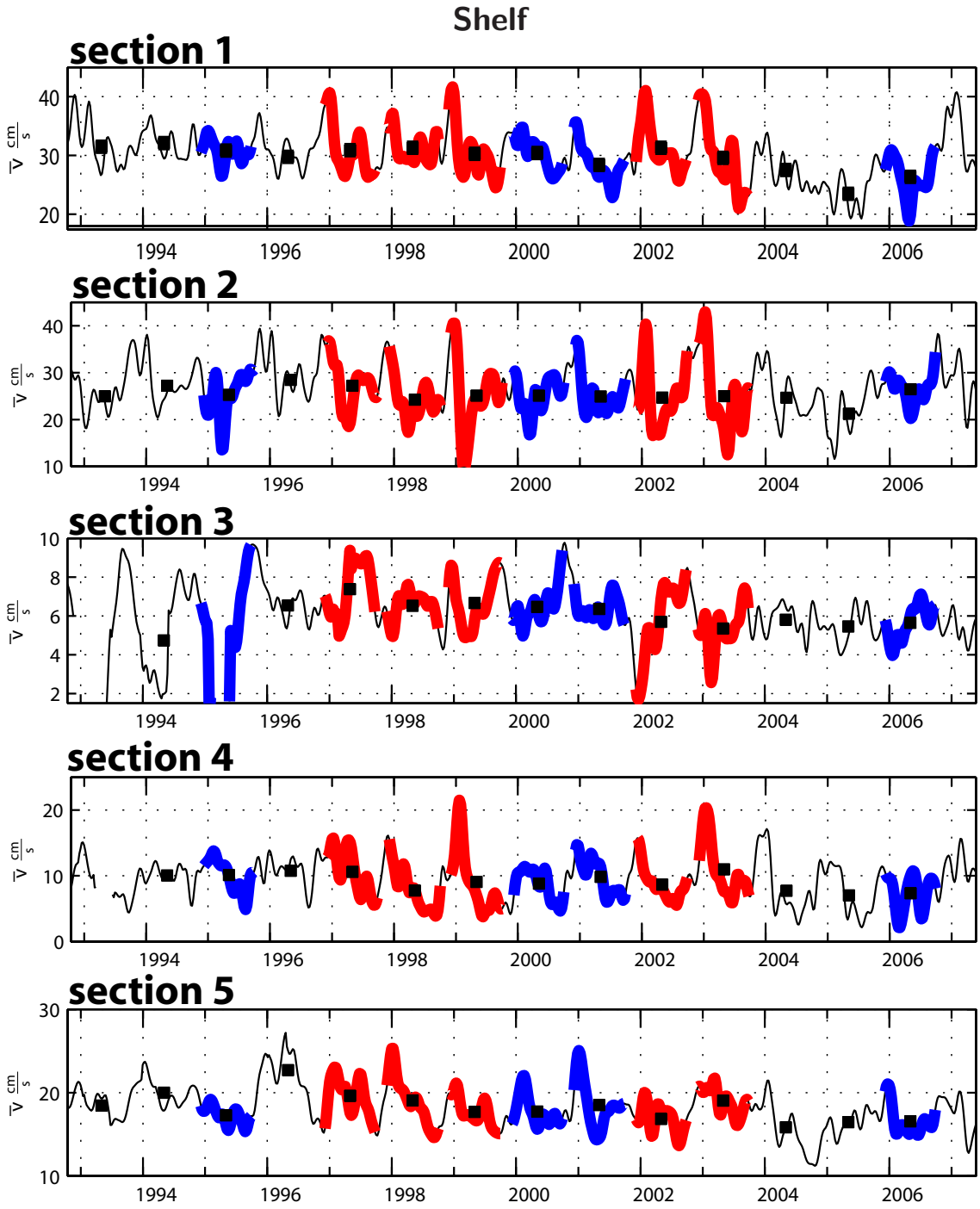

Figure 4.12: On-shelf 30-day low pass filtered geostrophic surface velocity for the five sections shown in figure 4.10. EKE high years are marked red, low EKE years blue. The crosses indicate the December to October mean velocity. Counterclockwise around the Labrador Sea and orthogonal to section current velocities are positive.

30 $\frac{cm}{s}$ to 40 $\frac{cm}{s}$ for the first section. This behavior can be seen around the Labrador Sea more or less at all sections, except section 3. No other differences between high and low EKE years stand out.

The second dominant signal in the core velocities is the long term current speed decrease. This is most likely related to the decline of the subpolar gyre circulation (HÄKKINEN AND RHINES, 2004), though a short period of strengthening can be observed again from 2006. At section 3 the mean velocity decreases from above 7 $\frac{cm}{s}$ to just above 5 $\frac{cm}{s}$, which corresponds to a decrease in geostrophic surface current velocities of about 30%.

4.3.2 offshelf geostrophic surface velocities

Analogous to figure 4.12, figure 4.13 shows the offshelf geostrophic current speeds for the five Labrador Sea sections.

As assumed in figure 4.10, the difference between the phases are opposite to that of the core for some low EKE years. In most high EKE years the velocities are slightly higher. This results in a $1-4\,\frac{cm}{s}$ higher average velocity and thus an increased Irminger Sea Water transport. 1999 and 2002 don't show this increase as strongly as expected, likely due to the following reasons. The year 1999 has a low average but the highest recorded velocities in that region for December and January. As the EKE propagates slowly through the Labrador Sea the switch from high to low in the boundary current might have occurred significantly earlier. 2002 was declared a high year for other reasons than high EKE in area B, as mentioned above, thus is not expected to be representative for a high EKE phase in the West Greenland Boundary Current. The decline of the subpolar gyre and its increase after summer 2006 can also be seen in these offshelf parts of the boundary current.

Concluding from figures 4.12 and 4.13, the difference between high and low EKE phases is detectable in the offshelf part of the boundary current at the first section. An offshelf increased Irminger Current or enhanced entrainment of Irminger Sea water is found during years of high EKE.

Further offshore the variations and seasonal cycles are reduced but still visible (lower panel of figure 4.13). The variability of EKE high and low years is of the same order of magnitude with a similar seasonal cycle. Maximum velocities are once again found in December/January but are decreasing more slowly in the course of the season. Increased mean velocities offshore at this second section are found during high EKE phases, similar to the first section, but with increased differences. High EKE phases have an up to 5 $\frac{cm}{s}$ faster geostrophic surface current. Comparing this with figure 4.10 downstream of this section, these offshelf anomalies move further offshore, closer to the area of highest EKE in the Labrador Sea.

At the second section through the West Greenland Current, just before the bifurcation, a distinct seasonal signal on the shelf is present, with maximum EKE in December and minimum around April (figure 4.12). The offshelf current is strengthened during EKE high phases. How do the boundary current velocities and its dependence to the EKE phases change after the bifurcation of the southern West Greenland Current branch, at section 3?

The southern West Greenland Current branch is meandering strongly (see also CUNY ET AL., 2002). The low pass filtered velocities are between 2 $\frac{cm}{s}$ and 8 $\frac{cm}{s}$. The mean

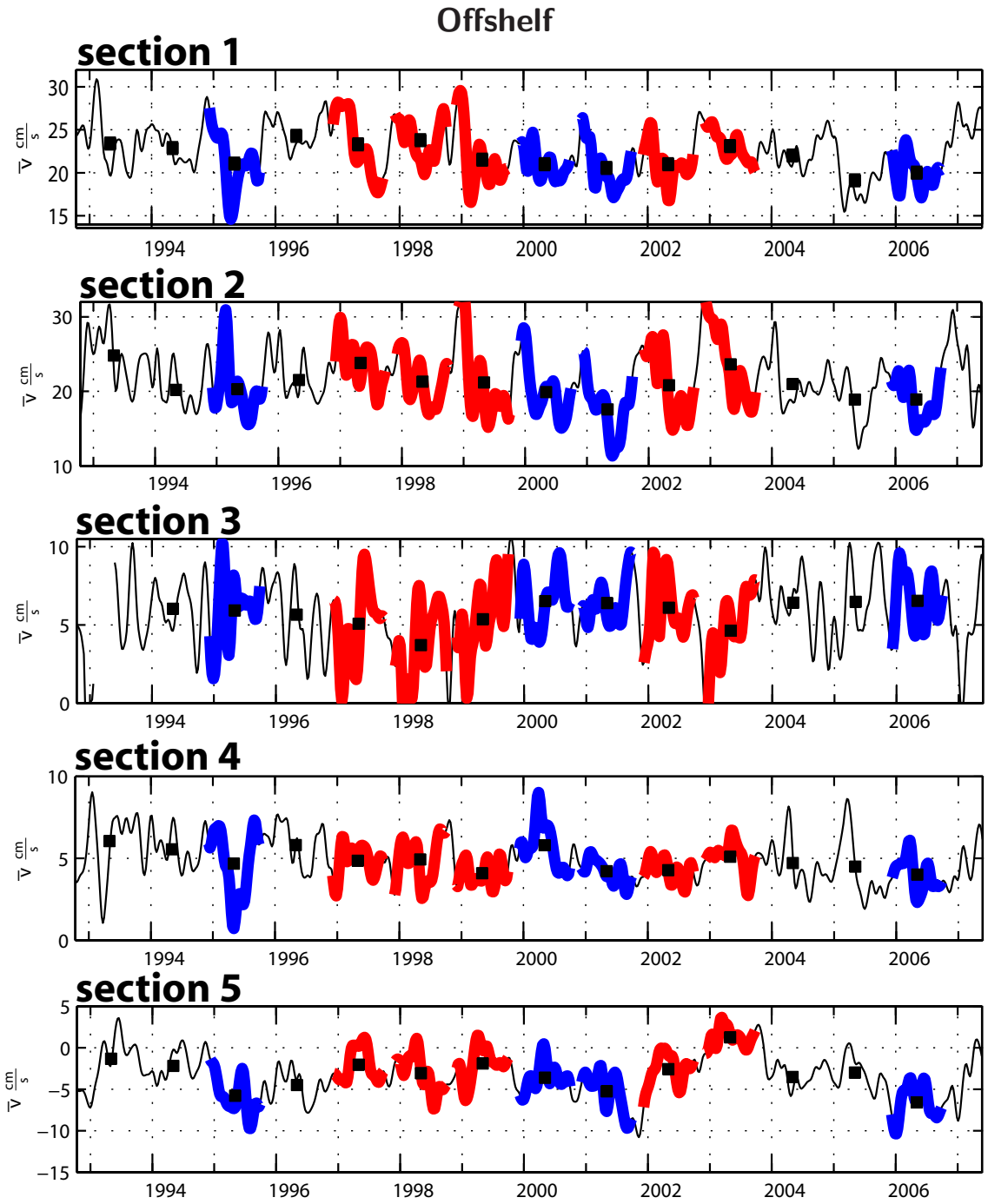

Figure 4.13: Offshelf 30-day low pass filtered geostrophic surface velocity for the five sections shown in figure 4.10. EKE high years are marked red, low EKE years blue. The crosses indicate the December to October mean velocity. Counterclockwise around the Labrador Sea and orthogonal to section current velocities are positive.

velocity during EKE low phases is higher than during low phases. This is surprisingly opposite to the previous two sections. The offshore part of the West Greenland Boundary Current was enhanced during high EKE phases. The southern branch of the West Greenland Current shows an inverted behavior to the offshelf part of the boundary current before the bifurcation (see figures 4.12 and 4.13). The velocity is reduced by up to a third during high EKE phases.

2002 again shows behavior atypical for a high EKE phase year, likely for the reason of selection mentioned above. Not classified years do not show a significant decrease compared to low EKE years. Current velocities during high EKE phases are more oscillating. This oscillation might be related to the pronounced EKE along the southern branch during high phases as seen in figure 4.7. Without commenting on the mechanism it can be summarized that high EKE in area B or F, thus a pronounced EKE maximum, reduces the southern West Greenland Current branch.

Can the surprising signal from the southern West Greenland Current branch be found in the Labrador Current? Figures 4.12 and 4.13 panel 4 show the geostrophic surface current structure at section 4 on the Labrador shelf

The offshore component illustrates the same long term trend, but not the intensified January impulses during high EKE phases. The year 2000 has higher velocities, but this is not apparent in any other EKE low years. The surprising increase of the southern West Greenland Current branch during low EKE phases cannot be found on the Labrador side anymore. No significant difference between high and low EKE phases is apparent in this section west of the convection site.

To complete the turn around the Labrador Sea hhhhh and hhhhh show the last section at the exit of the Labrador Sea. Most obvious is the strong offshore recirculation cell at this section. From figure 4.10 the strongest anomaly of currents on very low mean current speeds can be found offshore of the $3000\,m$ isobath, thus in the transition between boundary current and recirculation cell. The anomalies of up to $4.5\frac{cm}{s}$ are in the same order of magnitude as the mean speed. Comparing this with the results from high and low EKE phases in figures 4.7 and 4.8, leads to the suggestion that the geostrophic surface current part of the recirculation cell is strongly influenced by high and low EKE phases. Figure shows the transition between boundary current and recirculation very close to the 3000 m isobath. Both currents have about the same width of around $120 - 150\,km$. The mean geostrophic surface velocity of the boundary current is $18.2\frac{cm}{s}$ and the velocity of the recirculation cell is a factor three less, about $-5.8\frac{cm}{s}$. There is no correlation between those two in the geostrophic surface currents ($R = -0.06$ with 95% confidence interval $R_{low} = -0.13$, $R_{up} = 0.06$). Fischer et al. (2004) describe this section in detail. They determined absolute speeds from 51 lADCP profiles measured during 1996-2001 on this section as well as the geostrophic currents from mooring and float data. They found a northward flowing recirculation cell with speeds between $4 - 10\,\frac{cm}{s}$ between the $3200\,m$ and $3800\,m$ isobath. Mooring K10 in the middle of this recirculation cell shows a mean northward speed of $2.2\,\frac{cm}{s}$ with large standard deviation of $8.76\,\frac{cm}{s}$ in the upper most current meter instrument in 200 m depths. Since these mooring measurements took place between 1997 and 1999, they represent mainly the high EKE phase. The mean geostrophic speeds found here at the surface are higher, but mirror the findings of Fischer et al. (2004).

The transition between the boundary current and the recirculation cell shows increased

absolute velocities in all low EKE years, leading to an enhanced recirculation cell close to the shelf break. The consequences of this remain unclear.

Summarizing the main SSH-derived geostrophic surface current differences, two features have to be pointed out for the high EKE phase compared to the low phase with possible effects on the hydrography of the central Labrador Sea. The offshelf West Greenland Current is strengthened from the beginning up to the EKE hot spot, thus an increased import of salty Irminger Sea Waters during EKE high years is expected (compare figure 3.10.

This intensification reverses behind the EKE hot spot leading to the second notable feature, the significant reduction of the mean flow in the southern West Greenland Current branch during EKE high phases.

4.4 Hydrographic differences

Do these described geostrophic velocity changes have any influence on the central Labrador Sea hydrography? Can a further influence of increased EKE traveling into the central Labrador Sea during EKE high years be found?

In the following it is tried to relate the found anomalies accompanied with high or low EKE phases to hydrographic differences observed during those years. This can help to understand processes like the unexplained first freshening in central Labrador Sea seasonal cycle, or its absence in several years better.

Currently there is no historical proxy that can be used for estimating the EKE in the Labrador Sea. Thus only four years of low and five years of high EKE are confirmed from satellite data. As there is not enough hydrographic data in 1995, a hydrographic analysis of low EKE will have to be done with only three years of data (2000, 2001 and 2006). For the high EKE phase the above used years of 1997-1999 and 2002-2003 could be used and lead to a sufficient data coverage. The central Labrador Sea data set available for 1999 (compare 2.3.4) is strongly biased due to a non dissipated long lived boundary current eddy in area D in 1999, as seen in the EKE intensity in figure 4.3 and described in detail by Lilly et al. (2003). Since the data set for 1999 consists mainly of mooring data, the hydrographic data more strongly represents the water properties of the boundary current eddy than the surrounding central Labrador Sea. For these reasons 1999 was not used in the hydrographic analysis.

Unfortunately this reduces the hydrographic data set to three low EKE years and four high EKE years.

As described in section 3.2.1 and figure 3.5, the strength or absence of previous winter convection as well as interannual variability has a large influence on the following summer salinities (Lab-Sea-Group, 1998). Therefore in order to compare years with different starting conditions only the monthly salinity change is used. Figures 4.14 and 4.15 show the salinity and temperature development from January to October for high and low EKE phases. All left panels show the low EKE phase, the right panels the high EKE phase. The upper panels of each figure are the changes for the top 120 m of the water column, the lower panels describe the changes in the range between 200 m and 300 m. Shown is the difference in salinity (temperature respectively) from month to month. The colored dots represent the data from the years used, the yellow bars are the monthly mean of the years and the

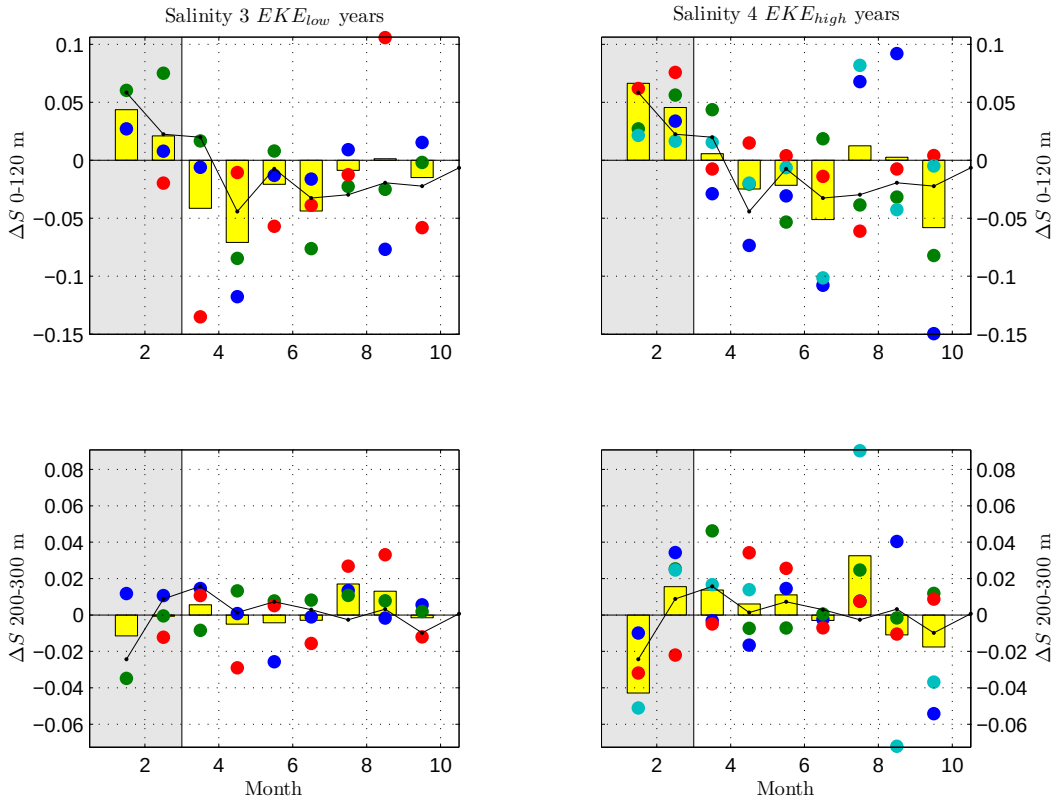

Figure 4.14: Monthly salinity change from January-February to September-October. Left panels show low EKE years, right panels high EKE years. Upper panels demonstrate the mean from 0-120 m, lower panels from 200-300 m. The black line is the overall monthly mean salinity change. The colored dots represent the different years consistent within the panel, unequal for high and low EKE panels.

black lines indicate the climatological mean from section 3.2.1. A climatological cycle is not shown for the temperature, as it is even more variable to changes in the atmospheric forcing.

The changes from January to March are shaded in gray and will not be discussed here. Changes in salinity and temperature in January to March depend strongly on previous summer surface freshwater, underlying salinity of upper Labrador Sea water and convection depths resulting especially from the strength and duration of atmospheric forcing (in particular radiation, temperature and wind). The March-April values (first non shaded) have to be treated with caution, as late convection can still happen, but surface salinification is mostly stopped. For a better understanding of the following description it has to be kept in mind that, when looking at monthly changes, an overestimate in one month leads to an underestimate in the next month, without addressing the reason of the initial overestimate.

Salinity changes in the top 120 m during low EKE phases (figure 4.14 upper left panel) illustrate a strong early freshening signal between March and May. When looking at individual years, it is apparent that this freshening is only a short pulse. All 3 years show this

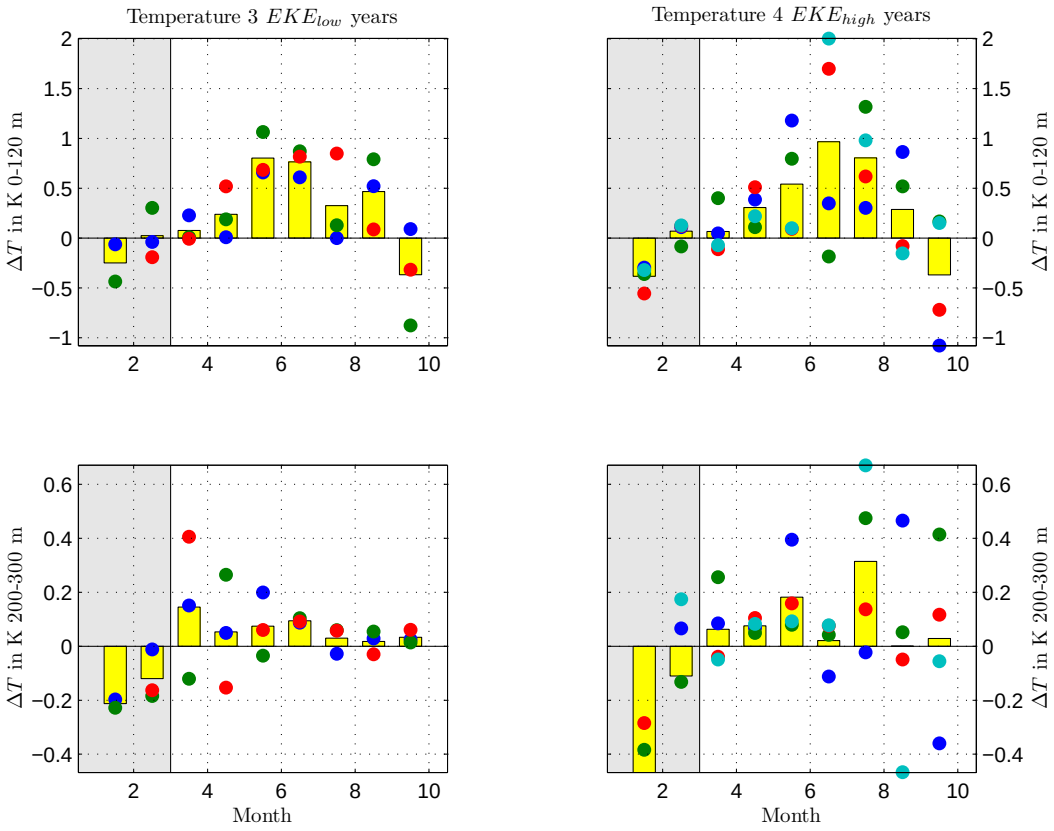

Figure 4.15: Monthly temperature change from January-February to September-October. Left panels show low EKE years, right panels high EKE years. Upper panels demonstrate the mean from 0-120 m, lower panels from 200-300 m. The colored dots represent the different years consistent within the panel, unequal for high and low EKE panels.

freshening, 2000 (blue) and 2001 (green) from April to May and 2006 (red) already earlier from March to April. After the first freshening signal the next month has low change (red - 2006 is again one month earlier), followed by a moderate and bit lower than average freshening for the rest of the season. The mean cycle of the three low EKE years (yellow bars) fits surprisingly well to the climatology (black curve), but with a much more pronounced first freshening pulse and a slightly weaker second freshening.

The salinity mean cycle during EKE high phases (same figure upper right panel, yellow bars) does not show the first short freshening. Only 1997 (blue dots) has a stronger than average first impulse. The phase of low or no further freshening from July to September can be due to an overestimate in the preceding and following change. This is likely as the individual monthly changes (dots) show a large variance.

For the top 120 m it can be said that, the first freshening as seen in the climatology is significantly strengthened in the mean for low EKE years and there even more pronounced in every single year. It is absent or low during the high EKE years analyzed. There is only a low, probably not significant, difference in second freshening between high and low EKE years. These conclusions are drawn from a very small data set of 3 and 4 years, but all individual years do confirm these general findings.

In the following I try to extract the influence of dissolving eddies on these hydrographic changes. For this it is assumed that dissipating eddies provide the same type and amount of water into the 200 m to 300 m layer as to the top (Lilly et al., 2003). This layer is used because it has low variability compared to the surface and is well under the surface mixed layer from March to October. This is only a crude estimate but sufficient for the analysis performed below. With the above mentioned assumption the difference between the layers show the difference between high and low EKE years with the influence of the dissipating eddies removed.

Variance of salinity change in the 200 m to 300 m layer is low during EKE low phases (figure 4.14 lower left panel), the individual years spread around the climatology for the time analyzed. There is a minor salinification between July and September, present in all years. It cannot be determined what the origin of this salinification is nor if this is significant or not. Since it shows up with a similar structure during EKE high phase, as discussed below, it is not further analyzed here.

During EKE high phase the variability is much stronger in this depth interval compared to the low phase. Salinification is stronger than in EKE low years, but on the same order of magnitude as the climatological mean for most months. The July/August change is higher than expected mostly due to the large change in 2002, thus not significant for the high EKE phase.

If more years of EKE data confirm that high EKE phases induce high variability in a certain layer at the area of Ocean Weather Ship Bravo, these variabilities between 200 m and 300 m could be used as proxy for high or low EKE. Thus many more years of historic pre-satellite hydrographic data could be included in the here performed crude analysis. An even more reliable conclusion could be drawn then.

Before discussing the detail between upper and lower layer analyzed in detail figure 4.15 shows a similar analysis for temperature. As temperature is strongly influenced by the atmospheric forcing, it is not surprising that no major differences can be found between the EKE phases for the upper water layer. The lower layer shows a constant warming with an increased warming during EKE high phases. The increased warming during high EKE phases is accompanied by higher variability for all years except 2002 (red right panels), as expected from the higher variability in salinity for this layer.

To illustrate and discuss the difference of the development of the freshening cycle in the Labrador Sea between high and low EKE phases better, figure 4.16 combines low and high EKE phases in each panel. The upper panel of figure 4.16 shows the top 120 m cycles of salinity change for low (blue) and high (red) phases as well as the difference of those (yellow). The changes prior to March are ignored because of the above mentioned reasons. Most changes during the second freshening balance each other except in the end of the freshening season. The reason for this is likely the already fresher Labrador Sea in low EKE phases. [2] Thus in the top layer the only unexplained significant difference is, as already

[2] After a reasonable amount of freshwater is supplied, the surface layer deepens and extends 120 m. This might be earlier the case for low EKE phases. As a result further freshwater supply would only lower the surface salinity to a small degree because some of the freshwater is lost through the 120 m corresponding isobar. Another reason might be that October is already under the influence of strong atmospheric forcing,

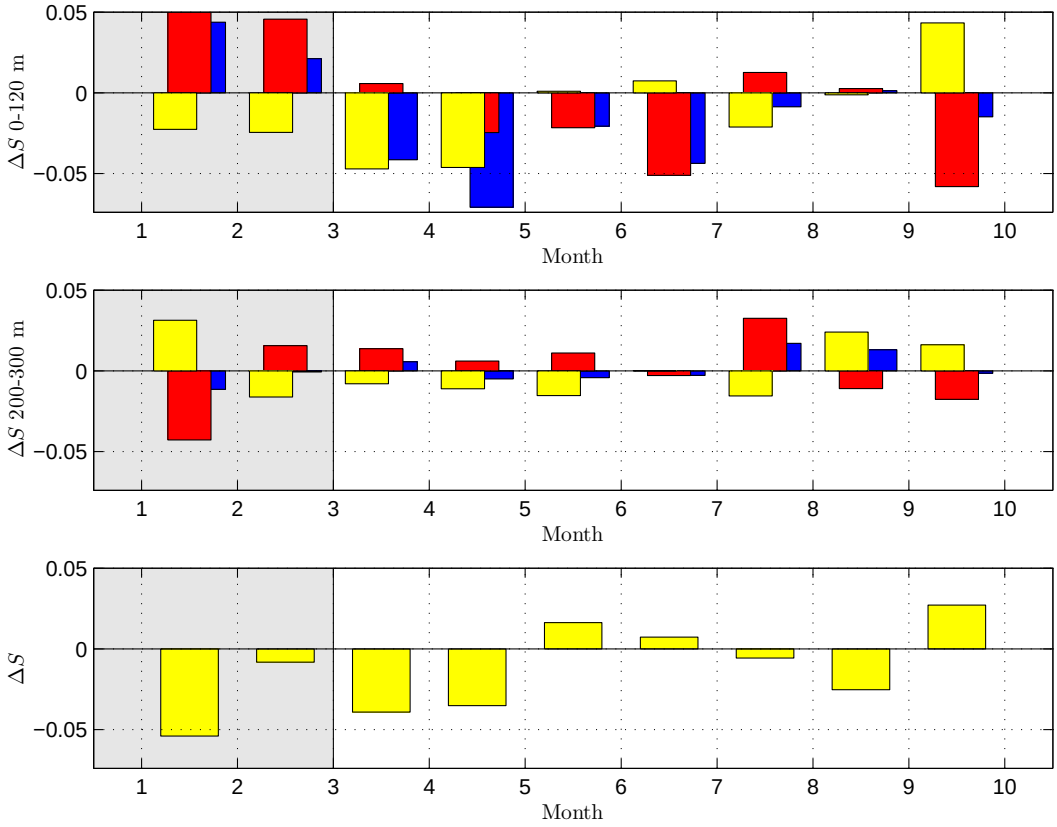

Figure 4.16: Monthly salinity change from January-February to September-October. Red indicates low EKE phases, blue high and yellow the difference. The upper panel is the layer 0-120 m, middle panel from 200-300 m. The lower panel is the difference between the layers,thus showing the salinity changes in EKE low years compared to high years with the removed effect of dissipating eddies.

suggested by figures 4.14 and 4.15, the first freshening impulse, on the order of 0.09 psu salinity change.

For the second layer analyzed the same difference is plotted in figure 4.16, middle panel. The first three months from March to June show a constant but low freshening on the order of 0.035 psu. This is the difference that is absent in the seasonal cycle during high EKE phases compared to low. The later part of the season has some higher fluctuations with an average salinification of 0.025 psu.

The crude estimate that the changes in this depth interval originate solely in dissipating eddies north of the convection side, with otherwise constant environmental influences is made. Together with the above mentioned estimate, that dissipating eddies provide the same water properties to this depth as to the surface, allows me to subtract these differences from the surface layer. This determines the changes in the central Labrador Sea that are not induced by a salt flux due to dissipating eddies, but must have a different origin. Part of this assumption is supported by the much lower variation in salinity and tempera-

capable of changing water properties in the surface layer (by inducing turbulence thus mixing up of underlying saltier waters or lateral advection by Ekman drift), which is reflected indirectly by the higher variability in the change from September to October (all panels of figures 4.14, 4.15 and 4.16).

ture in this depth level during EKE low phases compared to high phases as discussed above.

This described difference is plotted in the lower panel in figure 4.16. The 200 m to 300 m layer changes subtracted from the top layer results in the lower panel (yellow bars all panels) and thus is showing the salinity change difference between low EKE years and high EKE years, without the influence of dissipating eddies.

Doubts about subtracting salt differences of different reference salinities can be dispelled, because the error of using salinity change for the difference compared to absolute freshwater amount is in the order of S_{ref1}/S_{ref2}, thus around 1% for a difference between the surface and the lower layer of 0.2 psu and even lower in the beginning of the freshening season. The following equation can be used as a proof for these small errors:

$$\Delta v_{fw} = \frac{\Delta S}{S_{ref}} v_{ref} \tag{4.4}$$

where Δv_{fw} is the difference of freshwater evoked by the observed change in salinity ΔS, with S_{ref} the salinity of the water amount v_{ref}. Therefore the error in Δv_{fw} for different S_{ref} is,

$$\frac{\Delta v_{fw1}}{\Delta v_{fw2}} = \frac{S_{ref2}}{S_{ref1}}. \tag{4.5}$$

This error is well below the variability from only a few years of data and can be disregarded.

The so far unexplained lower salinities during low EKE years compared to high is between 0.06 and 0.075 psu using the time March to June or March to May (lower panel figure 4.16). The changes from August to October balance each other out.

In summary it can be said that significant hydrographic changes in the upper water layers of the central Labrador Sea can be found even using only a few years of data. Phases of high EKE have only a low first freshening pulse. This absent early freshwater pulse during EKE high phase is, with the above made assumptions, not lost to increased salt flux into the central Labrador Sea and must have a different advective reason.

These findings do surprise, since one could assume that enhanced EKE close to the boundary currents mixes more fresh shelf waters into the central Labrador Sea. The opposite is the case, lower EKE is associated with a higher freshwater flux into the Labrador Sea.

4.5 Pathway hypothesis and Conclusion

After summarizing the found differences in hydrography and geostrophic surface currents between high and low EKE phases it is tried to give a hypothesis propagation scheme for the seasonal Labrador Sea salinity cycle during high and low EKE years.

By using these very limited seven years of hydrographic data the following conclusions can be drawn. Enhanced EKE seems to have a stronger influence on central Labrador Sea hydrography than just transporting salt within the eddy field south and dissipating. The intense early freshening between March and May in the central Labrador Sea is inversely correlated with the EKE intensity at the eddy hot spot off Cape Desolation.

This highly variable early freshening pulse was first described by SCHMIDT (2003) and analyzed by SCHMIDT AND SEND (2007) and in detail above and in chapter 3.

The anti-correlation of this freshening to EKE intensity might be the reason why STRANEO (2006) did not find two freshwater events in her later data set. The two freshenings as described in chapter 3 and SCHMIDT AND SEND (2007), are not found by STRANEO (2006), as her later data set mainly covers the high EKE phase 1997-1999. STRANEO (2006) is addressing a lack of second impulse, the reason here might be that the smaller first pulse does not show a flux minimum before the second flux starts (compare figure 4.14 upper right panel and 4.16 upper panel).

It was found that geostrophic surface current changes notably at two places between high and low EKE phases in the Labrador Sea.

During EKE high years compared to EKE low years the offshelf West Greenland Current is strengthened from the beginning up to the Labrador Sea EKE maximum, thus an increased import of salty Irminger Sea Waters during EKE high years is expected (compare figure 3.10).

The opposite is found for the southern West Greenland Current branch. The mean speeds in this southern bifurcation are reduced significantly during high EKE years (compare panel 3 figure 4.13).

Combining the known origins (e.g. SCHMIDT AND SEND, 2007) and new findings discussed above, a hypothesis for likely pathways for high and low EKE phases can be developed.

Figures 4.17 and 4.18 sketch the conceptual differences between low and high EKE phases. Freshwater pathways are plotted in blue, EKE and eddy propagations in red. During high EKE phases, there is a decrease of the mean current speed of the southern West Greenland Current branch. Thus this southern West Greenland Current branch is developed during low EKE phases and transports fresh Greenland boundary current waters (compare figure 3.10). This freshwater is transported into the northern Labrador Sea and continuing on to the central Labrador Sea, and passing through the area of low mean EKE region very close to the site of maximal convection. This is the first freshening pulse.

Why is this the first freshening pulse? Several observations support this view. The seasonal cycle of the north western Labrador Sea demonstrates a much stronger first freshening than the central Labrador Sea (section 3.2.2). Thus it is likely that the freshwater impulse either travels via this area, or the source of the first pulse supplies more to the northern Labrador Sea than the central Labrador Sea. Both make the southern West Greenland Current branch the only plausible source.

How does this change during the high EKE phase? Figure 4.17 exemplifies the sketch for high EKE phases. The partly imported and generated EKE builds up at the so called eddy hot spot with a maximum in December/January. Thus lowering by a (in this thesis) unaddressed mechanism the mean geostrophic velocities of the southern West Greenland Current branch. This is especially pronounced during December/January (compare figures 4.12 and 4.13). With the mean observed advection speed of roughly 5 $\frac{cm}{s}$ a pulse traveling along the southern bifurcation would need around 4 months into the central Labrador Sea. Thus if the southern West Greenland Current is suppressed or significantly reduced in December and January a significant freshening in the Labrador Sea via this pathway would not take place.

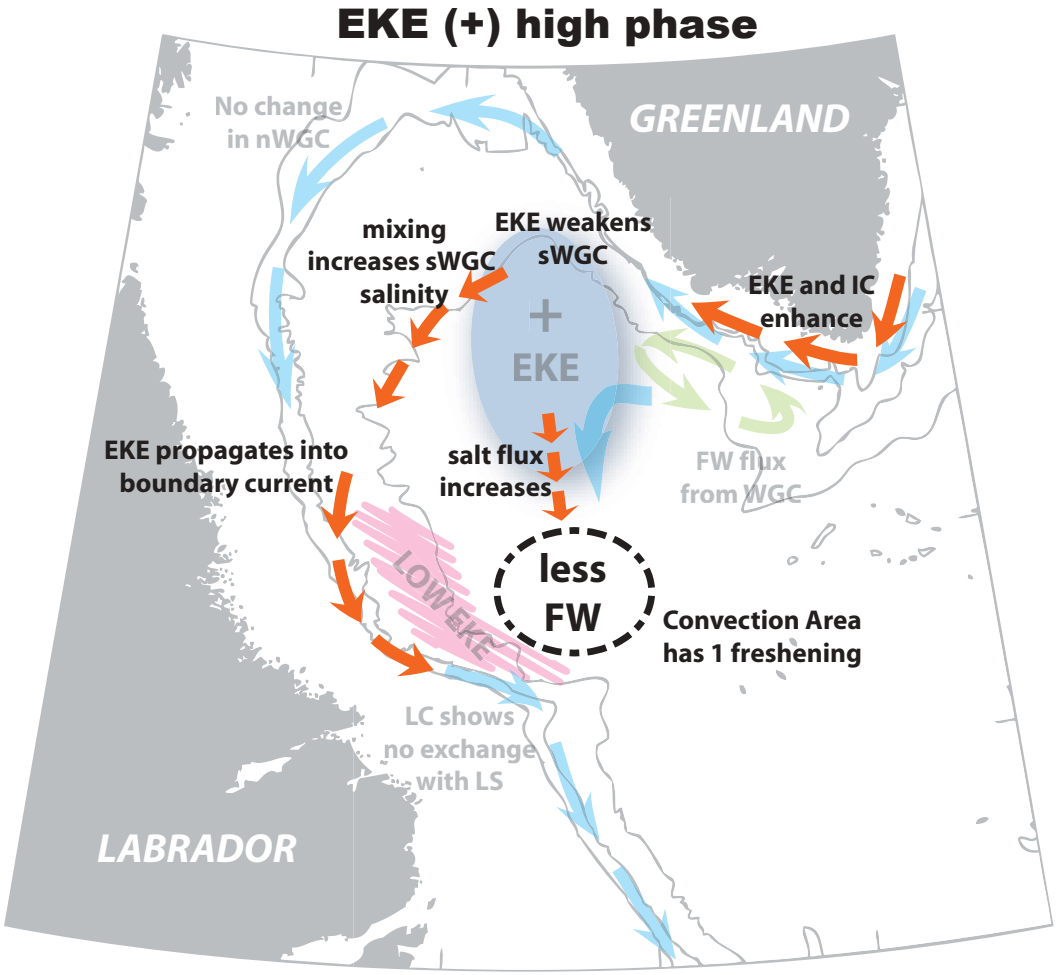

Figure 4.17: Schematic pathways during EKE (+) high phase. Blue arrows indicate freshwater pathways, red arrows EKE pathways. Green arrows indicate an interchange between boundary current and interior.

Furthermore some EKE travels along the path of the southern branch (see figure 4.7) and is likely decreasing the salinities in the remaining southern West Greenland Current branch further by mixing with warm and salty Irminger current waters from the eddy cores. Therefore the southern West Greenland Current branch cannot supply an early freshwater impulse into the central Labrador Sea during years of high EKE.

This view leads to the following consequences: The southern West Greenland Current freshwater supply is lowered or stopped if the EKE intensifies over a certain level. The seasonal maximum in EKE in December would trigger the existence of the first freshening pulse of the central Labrador Sea. An early seasonal maximum at the EKE hot spot would decrease the freshwater supply to the central Labrador Sea during active convection, thus increasing the chance and intensity of deep convection, assuming adequate atmospheric forcing. A late seasonal EKE maximum is likely not to have major influence on the first freshening as an EKE maximum in December has.

Furthermore enhanced EKE transports more salt and heat along the West Greenland Current and into the central Labrador Sea, but arriving in the convection area not

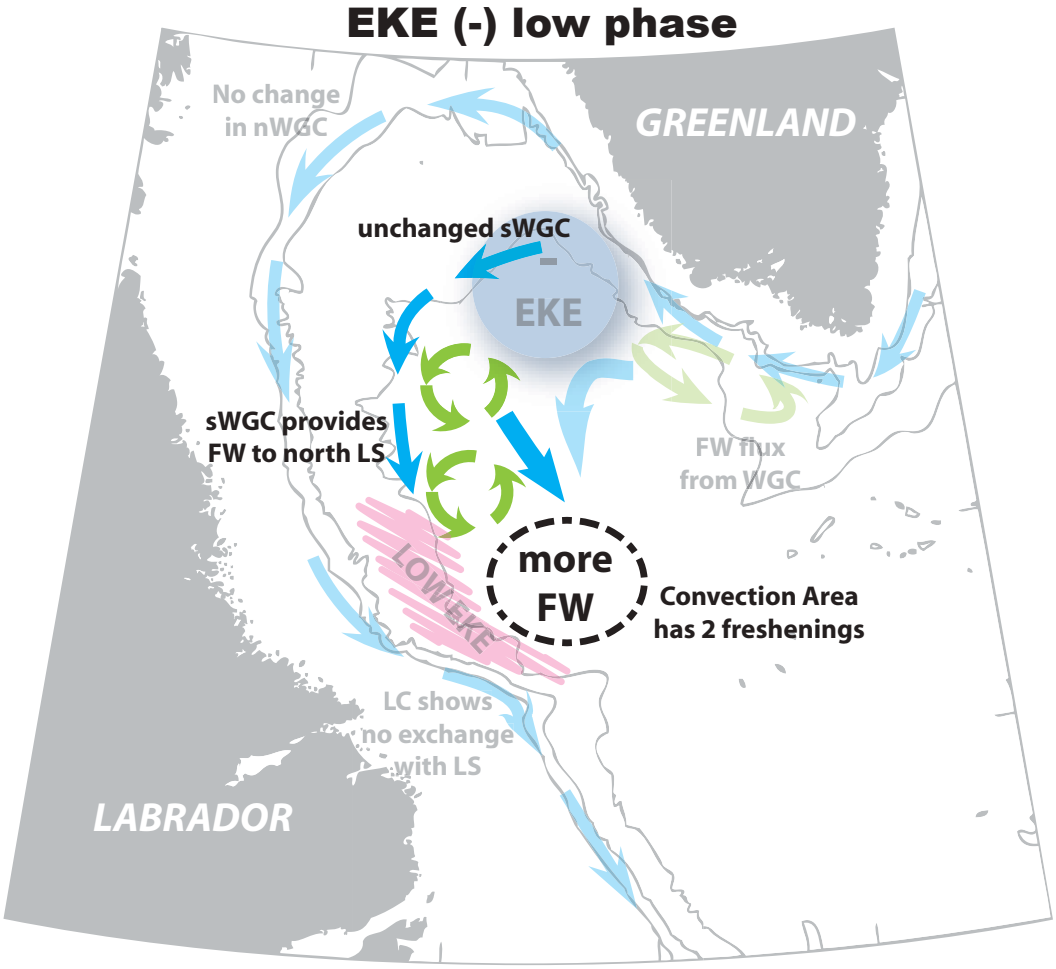

Figure 4.18: Schematic pathways during EKE (-) low phase. Blue arrows indicate freshwater pathways, red arrows EKE pathways. Green arrows indicate an interchange between boundary current and interior.

prior to May and thus supports restratification (e.g. Lilly et al., 2003). Due to the timing it can not be responsible for the end of convection under prevailing heat loss in April.

Whether the observed variation of the recirculation cell at the exit of the Labrador Sea plays a further role for the upper Labrador Sea freshwater layer could not be determined.

The hypothesis of freshwater pathways of high and low EKE phases are coherent with the observations available. It explains the reason of the first freshening as well as its absence and different strength in some years. As the Labrador Current shows no significant variation during high or low EKE phases it is unlikely to be the source of the large hydrographic differences between those phases in the central Labrador Sea. The only remaining uncertainty is the hydrographic basis of three EKE low years and four EKE high years.

These new found understandings of Labrador Sea freshwater should be reviewed in a model that can represent a seasonal EKE maximum and the southern West Greenland Current branch.

This view of the central Labrador Sea first freshening impulse would explain some unaddressed questions to date about the Labrador Sea and has further consequences. The following consequences need to be confirmed by model analysis or further years of EKE observations.

The reason for the rapid restoration of the surface fresh layer after convection could be explained with surface advection of freshwater along the southern West Greenland Current branch into the central Labrador Sea.

It could also explain why there is no observed deep convection in the northwestern Labrador Sea as one would expect from regional heat loss. Freshwater flux from the West Greenland boundary current is found in these regions between February to March, preventing deep convection and ventilation of deep water to occur (compare figure 3.10).

These results lead to the fact that modeling convection in the Labrador Sea will overestimate convection depths if the seasonal EKE maximum and the southern West Greenland Current branch are not represented, since it seems that the freshwater transported along the southern West Greenland Current branch is necessary for the early restratification and the end of convection.

Furthermore this would be an explanation that could try to answer why surface waters in the deep convection area have lower salinities than the surrounding waters (e.g. Pickart et al., 2002). At the convection site salty water from below is mixed up in correspondence with convection depths. Surrounding waters with no deep convection but similar late summer stratification have higher salinities. This so far unanswered and often ignored paradox could be explained by a freshwater supply to the convection site that is being mixed down in the water column on the way and at the convection site. For high EKE phase a saltier or similar to the surrounding convection site would be expected with this hypothesis. Pickart et al. (2002) collected their data in winter 1997, thus it would contradict this hypothesis at first glance, because 1997 was a high EKE year. Looking at figure 4.3 area B it can be observed that the seasonal EKE maximum at the eddy hot spot was late in January 1997 and EKE was low at the end of 1996, thus for the above explained hypothesis the current would not have been decreased until some freshwater passed.

The hypothesis presented here is consistent with many observations. Further hydrographic data and model analysis will have to show if this mechanism is indeed correct and can be used in the future for improved forecasting and modeling of Labrador Sea convection.

Apart from the pathway hypothesis it was found that phases of high EKE correlate with an increased import of Irminger Sea water and a reduced southern West Greenland Current branch. Low EKE years show significant higher central Labrador Sea salinities and two freshening pulses. The earlier pulse is absent in high EKE years. High EKE at the bifurcation of the southern West Greenland Current branch, close to the boundary currents and in the boundary currents is not leading to lower central Labrador Sea salinities.

Chapter 5

Decadal variability

Decadal salinity fluctuations in the Labrador Sea have been discussed by various authors before (e.g. Dickson et al., 1988; Houghton and Visbeck, 2002). What is different that promises new results in redoing this analysis?

It is believed that more favorable setting of the regions from chapter 3 will reveal different results. To my knowledge no prior analysis examines an offshelf part of the boundary currents, as all data offshelf is used for central Labrador Sea calculations. Figure 3.1 and the climatological salinity cycles (figure 3.10) suggest that a separation into offshelf and on shelf is necessary. Another major difference to other studies is the limitation to the top 100 m in this study compared for instance to the 300 m used by Houghton and Visbeck (2002). Using the top 300 m averages for some regions over different water masses (compare figure 3.2). A better determination of the origin of long term changes with a better layout is the motivation to repeat the analysis. Especially since the Labrador Sea is known to experience prolonged decadal anomalies known as Great Salinity Anomalies (GSAs).

In the following section the method used will be introduced. Afterwards, each region will be presented and briefly discussed. There will then follow a general discussion, correlation analysis and comparison of the results.

5.1 Method

The area layout was adopted from chapter 3 and is discussed there in detail. The same reasons leading to the layout for these areas for the seasonal cycle can be applied for the decadal analysis performed here. The method applied to derive the long term variabilities in salinity was the same for all areas. Some areas proved to have an insufficient amount of monthly observations to acquire meaningful long term variations. The procedure is illustrated as a workflow diagram in figure 5.1 similar to chapter 3 and is described briefly again in the following.

A first guess salinity cycle was subtracted from the data. The gaps in the data were then filled with a shape preserving cubic interpolation. A two year running mean was used to eliminate short term fluctuations and interannual variability. The problem here is that individual observations with no nearby data have to be seen as accurate, without addressing the possible monthly fluctuations that are high in some areas. This running mean was used

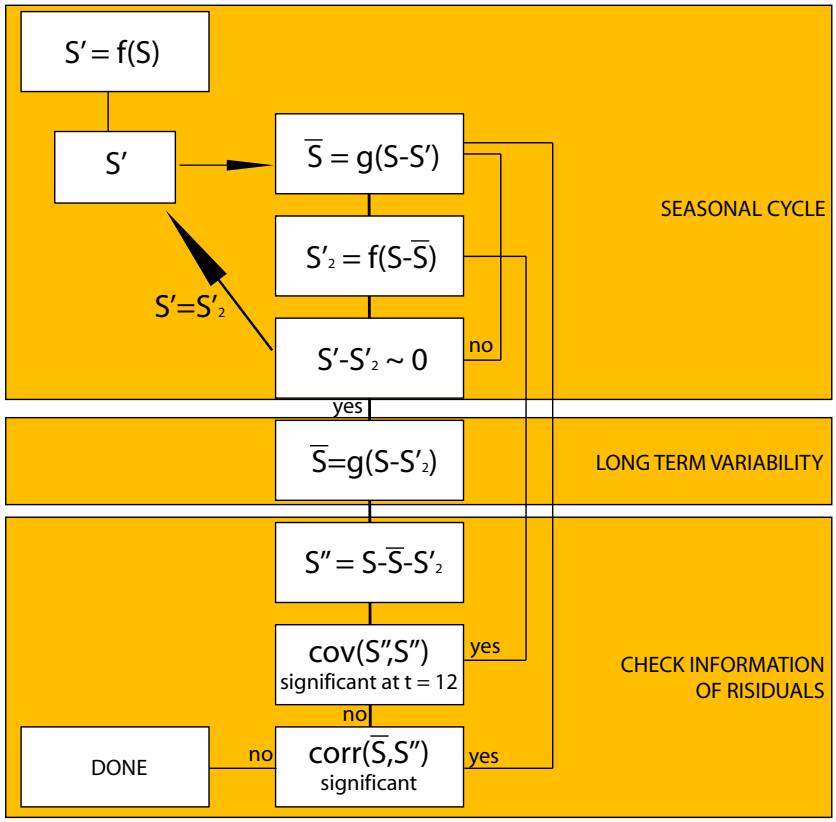

Figure 5.1: Workflow of constructing the seasonal cycle and the long term variability. S is the monthly salinity data set, S' and S'_2 the seasonal cycle, $\overline{S}$ the long term trend and S'' the short term fluctuations and variations from the mean seasonal cycle. $f(x)$ is the procedure to derive a seasonal cycle from a data set x and $g(x)$ the procedure for interpolating the gaps and acquiring a long term variability.

for a first guess of the longer than seasonable variability and removed from the original data set. Again the seasonal cycle was constructed using this new data set. If the new cycle differed significantly from the first one it was used in the following. If the differences were marginal the first cycle was used, since removing a term trend can cause minor unwanted distortions in the seasonal cycle.

This distortion can happen if one part of the seasonal cycle is more strongly effected by long term fluctuations than another. This is for instance the case for the central Labrador Sea. End of winter salinity values vary only slightly between fresh and salty periods (except if convection is totally repressed as was the case during the Great Salinity anomaly of the 70's (Dickson et al., 1988)), but summer values show a major influence. Since subtraction of long term changes effects summer and winter values similarly it has the result of only partly reducing long term trends in summer and falsely shifting values in winter. These effects are small but cannot be neglected. Due to the fact that the end of winter period has a length of 1 to 2 months but the effected summer period exceeds 10 months the bias is reduced to a degree that it is small when compared to others. Iterative construction of the seasonal cycle can sometimes help to reduce this bias.

The final climatological salinity cycle was subtracted from the original data set. The

gaps were again filled with a shape preserving cubic interpolation. The residual data with interpolated gaps were filtered with a low pass butterworth filter with a cut off frequency of three years. The filtered cycle was used as a long term trend for the region analyzed (shown in the middle part of figure 5.1).

The removal of the seasonal cycle is necessary since otherwise isolated measurements would not represent the difference from the mean cycle for this period.

The use of a butterworth filter can enhance some frequencies in the data set, depending on its order and the cut off radius. Therefore it must be used with caution if a frequency analysis is performed afterwards. This will be seen below and discussed for the Labrador Current, area LC. It is still favored for a frequency analysis, compared to for instance a running mean, since the running mean reduces but does not eliminate short term fluctuations. This results in higher power for low frequencies and their multiples, thus reducing the significance of other signals.

To take large areas of interpolated values into account that might not represent the observed variations the long term variations were flagged. Long term variations with less then 3 months observations within 7 months (3 out of x$\pm$3) were flagged as doubtful, while others were trusted. Thus for all correlation analyzes performed below only the trusted long term trend was used.

As a control mechanism (last three steps of figure 5.1) for the quality of the derived values the autocorrelations of residuals were calculated. If the autocorrelation with a lag of 12 months shows a significant value, then the seasonal cycle includes a signal with the period of one year in the monthly fluctuations. The only region that failed this test was area WGCn. The West Greenland Current shelf area shows an autocorrelation on lag 12 despite all attempts of different seasonal cycle construction. It is believed that the reason for this is found in the composite of the seasonal freshwater cycle of three different sources with individual cycles, resulting in very different strengths of seasonal cycles, this is also reflected in the high monthly variability (compare section 3.3.1). All other areas passed this test and showed no significant value at a lag of 12 months. A further validation of the quality of the found trends and long term variabilities was performed. To check the trend the correlation between long term trend and monthly fluctuations was calculated. No significant values were found here with the procedure described above.

For analysis purposes the data set with removed seasonal cycle (in blue), the interpolated value (in gray), the long term variations (in magenta) and the trusted long term variations (in red) are presented in the following for each region. Further, the autocorrelation of each of them is displayed and discussed briefly individually and afterwards compared and discussed. The autocorrelation analysis gives a more objective view about the properties of the time series and its variabilities.

These analyzes will provide the possibility to track long term variations in the central Labrador Sea. This is discussed and shown in lag and correlation analyzes afterwards.

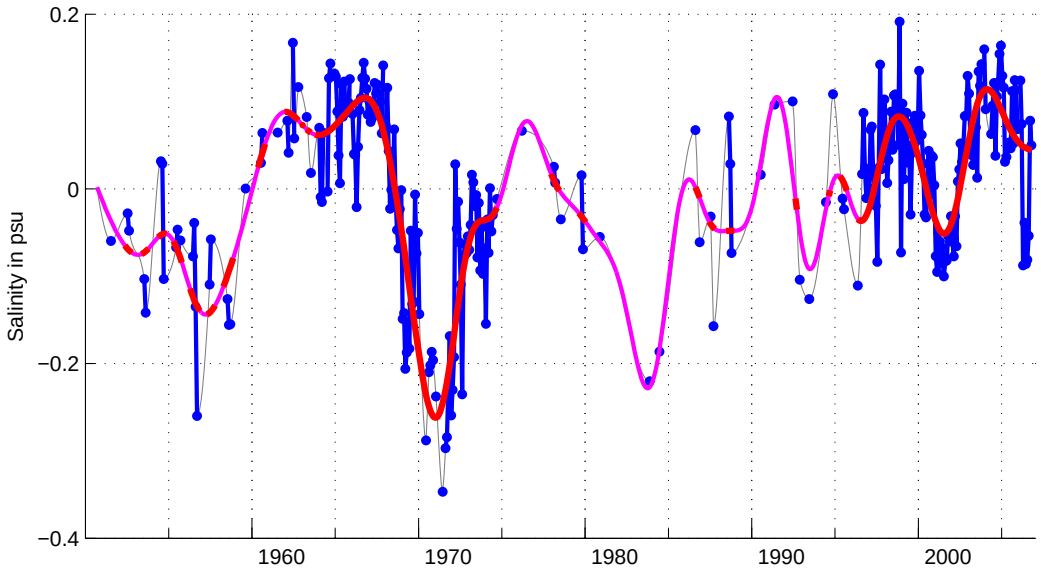

Figure 5.2: Central Labrador Sea (area cLS) salinity time series without seasonal cycle (blue dots and curve), missing years filled with cubic interpolation (gray curve). The long term variability (low pass butterworth filtered with 3 years cut off frequency) is marked magenta and red for the trusted part.

5.2 Labrador Sea

5.2.1 central Labrador Sea (area cLS)

The central Labrador Sea area has two well observed time periods that stand out in figure 5.2. The 60's and beginning of 70's during the time of Ocean Weather Ship Bravo and from the mid 90's onward. For the rest of the time only random monthly observations are available.

Before addressing the long term variations it should be clarified how much you can trust these individual observations. A good measure is the relation of the standard deviations from the short term variability and the long term variability.

$$\varsigma_{(x,y)} = \frac{\sigma_x}{\sigma_y}$$

Let x be the long term variability and y the short term fluctuations, thus σ_x and σ_y their standard deviations . If $\varsigma \gg 1$, individual measurements are likely to represent the long term variability. For the case $\varsigma \ll 1$, short term variations exceed the long term variations, thus their use for diagnosing long term variability is not suggested. In the central Labrador Sea area ς is about 2, thus interpolation over larger periods with only few months of observations will represent at least the general shape of the variability.

Three major fresh water events in the Labrador Sea stand out. The later two are well described, the Great Salinity Anomaly of the 70's (Dickson et al., 1988) and the Salinity anomaly of the 80's (Belkin et al., 1998) stand out, though the trusted cycle does not

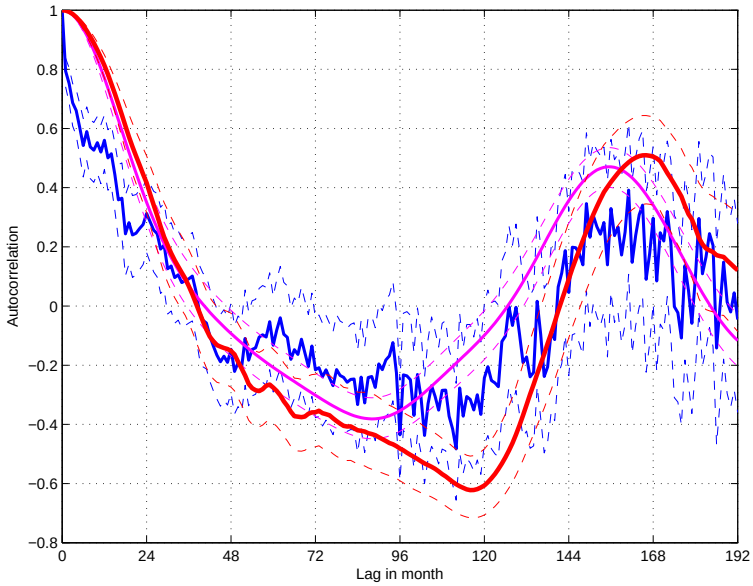

Figure 5.3: Autocorrelation function of central Labrador Sea (area cLS) salinity time series. Available monthly data without season used for blue curve, the trusted long term variability is shown in red, the complete long term variability including the doubtful in magenta. 95% confidence bounds are indicated by dashed lines.

include the salinity anomaly of the 80's. The often discussed salinity anomaly of the 90's can not be seen in this data set. Still another to my knowledge not described large salinity anomaly in the late 50's stands out. That anomaly of the 50's was for the deep Labrador Sea sampled even better than the anomaly of the 80's. The large anomalies seem to reoccur on a regular basis.

The regular timing of the anomalies is also found in the autocorrelation of the data and displayed in figure 5.3. All three data sets show a peak around 13 to 14 years. The blue curve that includes the short term fluctuations has lower 95% confidence bounds around 0 during that maxima, but the trusted long term trend data stays with the lower 95% confidence bounds above 0.3. Thus the maximum at 13-14 years is notable. The timeseries with 57 years is too short to classify this periodicity of 13-14 years significant. The same is true for a distinct minimum at around 10 years. The minima is not represented by the long term variability using also the doubtful periods (magenta curve).

The for itself surprising result from the central Labrador Sea region is the regular occurrence of Great Salinity anomalies, in the late 50ies, early 70ies and mid 80ies. Suggesting a period of 12 to 14 years. There is no study mentioning a Great Salinity around the year 2000 as one would expect extrapolating these events, but as seen in figure 1.7 the years 2000 and 2001 show a significant higher than normal freshening.

5.2.2 northwestern Labrador Sea (area LSn)

The data base in area LSn is very low (figure 5.4) and thus only shown for completeness. The only reasonably sampled times are data during the Labrador Deep Sea Experiment and the ARGO Programme by floats. Some CTD measurements in the 50's and 60's suggest a similar signal to the central Labrador Sea with a larger amplitude. The salinities in the 90's

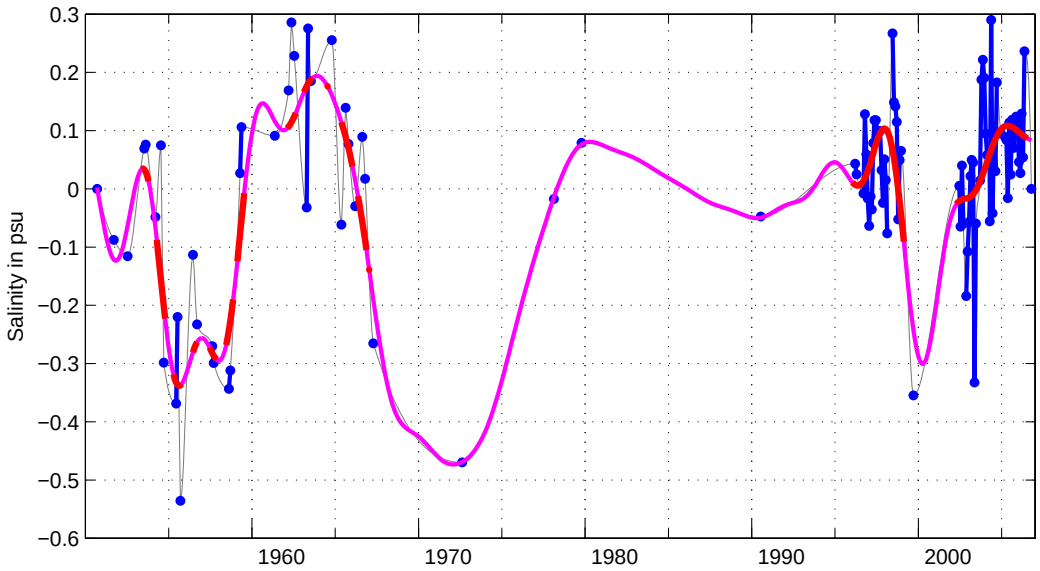

Figure 5.4: Northern Labrador Sea (area nLS) salinity time series without seasonal cycle (blue dots and curve), missing years filled with cubic interpolation (gray curve). The long term variability (low pass butterworth filtered with 3 years cut off frequency) is marked magenta and red for the trusted part.

show no major difference to the ones after the year 2000. Further conclusions from figure 5.4 would be speculation. For these reasons a further long term analysis of this area is not possible and omitted.

Due to this too low data basis area LSn is excluded from all further statistical comparisons and discussions below.

5.3 West Greenland Current

Since the seasonal analysis in chapter 3 showed very similar shelf cycles and large differences between the shelf and offshelf areas the same is expected for the long term variability. Since shelf and offshelf regions have completely different origins, waters with salinities continuously above 34.7 for the offshelf area (Irminger Sea Water of North Atlantic Current origin) and continuously below 33psu for the shelf area (polar waters of Nordic Seas origin and Greenland runoff waters) at the entrance of the Labrador Sea, no major similarities are expected. Surprisingly they do show unexpected similarities, as I will show in the following.

5.3.1 On shelf variations (area WGC and WGCn)

The West Greenland Current shelf is better sampled past Cape Desolation. This has been seen and explained for the seasonal cycle (sections 3.3.1) and can be seen again when comparing figure 5.5 for area WGC and figure 5.6 for area WGCn. These two figures also demonstrate well the problems of interpolating with a high monthly variability. The (in equation 5.2.1 introduced) measure ς is in both areas well below 1 and even below 0.5 for area WGC, thus an interpolation is likely to be misleading. Looking at the long term

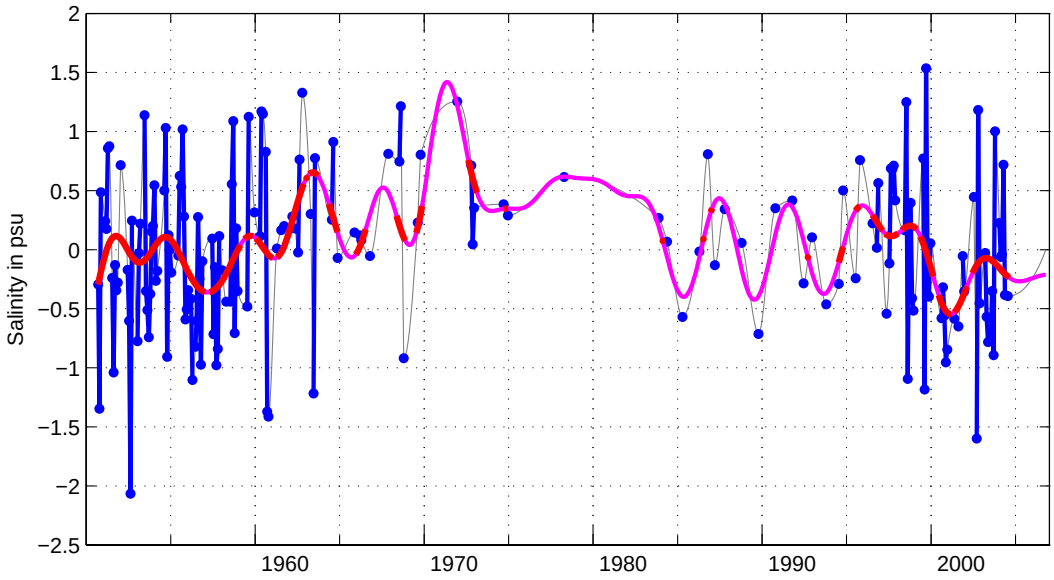

Figure 5.5: West Greenland Current on shelf before Cape Desolation (area WGC)salinity time series without seasonal cycle (blue dots and curve), missing years filled with cubic interpolation (gray curve). The long term variability (low pass butterworth filtered with 3 years cut off frequency) is marked magenta and red for the trusted part.

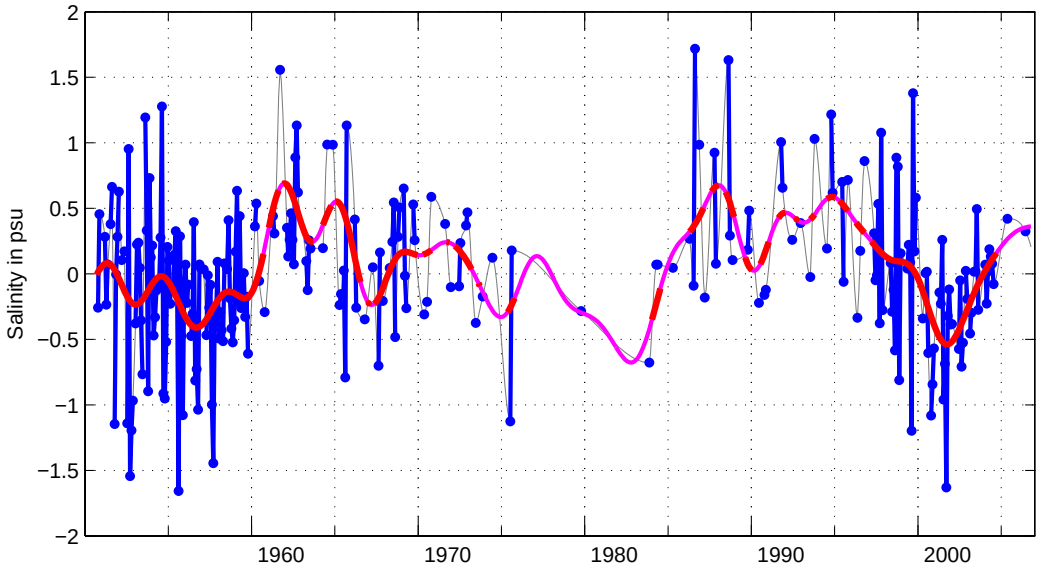

Figure 5.6: West Greenland Current on shelf north off Cape Desolation (area WGCn) salinity time series without seasonal cycle (blue dots and curve), missing years filled with cubic interpolation (gray curve). The long term variability (low pass butterworth filtered with 3 years cut off frequency) is marked magenta and red for the trusted part.

variability it becomes obvious that the trusted parts of the long term variability (more than 3 out of 7 measurements available) look very similar. The correlation of the trusted parts is 0.73, while the part flagged doubtful has a correlation of -0.36. Since area WGCn is the continuation of the West Greenland Current on the shelf from area WGC a high correlation is expected.

Both areas have long term variability of the order of 5 times the central Labrador Sea variability but still the monthly fluctuations dominate those area. In the following the discussion will concentrate on the better sampled area WGCn, but all features of area WGCn can be found also in area WGC as far as that period is sampled sufficiently.

There are indications of fresh anomalies around 1957 and 2002 and salt anomalies in the beginning of the 60's and the end of the 80's to mid 90's. It is surprising that at the time of the Great Salinity anomaly of the 70's no strong anomaly is found on the West Greenland shelf. One could assume a small negative anomaly just before (1967) or afterwards (1974-5), but during the years of the GSA 1969-70 (Dickson et al., 1988) a small positive anomaly is seen. The implicit conclusions from this are discussed further below in section 5.5.

The 80's anomaly can neither be confirmed nor denied with only two months of observations and thus remains doubtful.

A frequency analysis of area WGCn is found in figure 5.7. The autocorrelation of area WGC is omitted due to a deficit of data. The correlation analysis shows large errors from 10 years onward. This is not surprising since looking at figure 5.6 the longest trusted part is about 14 years. Thus an autocorrelation with a lag larger than 10 is not significant. There

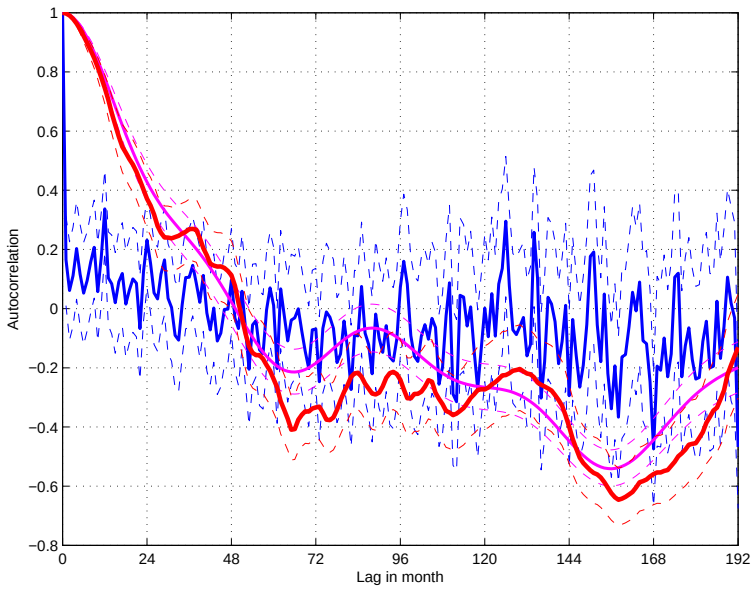

Figure 5.7: Autocorrelation function of West Greenland Current on shelf north off Cape Desolation salinity time series (area WGCn). Available monthly data without season used for blue curve, the trusted long term variability is shown in red, the complete long term variability including the doubtful in magenta. 95% confidence bounds are indicated by dashed lines.

are no significant oscillations found in this data set for the West Greenland shelf.

5.3.2 offshelf trends (area WGC-ic and WGCn-ic)

The long term variability in the offshelf part of the West Greenland current are illustrated in figure 5.8 and figure 5.9. Similarly to the shelf part, the southern part, area WGC-ic, is significantly less sampled than the northern part, area WGCn-ic. Comparing area WGC-ic with area WGCn-ic, the trusted salinity features in figure 5.8 can also be found in figure 5.9, thus analysis will concentrate on the latter area.

ς is in the order of 0.75 indicating the dominant influence of short term fluctuations. Area WGCn (figure 5.9) captures well the salt anomaly of the 50's and the 70's. There is no data available to confirm the GSA of the 80's. A small fresh anomaly can be seen around the year 2000. It is Surprising that the anomaly of the 50's and 2000 that were also seen on the shelf, occur offshelf 2-3 years prior to on the shelf (compare figure 5.9 (offshelf) and figure 5.6) and that the GSA of the 70's is seen offshelf but not on the shelf. A detailed discussion about these results will follow below.

The autocorrelation analysis for the offshelf West Greenland Current (figure 5.10) suffers from the same problem as the on shelf. Since no continuous record reaches 15 years, the autocorrelation becomes more insignificant with increasing periods than the upper and lower bounds indicate. This is due to less data overlapping each other with increasing lag.

The autocorrelation shows a significant negative correlation around 6 years that could indicate a 12 year cycle. Due to insufficient data coverage further conclusions cannot be

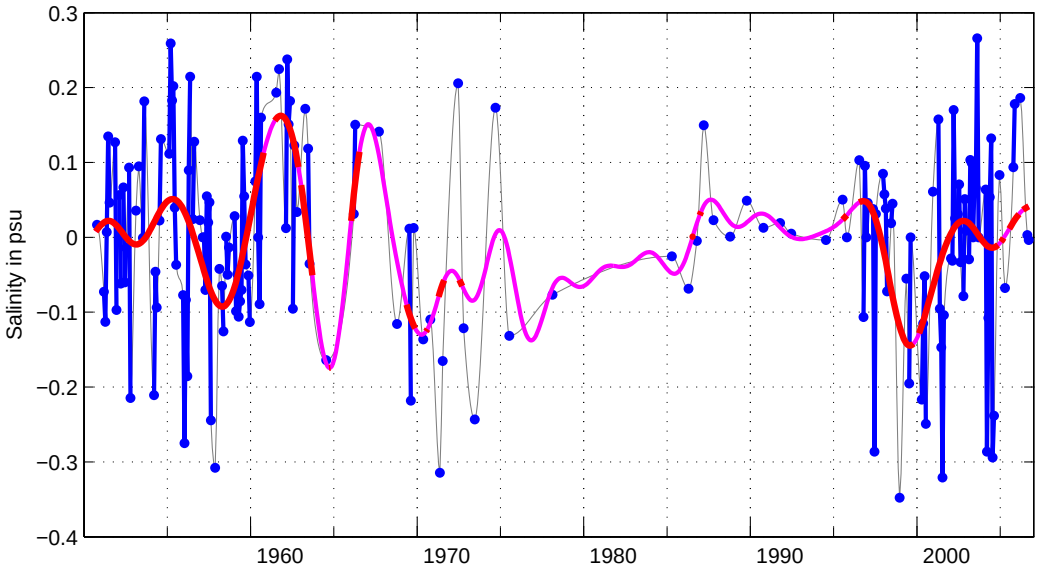

Figure 5.8: West Greenland Current offshelf before Cape Desolation (area WGC-ic) salinity time series without seasonal cycle (blue dots and curve), missing years filled with cubic interpolation (gray curve). The long term variability (low pass butterworth filtered with 3 years cut off frequency) is marked magenta and red for the trusted part.

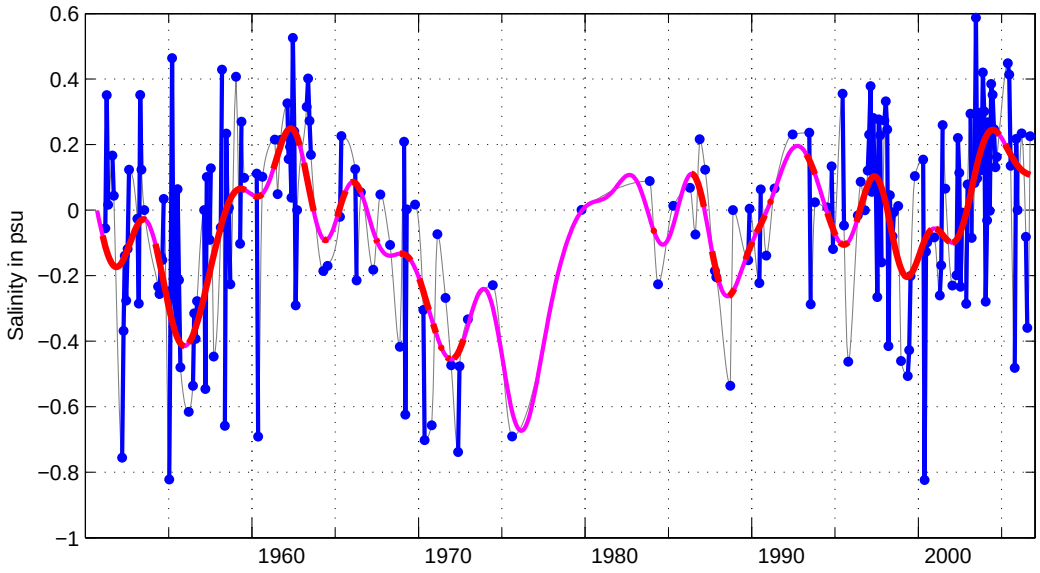

Figure 5.9: West Greenland Current offshelf north off Cape Desolation (area WGCn-ic) salinity time series without seasonal cycle (blue dots and curve), missing years filled with cubic interpolation (gray curve). The long term variability (low pass butterworth filtered with 3 years cut off frequency) is marked magenta and red for the trusted part.

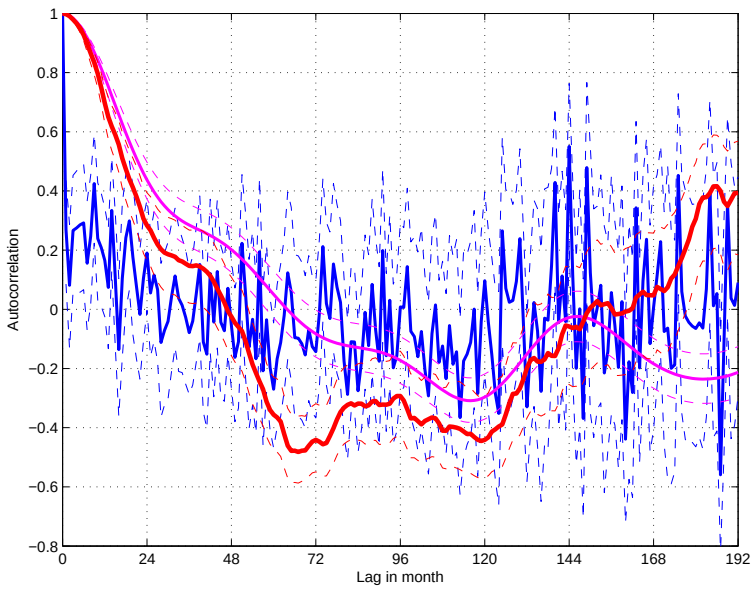

Figure 5.10: Autocorrelation function of West Greenland Current offshelf north off Cape Desolation salinity time series. Available monthly data without season used for blue curve, the trusted long term variability is shown in red, the complete long term variability including the doubtful in magenta. 95% confidence bounds are indicated by dashed lines.

made.

5.3.3 southern West Greenland Current branch (area sWGCb)

There is not enough data for the southern West Greenland Current branch to perform a long term variability analysis. Figure 5.11 displays the available data that indicate the two above addressed salinity anomalies of the 50's and 70's. No further conclusions can be drawn.

As for area LSn no further statistical analysis will be made for this area.

5.4 Labrador Current

The Labrador Current is the best sampled area from all areas analyzed. A nearly continuous data record since 1950 exists on the shelf with more than 9 months of data for every year. The offshelf region is sampled less frequently but well spread over the 57 years analyzed here. Thus it is expected that all major anomalies that occurred in the Labrador Sea area show up in the Labrador current.

5.4.1 On shelf trends (area LC)

The Labrador shelf is sampled nearly monthly for the last 57 years in area LC, except for April and May. This provides the best record for long term variability analysis in the Labrador Sea. This is illustrated in figure 5.12. Like the West Greenland current, the monthly fluctuations exceed in general the long term trend. Salinity minima can be found

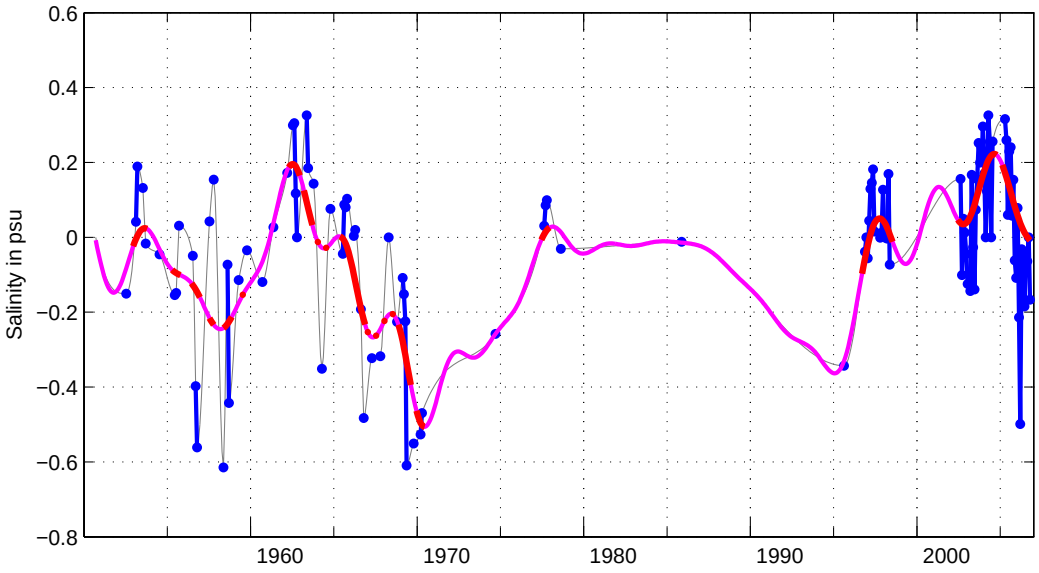

Figure 5.11: Southern West Greenland Current branch (area sWGCb) salinity time series without seasonal cycle (blue dots and curve), missing years filled with cubic interpolation (gray curve). The long term variability (low pass butterworth filtered with 3 years cut off frequency) is marked magenta and red for the trusted part.

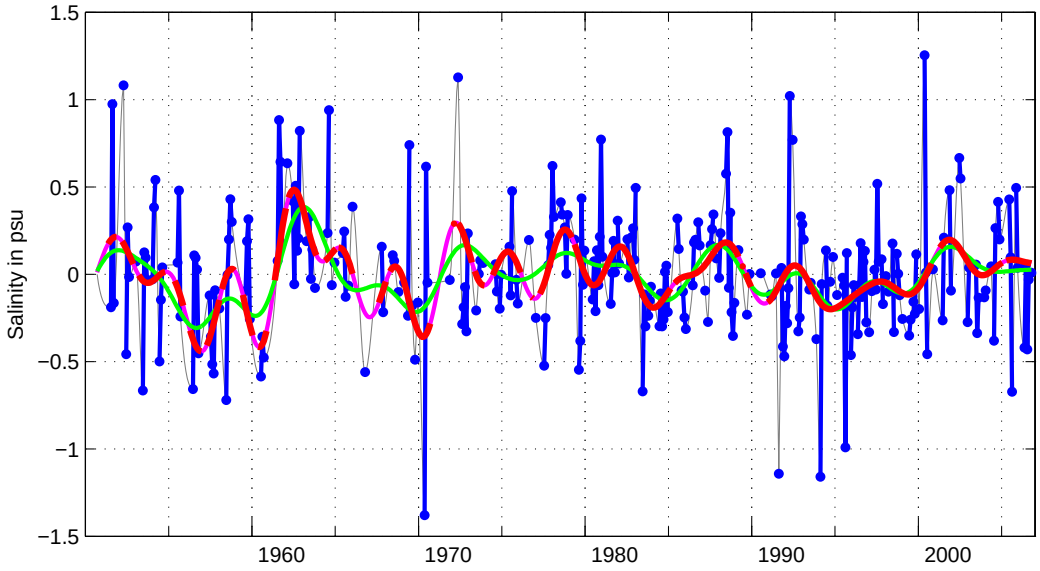

Figure 5.12: Labrador Current (area LC) salinity time series without seasonal cycle (blue dots and curve), missing years filled with cubic interpolation (gray curve). The long term variability (low pass butterworth filtered with 3 years cut off frequency) is marked magenta and red for the trusted part. In green the time series filtered with a butterworth filter close to 4 year cut of frequency is shown.

in the 50's and beginning of the 70's, mid 80's and mid 90's. The anomaly of the 90's as described by Belkin (2004) is found in this area for the first time and has not been seen in the previously discussed areas. The anomaly around the year 2000 seen in the West Greenland Current area cannot be seen.

Also obvious is a high periodicity of variations around 3.3 years (red curve). This can be removed by using a wider cut off frequency for the butterworth filter in the order of 3.9 years (green curve).

The autocorrelation function figure 5.13 is dominated by the period of 3 years and its multiples that show up in the autocorrelation function. The reasons for this and further frequency analyzes of this best sampled area are provided in detail below in section 5.6.

5.4.2 offshelf trends

The off shelf long term salinity variability of the Labrador Current (figure 5.14) looks similar to the central Labrador Sea seen before in figure 5.2. For this offshelf area, as for the Labrador Sea, the short term fluctuations are small compared to the long term variability.

All salinity anomalies described in literature can be seen, the 70's, 80's and even 90's one that cannot be found in the central Labrador Sea. Also the anomaly of the 50's is represented.

The variability seems to have decreased since the 70's, with no larger salinity variability in the last years.

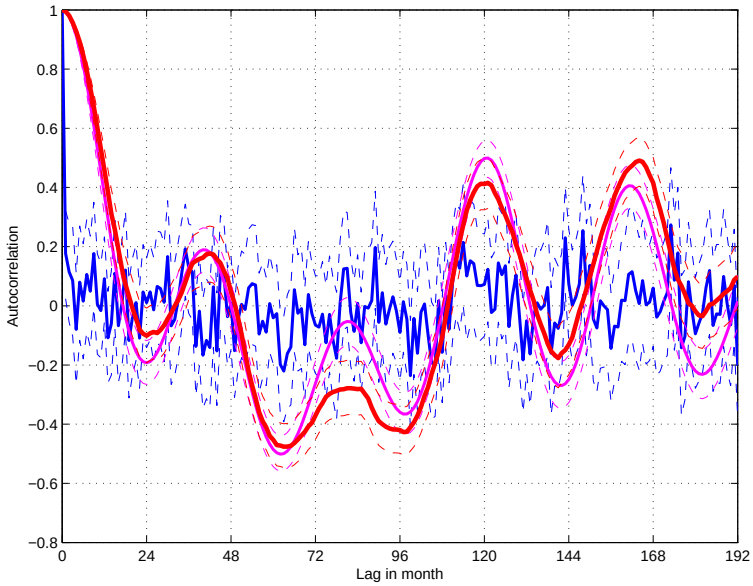

Figure 5.13: Autocorrelation function of Labrador Current salinity time series. Available monthly data without season used for blue curve, the trusted long term variability is shown in red, the complete long term variability including the doubtful in magenta. 95% confidence bounds are indicated by dashed lines.

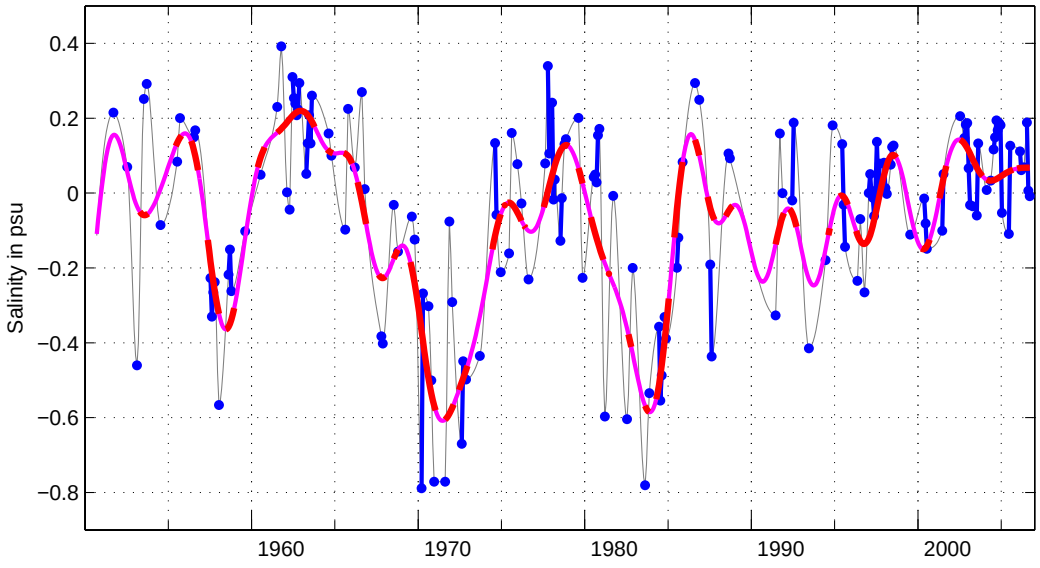

Figure 5.14: Labrador current offshelf (area LC-ic) salinity time series without seasonal cycle (blue dots and curve), missing years filled with cubic interpolation (gray curve). The long term variability (low pass butterworth filtered with 3 years cut off frequency) is marked magenta and red for the trusted part.

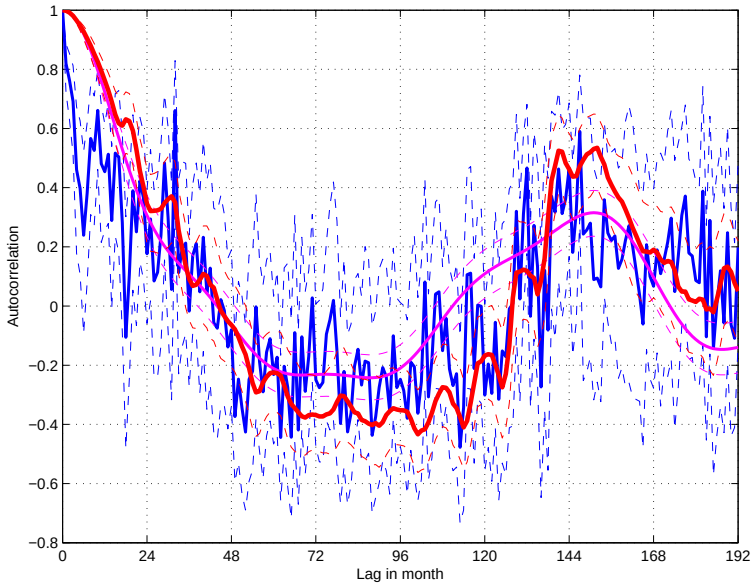

Figure 5.15: Autocorrelation function of Labrador current offshelf salinity time series. Available monthly data without season used for blue curve, the trusted long term variability is shown in red, the complete long term variability including the doubtful in magenta. 95% confidence bounds are indicated by dashed lines.

Autocorrelation functions in figure 5.15 have a significant maximum around 12 years, other maxima are not obvious. A further discussion of periodicities in area LC-ic can be found in the discussion below.

5.5 Inheritance and correlations

Can a correlation analysis give evidence on how the Labrador Sea areas are connected in long term variability?

From chapter 3 as well as figures 5.5 and 5.6 for the shelf and figures 5.8 and 5.9

area	WGC-ic	WGCn	WGCn-ic	LC	LC-ic	cLS
WGC	0.59 (23)	0.73 (4)	0.69 (18)	0.46 (6)	0.28 (-5)	0.25 (0)
WGC-ic	1	0.44 (-23)	0.39 (5)	0.42 (-5)	0.74 (-8)	0.35 (-8)
WGCn	-	1	0.60 (30)	0.32 (-5)	0.24 (-6)	0.26 (6)
WGCn-ic	-	-	1	0.39 (-11)	0.64 (-4)	0.73 (-2)
LC	-	-	-	1	0.59 (-7)	0.49 (-12)
LC-ic	-	-	-	-	1	0.82 (6)

Table 5.1: Correlations table for the areas analyzed. Maximum correlations within plus minus five years shown, months of lag of maximum correlation in brackets. Correlations with an area of low data coverage is shaded light gray (use with caution). Significant data are colored red, white and green. Uncorrelated connections are colored red ($R < 30$), unsure white ($30 \leq R \leq 50$) and correlated ones green ($R > 50$).

for the offshelf part it can be stated that area WGCn and WGCn-ic represent well the upstream areas WGC and WGC-ic, thus they do represent the inflow of Irminger Sea Water (WGCn-ic) and of waters with East Greenland Current origin (WGCn) into the Labrador Sea area. For these reasons the discussion will focus mainly on the two northern West Greenland Current regions.

The correlations between all areas were calculated in table 5.1. Only the trusted parts of the long term variability were used. The maximum correlation within a lag of plus/minus five years is given. The lag in months is indicated in brackets behind the given correlation. The lag corresponds to the area in the column, thus positive lag the column area lags, for negative lag the column area leads. Areas with low data coverage were colored gray and need to be used with caution. Correlations below 0.3 are marked red for showing nearly no correlation and green for showing correlations above 0.5.

The only area that shows no correlation with the central Labrador Sea area (area cLS) is the shelf part of the West Greenland current, area WGCn. The long term variability of area WGCn has a correlation to the offshelf area WGCn-ic with a lag of 2.5 years and is uncorrelated to the offshelf Labrador Current and the central Labrador Sea. This is surprising since the fresh shelf waters of the West Greenland Current are commonly believed to be the origin of the GSAs observed in the Labrador Sea. Further more it surprises that the Irminger Sea Water, area WGCn-ic, is correlated with the central Labrador Sea and the other regions. The found lags for the maximum correlations suggest that the Irminger Sea Water is the origin of most long term variability in this region.

To verify the significance of the found lags of significant correlations figure 5.16 illustrates the cross correlation functions of the five found significant correlations. 5 out of 9 areas are emphasized blue, they showed sufficient data coverage and are discussed. The green numbers give the found maximum correlation from table 5.1 at the lag in months (black numbers). The sign of the lag is represented by arrows. The 95% confidence intervals for the cross correlation functions are indicated as dashed lines. The following can be said about the 5 found significant correlations:

1. The 30 months lag between area WGCn and WGCn-ic proofs to be a high estimate for a significant lag between 18 and 30 months, thus a lag of about 2 years can be accepted for this correlation.

2. The 4 months lag between area WGCn-ic and LC-ic is a very low estimate. The cross correlation function suggests that it is likely that area LC-ic lags further behind area WGCn-ic. In the following a lag of about 1 year is used for discussion.

3. The lag of 2 months between area WGCn-ic and area cLS is not significant. But the autocorrelation indicates a slight tendency of anomalies in area WGCn-ic leading area cLS.

4. 7 months of lag between the area LC and area LC-ic seem to be significant since the cross correlation function decreases strongly in both directions. Thus a significant correlation at a lag of roughly half year is found.

5. The last lag to be addressed is the correlation of 6 months between area cLS and area LC-ic. The cross correlation function shows the maximum at 6 months lag, but

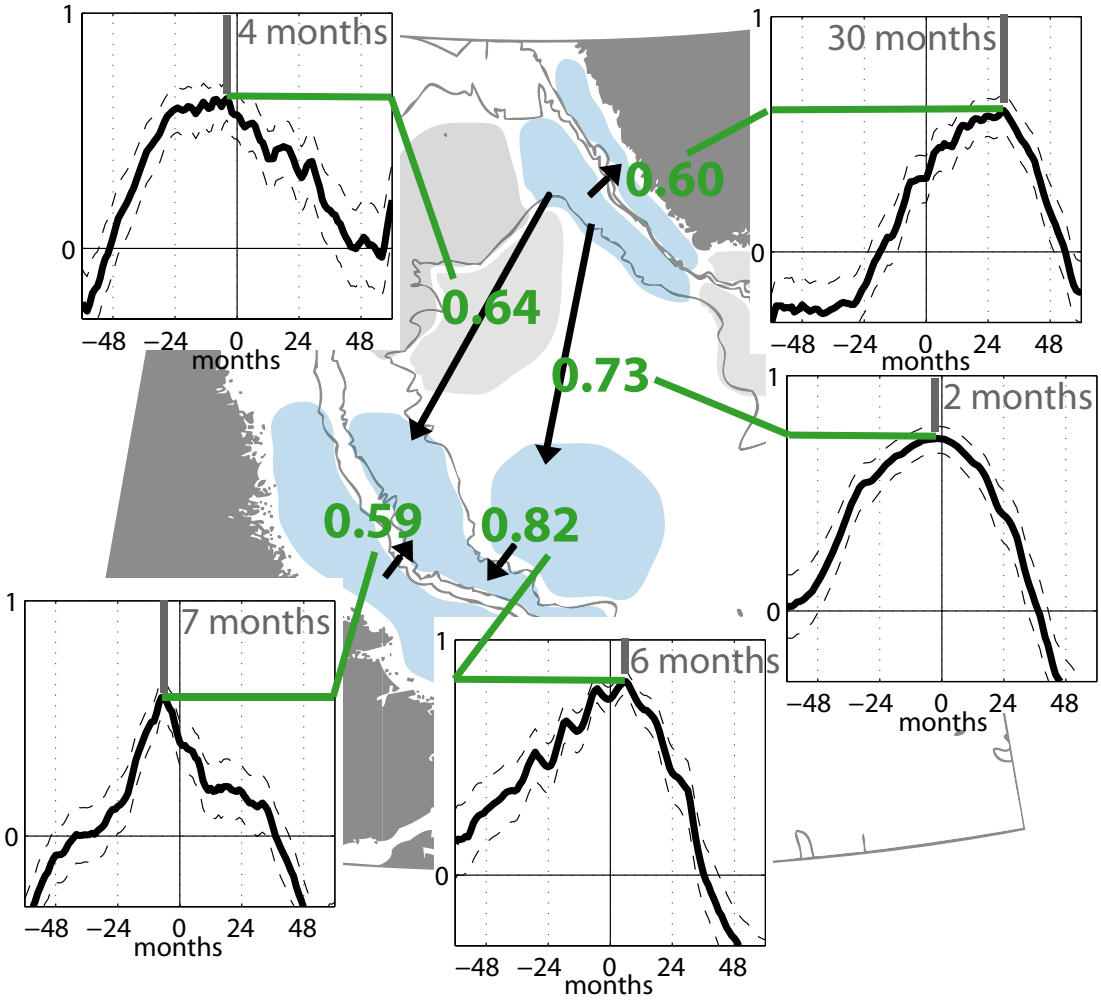

Figure 5.16: Correlations of long term variability in the Labrador Sea. The green numbers indicate the maximum correlation between the sketched areas, arrows indicate the likely propagation, gray numbers in sub panels the time in month for this propagation (lag). Sub panels give the ±5 year cross-correlation function between the areas, y-scale is always -0.3 to 1.

decreases stronger towards higher lags compared to lower. Comparing the individual salinity minima and maxima (figure 5.2 and 5.14) they all are found first in the central Labrador Sea and shortly afterwards in the Labrador Current. Thus a lag of ≤ 6 months is used for further argumentation.

Apart from the origin in the offshelf West Greenland Current Irminger Sea Waters rather than in shelf waters the lags and propagation pathways in general confirm the propagation pathways and advection velocities given for the so far observed GSAs in literature (e.g. Dickson et al., 1988; Belkin et al., 1998).

Since the consequences of this significant shelf - offshelf lag are large and the correlation as well as the lag is not visually obvious from data, it is further analyzed. Figure 5.17 shows all four salinity anomaly time series for the West Greenland Current. Red for the

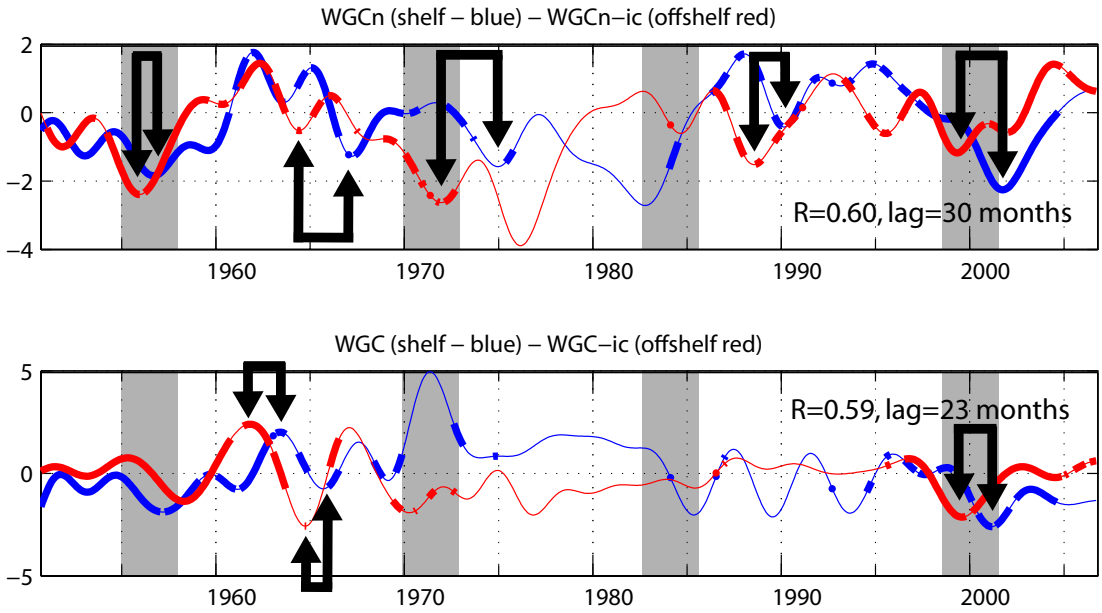

Figure 5.17: Comparison between the shelf (blue) and offshelf (red) West Greenland Current salinities, normalized by their standard deviation of the trusted long term variability. Upper panel the northern areas WGCn and WGCn-ic, lower panel the southern areas WGC and WGC-ic. Maximum ±5 year correlation at given lag is included.

salty offshelf areas and blue for the fresh shelf areas. The timeseries got normalized by their standard deviation. Maximum correlation at given lag is indicated. The passing time or estimated passing of the Great Salinity Anomalies are marked in gray. The arrows emphasize the lag for certain events.

The two shelf areas lag behind both offshelf areas between 2 and 2.5 years. The cross-correlation panel figure 5.16 suggested that a medium lag around 2 years is expected to be a robust value. The observed variations are too large for ice-melt or ice formation on the shelf to modulate the shelf signal to the observed values. A direct comparison of the shelf and offshelf data in figure 5.17 confirms the statistical found lag for most major anomalies that got observed.

This lag will be exemplarily discussed for the often discussed and most well known GSA of the 70ies in the following.

The Great Salinity anomaly arrived in the Labrador Sea around 1970 (Dickson et al., 1988, and figure 5.2). There is no trace of a negative salinity anomaly on the shelf during these years (blue curves upper and lower panel in figure 5.17). The opposite can be seen offshelf (red curves upper and lower panel in figure 5.17), decreasing salinities are found from 1967 up to the minimum in 1972 in the waters with salinities higher than 34.7 at the entrance of the Labrador Sea. About 3 years later in 1975 a minimum of a negative salinity anomaly can be seen on the shelf (blue curve upper panel in figure 5.17).

This order of occurrence can be seen more or less for all larger long term variations (figure 5.17). They all occur first in the offshelf areas and a second time with a lag of around 2 years on the shelf of the West Greenland Current.

The consequences are that long term salinity variations in the Labrador Sea are inherited from variations in the extension of the Irminger Current and from there spread around the Labrador Sea. Two years later a similar anomaly signal can be observed in the polar waters on the West Greenland shelf, but has no further impact on the other Labrador Sea areas.

These findings have major influence concerning the origin and propagation of the Great Salinity Anomalies and is discussed below in section 5.7.

5.6 Periodicities

Two periodicities were obvious in the individual time series, a three year periodicity in the Labrador Current and the regular occurrence of the Great Salinity Anomalies. First the periodicity of the GSAs is described and afterwards the Labrador Current periodicities.

5.6.1 Occurrence of Great Salinity Anomalies

The Great Salinity Anomalies were observed in the end of the 50's, around 1970 and in the mid 80's. They all lie 12-14 years apart. 12 to 14 years after the GSA of the 80's no anomaly is observed in the central Labrador Sea, but all observations in the four West Greenland Current areas do show an anomaly during that period (e.g. figure 5.17 first offshelf and two years later on the shelf). In those West Greenland Current areas it is even more pronounced than several of the earlier anomalies.

Why does this last GSA in the West Greenland Current does not propagate into the central Labrador Sea the same way the previous ones did?

The GSA is entering the Labrador Sea around 1997 and is at is minimum in 1999 (e.g. red curve lower panel figure 5.17). Concurrent to the offshelf minimum a salinity maximum on the shelf possibly counteracted and might have partially diminished the anomaly along the West Greenland Current. But another reason might be more important, since the effect of the shelf area on the Labrador Sea seems to be small. 1997 to 1999 were three consecutive years of high EKE in the Labrador Sea (Brandt et al., 2004), as has been discussed in section 4.2 and following ones. Therewith a possible explanation for the pronounced GSA in the West Greenland Current not reaching the rest of the Labrador Sea might be found and even supports the results of chapter 4. Phases of enhanced EKE increase the Labrador Sea salinities and thus can be seen responsible for diminishing the GSA around the year 2000 that is clearly visible in the West Greenland Current.

Further more local effects like wind fields might play an important role about strengthening or eroding salinity anomalies in the Labrador Sea as suggested by Czeschel (2005)

The only GSA that has not been seen propagating into the Labrador Sea is the GSA of the 80's. Since Belkin et al. (1998) see that anomaly locally generated in the Labrador Sea, it should be clarified if this anomaly has the same origin as the others. If it is locally generated and not advected like the others any suggestions of periodicity in these events is void.

The 80's did not get sampled continuously at all on the Greenland side of the Labrador Sea. Even the data from both offshelf areas (figure 5.8 and 5.9) miss the 80's anomaly completely. An analysis of Irminger Current waters is also impossible since no available data along the East Greenland Current south of Denmark Strait between 1979 and 1985

was found. On the Labrador side and in the central Labrador Sea the anomaly looks very similar to the 50's and 70's one.

It cannot be determined if the 80's anomaly was advected, neither can be determined that it was not advected. But it is surprising that the time between the salinity minima in the 50's and 70's is the same as in the 70's and the 80's wherever all three were observed. And even a fourth anomaly with again the same period is observed around 1999. These conclusions make an explanation of a solely local generated 80's anomaly by Belkin et al. (1998) unlikely, though no observational proof exists.

Even though doubts remain in the following the discussion is assuming the same origin far the 80's anomaly as for the other anomalies.

This makes four Great Salinity Anomalies in the last 57 years for the Labrador Sea region, continuously since the mid 50's, all spaced about 12 to 14 years apart. Thus this might indicate the the Great Salinity Anomalies are a regular occurring phenomena in the Labrador Sea with a period of 12-14 years, originating in waters with salinities above 34.7. This will be further addressed in the discussion below (section 5.7).

5.6.2 Labrador Current periodicities

Since the Labrador Current is well sampled for 57 years and the period observed of around 3 years is many times smaller than the sampling period a power spectrum is calculated.

The analysis is applied on the data with removed seasonal cycle. No filtering was applied. A fourier transformation spectral analysis requires evenly spaced data and since interpolation of an unevenly spaced time series is equivalent to low-pass filtering that period, significant reddening of an estimated spectrum at wavelengths comparable to gaps will result and consequently a biased result may be the outcome (Press et al., 1992; Schulz and Mudelsee, 2002). Therefore a completely different method of spectral analysis for unevenly sampled data was developed by Lomb (1976) and additionally elaborated by Scargle (1982). The Lomb-Scargle method evaluates data, sines and cosines only at times that are actually measured. It is called the Lomb-Scargle Fourier transformation hereafter. The algorithm presented by Press et al. (1992, chap. 13.8) is used for calculation. Extended significance analysis was performed by Horne and Baliunas (1986) for white noise. Analogous to Horne and Baliunas (1986) a Monte Carlo approach for red noise was performed here. This was done by fitting a first-order autoregressive (AR1) process, being characteristic for many climatic processes (Hasselmann, 1976), directly to the unevenly spaced (gaps) time series. Thus the AR1 model had the same one lag autocorrelation, mean, variance and time steps as the data series. 1001 AR1 realizations were performed for each data set individually. A similar approach for red noise significance in the Lomb-Scargle Fourier transformation is analyzed and discussed in detail by Schulz and Mudelsee (2002).

The power spectra for the Labrador Current, area LC is given in figure 5.18, the confidence bounds for pure red noise and 95% limit is indicated. The lower frequencies area LC has a significant maximum in the range of 12 to 13 years. This has been discussed above for the GSAs. Area LC furthermore has significant power around 3.3 and around 2.6 years.

Since the previous sections 5.5 and 5.6.1 indicates that the offshelf West Greenland

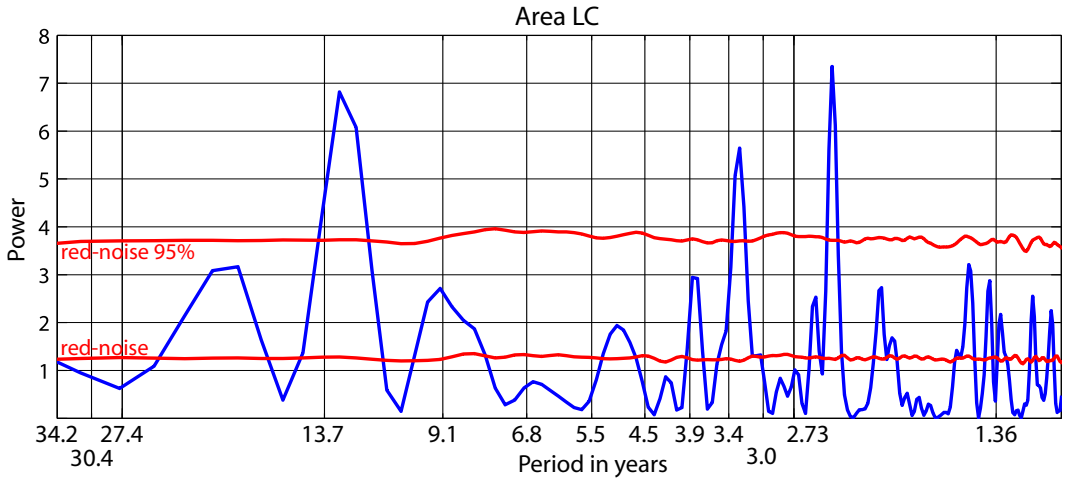

Figure 5.18: Power spectra of the Labrador Current, area LC. Lomb-Scargle Fourier transformation used, confidence bounds calculated by Monte Carlo approach, 1001 realizations of pure red noise (AR1 process) with same one lag autocorrelation, mean, variance and data distribution as data.

Current is the origin of long term variability, it could be that 2-5 year periodicity has the same origin. Area WGCn and WGCn-ic are both correlated with the Labrador Current shelf (compare table 5.1). Therewith the periods around 2.6 years on the Labrador shelf might be explained by the lag of around 2 years between the shelf and offshelf West Greenland Current. Thus providing signals that occur on and offshelf in the West Greenland Current twice to Labrador Current.

Both of these periods might be induced by the West Greenland Current, since an anomaly in the West Greenland Current must be either eroded in the area or must leave the Labrador Sea region again. It has several possible advective ways to reach the Labrador Current (e.g. Wang et al., 1994; Curry and Mauritzen, 2005): the southern West Greenland Current branch, the northern West Greenland Current branch, recirculation in Davis Strait joining the Baffin Island Current and in the north of Baffin Bay the remainders of the West Greenland Current do form the Baffin Island Current that is the major source of the Labrador Current. No known to me reliable drifter or model analysis show mean advection speeds for those later pathways in the Baffin Bay.

More of the unexplained variations or modulations of the Labrador Current might be found in variability of Greenland runoff, Canadian Archipelago through flow (Zweng and Münchow, 2006), Hudson Bay outflow (Straneo and Saucier, 2007) and as well as changes in the long term wind field (Czeschel, 2005). It might be questionable why these sources should have the periodicities found, especially since the power spectra suggests that these periods do not vary much.

Summarizing it can be said that the origin of the 2.6 and 3.3 year periodicities in the Labrador Current remains unclear, but different timescales of advection from the same signal are a plausible explanation.

5.7 Discussion

The long term variability analysis of Labrador Sea surface salinities shows some interesting new aspects not described before. The separation of the boundary currents in shelf and offshelf areas showed significant differences in long term variability as has been expected from the different seasonal cycles. These have not been seen in previous studies due to their combination of water masses of different origin, or the use of areas with large horizontal gradients.

Figure 5.19 combines a previously shown figure with the discussion from section 5.5. Maximum correlations within ±5 years are given in green (correlated) and red (uncorrelated). The arrows indicate the propagation or order of occurrence of salinity anomalies, retrieved from the lag of the correlation given in years (see section 5.5).

As can be seen in figure 5.19 and has been discussed in detail in section 5.5 most

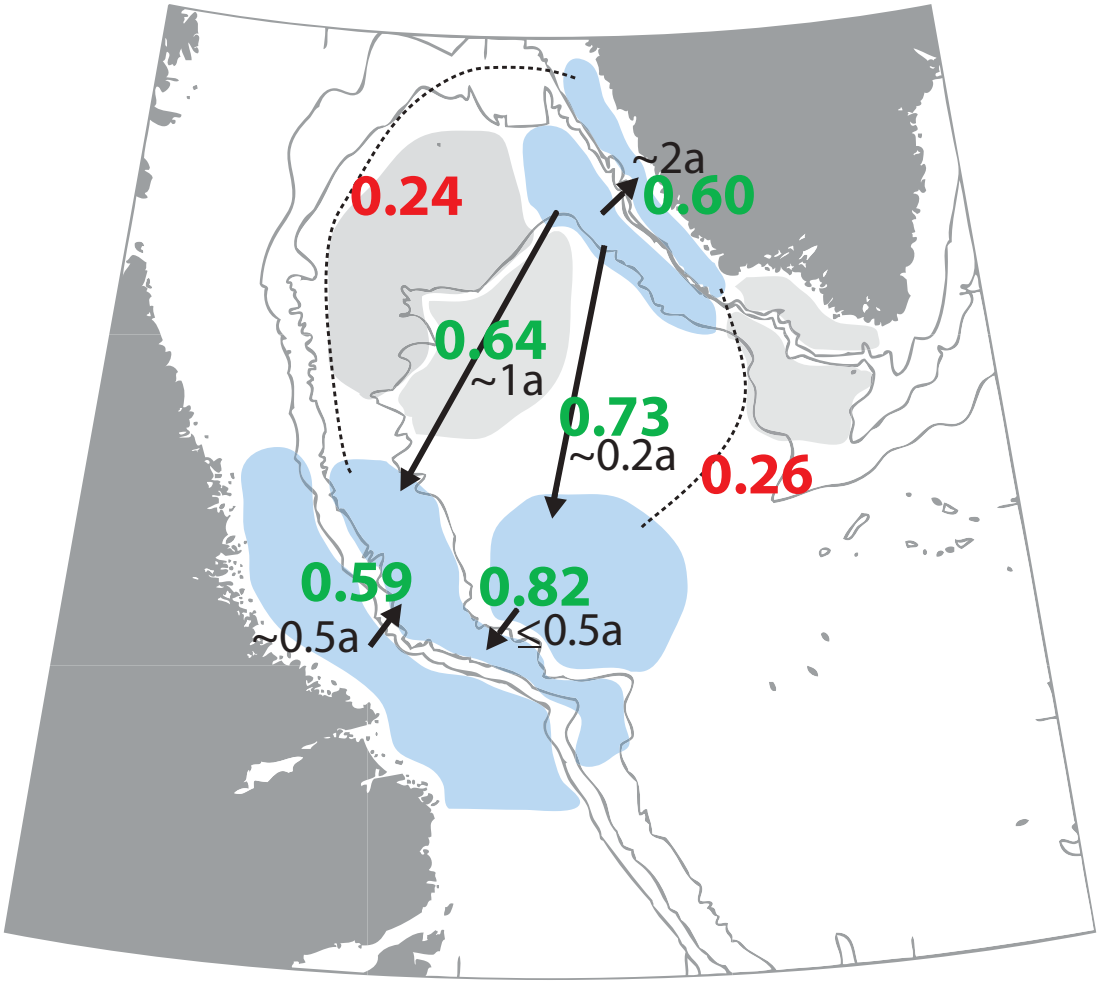

Figure 5.19: Correlations of long term variability in the Labrador Sea. The numbers indicate the maximum correlation between areas in green (correlated) and red (uncorrelated). The arrows indicate the propagation pathway or order of occurrence of the anomalies. In black is the lag in years retrieved from cross correlation analysis.

anomalies enter the Labrador Sea in area WGC-ic with salinities above 34.7 and spread from there around the Labrador Sea. The shelf part of the West Greenland Current is not correlated to the central Labrador Sea, but lags around 2 years behind the offshelf parts.

This implements that the GSAs in the central Labrador Sea do not originate in the polar Waters of the West Greenland Current, but in Irminger Sea water. Since all GSAs seem to be of the same origin (compare sections 5.5 and 5.6) the discussion will focus in the following on the most discussed GSA of the 70's.

Long term variability analyzes performed here confirm the advection of this Great Salinity anomaly into the Labrador Sea via the West Greenland Current as many others did beforehand. But in this case it could be specified that the salinity anomaly seen in 1969 and 1970 in the Labrador Sea was advected via the offshelf part of the West Greenland Current.

Thus it originates in Irminger Sea waters with lower than normal salinity more than in salinity variations of polar and melt waters on the shelf. The advected polar and melt waters of the Greenland Current do not show this signal prior to the offshore part, they show this anomaly about 2 years later.

The mean seasonal salinity of the water mass importing the anomaly into the Labrador Sea is 34.77 (area WGCic). These mean salinities of the anomaly are gradually decreased along the West Greenland Current by exchange with polar waters from the shelf (compare section of seasonal cycles 3.3.2), thus shifting the anomaly to lower salinities. A slight modulation of the signal does occur but the general shape in time is conserved (compare figure 5.17.

How can Irminger Sea Water origin be explained with the numerous studies seeing especially the Great Salinity anomaly of the 70's originating in the nordic seas?

In the West Greenland Current Dickson et al. (1988) saw the Great Salinity anomaly in waters with salinities less then 34. They found a decrease of salinities since 1960 with a minimum at 1966 around -0.3 psu. Area WGCn does show a decrease during that period. Area WGCn even shows small positive salinity anomaly. The shelf area shows a minor 1-2 year anomaly in 1967/68 and a second larger one in the mid 70's, but the here analyzed offshelf area WGCn-ic does show the decreasing trend from 1961/2 to 1971. The found anomaly of around -0.3 psu by psu is still in the range of monthly fluctuations.

Figure xx from Dickson et al. (1988) suggests that the anomalies around Iceland and Jan Mayen are observed simultaneously to the Labrador Sea between 1964 and 1971 in Salinity, without a decreasing or increasing trend but annual fluctuations (Dickson et al., 1988). The timing of these anomalies and the lag of the shelf current lead to two propagation possibilities of this anomaly:

1. Like it is commonly believed the salinity anomaly originated from the arctic or Greenland Sea (e.g. Häkkinen, 1993). The anomaly is advected around Iceland into the Irminger Sea without effecting the East Greenland Current. A propagation west of Iceland is not possible, since it would immediately affect the East Greenland current and would show in the shelf analysis in the Labrador Sea. The anomaly then propagated via the Irminger Current around Cape Farewell into the Labrador Sea (offshelf anomaly). The lag of the shelf current must be explained by remainders of the anomaly in the Greenland Sea that enter the East Greenland Current far north with a lag of two

years and is from there advected into the Labrador Sea again (shelf anomaly). How likely it is that a Nordic Seas anomaly does not get advected along the East Greenland Current immediately needs to be analyzed in detail. If the East Greenland Current north of Denmark Strait adapts the long term variability of the Nordic Seas on shorter time scales than propagation into the Irminger sea takes, this scenario is unlikely.

2. The great salinity anomaly originates from the North Atlantic current. The North Atlantic Drift supplies somehow a salinity anomaly into the Irminger Current. The anomaly propagates from there into the Greenland Sea via the West Icelandic Current and simultaneously is advected via the Irminger Current into the Labrador Sea (off-shelf anomaly). The reduced salt transport into the nordic seas leads to the observed enhanced sea ice formation and lower salinities between Iceland and Jan Mayen. From there the anomaly is advected via the East Greenland Current through the Denmark Strait along the Greenland coast a second time into the Labrador Sea with a varying lag of around two years (shelf anomaly).

Since I could not find any confident explanation why a Nordic Seas anomaly is not advected reasonable fast via the East Greenland Current the first suggested propagation pathway is much less likely than the second.

Using the more likely origin, the north Atlantic Current, for the Great Salinity Anomalies it needs to be discussed, why and how this very well sampled North Atlantic Current induces a salinity anomaly into the Irminger Current on a regularly 12 to 14 year basis.

For instance a regular position shift in the North Atlantic drift could regularly decrease and increase the amount of salt advected into the Irminger Current and thus into the Labrador Sea. The same could happen via regular increased currents in the North Atlantic Drift, or just by regular advected anomalies. The phenomena has a relative constant periodicity in the Labrador Sea, thus one would expect that it would have been seen in the North Atlantic before.

Some authors see a correlation between solar insolation variability and SST or air temperature on the decadal periodicity found above. These solar and astronomical summarized variations are in the order of $0.4 - 0.6\frac{W}{m^2}$ for the last 5 decades at $60°N$ (Loutre et al., 1992; Berger et al., 1992). But this is unlikely to be the origin of these decadal freshwater changes.

More promising is following hypothesis. Dickson et al. (1988) see the Great Salinity anomaly 6-7 years after the Labrador Sea in Europe. This is exactly half the period of the 12-13 year occurrence of GSAs. Thus a position shift of the North Atlantic current could also explain the so far unexplained crossing of the GSA of the 70ies of the North Atlantic Current. Thus the Labrador Sea salinity anomaly would end in the North Atlantic Current. This is likely when comparing the mass transport rates. A hypothetical 12-13 year oscillation of the North Atlantic Drift could reallocate its salinities on this frequency between Europe and the Irminger Sea, causing a "pseudo" advection time of 6-7 years. The mid Atlantic ridge south of Iceland could be splitting the current, while an oscillation of the position determines the amount that is cut off. Since the amount entering the Irminger current is significant smaller than the other part of the North Atlantic Current a detection of the signal on the European side of the Atlantic should be considerably more difficult.

Further promising connection are oscillations found in different properties the North Atlantic with a periodicity around 13 years:

- Deser and Blackmon (1993) found a 12-13 year period in their EOF analysis of SST and air temperature over the North Atlantic off Newfoundland as well as in EOFs of the combined fields of sea level pressure and zonal winds.
- (Hansen and Bezdek, 1996) see the reason for a decadal SST oscillation in the North Atlantic in propagation periods around the subpolar gyre or the Nordic Seas.
- Moron et al. (1998) see a 12.8 year see-saw pattern oscillation between the Gulf Stream and the North Atlantic Drift Current in SST.
- Black et al. (1999) see a dominant 12.5 year mode of Atlantic variability driven by coupled tropical ocean-atmosphere dynamics.

Solely SST and rainfall for instance is unlikely to be the origin. All authors only explains a little of the North Atlantic variability with these periods, while the effect is large on the Labrador Sea salinity anomalies.

A similar origin may, however, be likely.

5.8 Conclusions

With a favorable layout of the regions analyzed and much larger data set compared to previous studies significant new results concerning the origin and occurrence of the Great

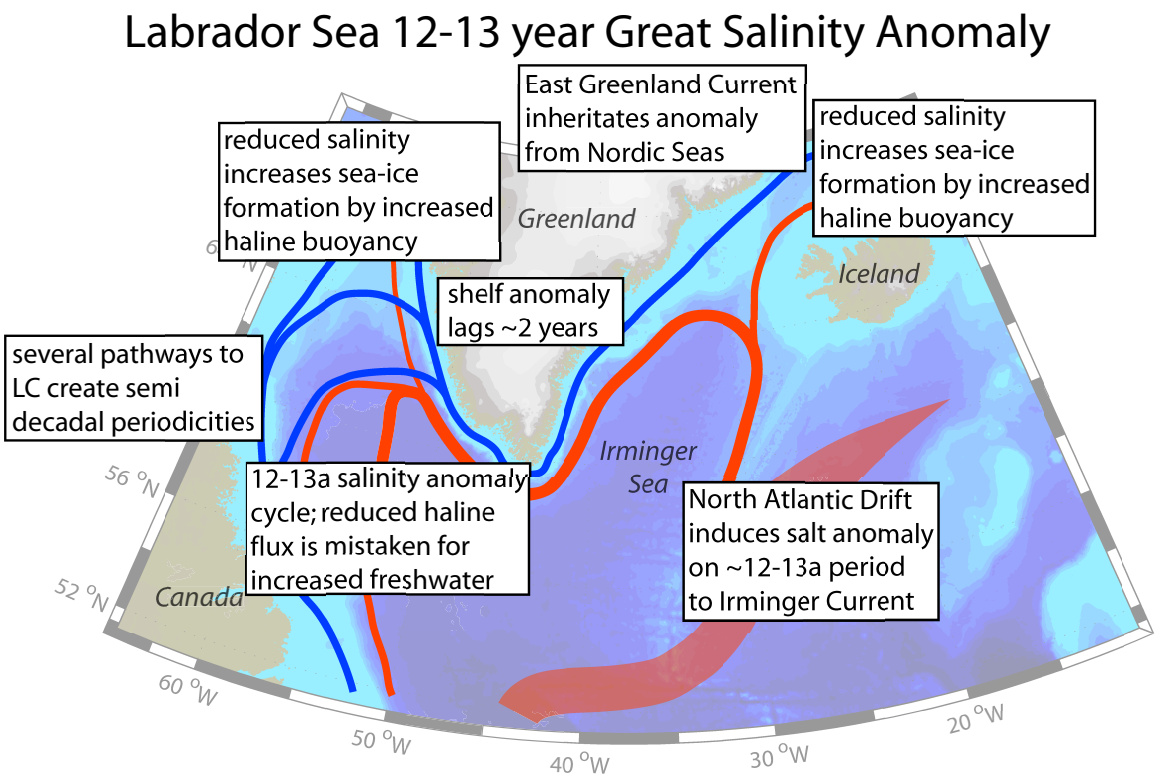

Figure 5.20: Schematic diagram of the 12-13 year occurrence of Great Salinity Anomalies in the Labrador Sea. Propagation paths correspond to surface currents. Currents saltier than 34.5 psu in red, otherwise blue.

Salinity Anomalies in the Labrador Sea were found.

The Great Salinity Anomalies are found first in the offshelf West Greenland Current with Irminger Sea origin. With a lag of two years the anomalies are observed on the shelf in water of polar origin.

A GSA originating in the Nordic Seas, that first seen offshelf in the Labrador Sea and around 2 years afterwards again in the originating polar waters on the shelf is unlikely. More likely the GSA originates in or along the North Atlantic Current, this is sketched in figure 5.20. From there the salinity anomaly is advected into the adjacent seas. Still this pathway hypothesis contradicting the common believed Nordic Seas origin can confirm the found salinity minima in the west North Atlantic as described by Dickson et al. (1988).

A key role in developing the differences in strength of these phenomena in the Labrador Sea seems play the EKE off Cape Desolation. Phases of high EKE erode this salinity anomaly probably by mixing with saltier underlying waters. This could be seen for the GSA around 1999 that collided with enhanced EKE from 1997 to 1999. The 1999 GSA was pronounced at the entrance of the Labrador Sea, but no longer detectable in the central Labrador Sea nor in the Labrador Current.

Further more it was found that the Great Salinity Anomalies occurred regularly every 12-14 years in the last 5 decades, showing 4 anomalies: 1957-58, 1970-71, 1984-85 and 1998-99 for the expected central Labrador Sea arrival. For three of these four the Irminger Current could be verified as the origin, the origin of the 80's anomaly has to remain uncertain. There was no available data for the anomaly of the 80's, but it is strongly believed that it has the same origin. The latest GSA (1998-1999) was suppressed by a high EKE phase and accompanying higher salt flux.

Such an oscillation is likely driven by coupled ocean-atmosphere response or larger feedback loops, evoking long term mean Ekman transport changes or wind stress curl change, capable of shifting a significant amount of the surface North Atlantic Current west and eastwards.

The relative constant periodicity and by various authors similar described periodicities in the North Atlantic make the next Great Salinity Anomaly in the Labrador Sea likely around 2011-13.

Chapter 6

Conclusions and Outlook

Several preliminary works proofed to be very crucial for the results of this thesis. The large hydrographic data base constructed from various sources in this study did allow to distinguish regions of reasonable homogeneous horizontal salinity. Thus set a more favorable layout of regions for analysis than previous studies did. The same needs to be said about the limitation of analysis to the top 100 m of the water column, since the water mass below the surface layer has very different properties and origins in many regions of the Labrador Sea. This needs to be kept in mind interpreting results of previous works by other authors averaging deeper than 100 m, since they do average the fresh surface layer with saltier often as well warmer subsurface waters, thus water masses of very different seasonal cycles and origins. This can explain why some surprising results from this study have been seen beforehand.

The large data base of several different sources as well as the layout of the regions made a revealing analysis of several Labrador Sea regions with the same procedures possible, without having to combine areas of different water masses, but still good temporal data coverage. It allowed to do intense seasonal to decadal analysis.

The first analysis of the regions showed that the boundary currents show significantly different salinity cycles between the shelf and offshelf. These cycles do not only differ in amplitude as suggested in previous works. Around the Labrador Sea shelf currents and offshelf currents originate from different water masses and do not only differ by a constant shift in salinities. This questions the results of many studies using a combination of both water masses for their results. For instance tracking long-term changes in a mixture of these water masses would provide very different likely misinterpreted results.

The separation of the freshening between April and September into two freshening periods for central Labrador Sea as described by Schmidt and Send (2007) was confirmed as well as the timing of the lowest salinities for the main freshening (strongest freshwater anomaly compared to a constant reference salinity in Schmidt and Send (2007)). The fact of Straneo (2006) not seeing two pulses in the mid-90's was addressed to the high variability of the first pulse and its absence in years with high EKE.

The central Labrador Sea salinity cycle has high similarities with two adjacent regions that both originate in the southern West Greenland Current branch. Thus it is undoubted that the central Labrador Sea acquires most of its seasonal salinity cycle from the West Greenland Current. This confirms the work of Schmidt and Send (2007) who showed

the West Greenland Current to be the origin by calculating a freshwater budget, but gives further clarity about the freshwater pathway. This study suggests a pathway further along the West Greenland Current before moving south again into the central Labrador Sea.

An analysis of the EKE in the Labrador Sea (chapter 4) gave information about the origin for the above mentioned early variable freshening in the central Labrador Sea in May. Analysis of hydrographic differences in the central Labrador Sea during high and low EKE phases showed the absence of the early freshening during high EKE phases. After ruling out the effect of eddy transports, the reason is believed to be found in advective changes. The average speed of the souther West Greenland Current branch decreases down to zero during years of high EKE while it has a mean flow of about 5 $\frac{cm}{s}$ during the low EKE phases analyzed here. This surprises since the souther West Greenland Current branch is mainly believed to be an eddy pathway, thus one would expect the opposite. The southern West Greenland Current branch has lower salinities than the central Labrador Sea and thus could be responsible for the observed freshening.

In general years with two freshening pulses, thus years of low EKE in the Labrador Sea region had an overall stronger freshening in the course of the year than years with high EKE. This is contradictory to the believe that high EKE close to the boundary currents enhances the exchange and leads to more freshening in the surface layer of the Labrador Sea.

The reason why and how enhanced EKE in the Labrador Sea is slowing down the southern West Greenland Current branch is not analyzed or answered in this thesis. Model analysis or process studies will have to be made to address this question.

Long term variability analysis of the regions used here, surprisingly see all major anomalies, in particular the observed Great Salinity Anomaly of the 70's first in water originating in the Irminger Sea. Not before two years later the observed Great Salinity Anomalies are found in waters of polar origin entering the Labrador Sea. Previous analysis not seeing this must be explained by the fact that they did sample over a mixture of polar water and Irminger Sea water, thus misinterpreted the anomaly as additional freshwater in the polar water and not as the here reduced freshwater in the Irminger Sea Water. Further correlation analysis show no significant correlation on long term time scales between shelf waters and the central Labrador Sea, but indicate a significant correlation between the offshelf Irminger Sea Waters with the interior. The observations do leave no doubt about this origin at the entrance of the Labrador Sea, though the pathways up to this point can be discussed.

The most likely pathway is probably an origin in the North Atlantic Current. The North Atlantic Current induces by a still unknown way a salt anomaly to the Irminger Sea. From there the anomaly propagates simultaneously to the Nordic Seas via the West Icelandic Current and the Labrador Sea via the Irminger Current. In the Nordic Seas the anomalies are entrained into the East Greenland Current and arrive with a lag of about 2 years a second time in the Labrador Sea. Further Nordic Seas analysis and data comparison has to be made to validate this pathway hypothesis, since many observations and studies assume a Nordic Seas origin of the Great Salinity anomalies.

The last interesting aspect of this thesis is the high probability that the Great Salinity Anomalies occur on a regular basis. The 57 year data set shows the trace of four Great Salinity Anomalies, all spaced 12 to 14 years apart. The same periodicity has been found in different studies concerning SST in the North Atlantic. Though the SST variations can

not be responsible, but may, however, have the same origin.

Since the last Great Salinity Anomaly around the year 2000 is pronounced at the entrance of the Labrador Sea, future North Atlantic studies from models and observations have a good chance to reveal the origin of this Great Salinity Anomaly, since this period is already quite well sampled. These or the confirmation of the periodicity of the Great Salinity Anomalies would make Labrador Sea salinity stratification much more predictable. This would lead to a much higher predictability of convection depths and occurrences assuming the knowledge of the strength of atmospheric forcing.

The observational results of this study can further be used to validate freshwater pathways in models, since it does show several new pathways for seasonal and decadal salinity anomalies in the Labrador Sea region that have not been described by observations so far. Leading again to a higher predictability of Labrador Sea deep convection, since haline buoyancy is the reason for reduced convection depths in many years.

Recent satellite sea surface height (SSH) measurements indicate a strong decline of this subpolar gyre circulation. The reason is found in a weak thermohaline forcing that allows the decay of the domed structure of subpolar isopycnals. Because the time series is too short it cannot be determined whether the 1990's slowing gyre is a part of a decadal cycle or the beginning of a loner term trend (Häkkinen and Rhines, 2004). Thus it is yet unclear if this will impact Labrador Sea convection in the long term, or if it is just the relaxation after the strong cooling of deeper waters during the beginning of the 90's. Further the influence of this weakening on the pathways and origins discussed in this study cannot be determined. No major trend was observed in surface salinities in any of the analyzed regions that could be correlated to the weakening of the subpolar gyre.

Even though it was possible to answer several questions concerning surface salinities in the Labrador Sea more questions came up. For the understanding the influence of EKE in the Labrador Sea it should be analyzed, why enhanced EKE is reducing the mean velocities of the southern West Greenland Current branch, though the southern branch is a major EKE pathway? Why is enhanced EKE not mixing more freshwater into the Labrador Sea, though it is close to the very fresh boundary currents and thus what parts of the boundary current are influenced by the EKE?

Discussing long term variability and Great Salinity anomalies in the North Atlantic the pathway hypothesis of this thesis questions the importance of Arctic freshwater variations for changes in Labrador Sea deep water formation. Seeing no long term influence (within five years) from reasonable salinity variations in the polar West Greenland Current or Labrador Current on the central Labrador Sea salinities it should be analyzed via models if this could also true for longer timescales. This is of main interest for instance regarding long term increased freshwater input into the subpolar gyre.

Future studies will need to show if the Great Salinity Anomalies are a regular occurring phenomena caused by feedback loops and atmosphere ocean coupling or have further unknown origin.

This thesis helped significantly to understand pathways of freshwater in the Labrador Sea region better on timescales from seasons to decades.

Chapter 7

Bibliography

Aagaard, K. and E. C. Carmack, 1989: The role of sea ice and other fresh water in the Arctic circulation. *Journal of Geophysical Research*, **94** (C10), 14485–14498.

Avsic, T., J. Karstensen, U. Send and J. Fischer, 2006: Interannual variability of newly formed Labrador Sea Water from 1994 to 2005. *Geophysical Research Letters*, **33**, 6.

Bacon, S., G. Reverdin, I. G. Rigor and H. M. Snaith, 2002: A freshwater jet on the East Greenland shelf. *Journal of Geophysical Research*, **107** (C7).

Belkin, I., 2004: Propagation of the Great Salinity Anomaly of the 1990s around the northern North Atlantic. *Geophysical Research Letters*, **31** (L08306).

Belkin, I. M., S. Levitus, J. I. Antonov and S.-A. Malmberg, 1998: Great Salinity Anomalies in the North Atlantic. *Progress in Oceanography*, **41**, 1 68.

Berger, A., M. Loutre and J. Laskar, 1992: Stability of the Astronomical Frequencies Over the Earth's History for Paleoclimate Studies. *Science*, **255** (5044), 560–566.

Black, D., L. Peterson, J. Overpeck, A. Kaplan, M. Evans and M. Kashgarian, 1999: Eight centuries of North Atlantic ocean atmosphere variability. *Science*, **286** (5445), 1709 – 1713.

Brandt, P., F. A. Schott, A. Funk and C. S. Martins, 2004: Seasonal to interannual variability of the eddy field in the Labrador Sea from satellite altimetry. *Journal of Geophysical Research*, **109** (C02028).

Brewer, P., W. Broecker, W. Jenkins, P. Rhines, C. Rooth, J. Swift, T. Takahashi and R. Williams, 1983: A Climatic Freshening of the Deep Atlantic North of 50 N over the Past 20 Years. *Science*, **222** (4629), 1237–1239.

Bronstein, I., K. Semendjajew, G.Musiol and H. Mühlig, 1997: *Taschenbuch der Mathematik*. Verlag Harri Deutsch, Thun, Frankfurt am Main, 3rd Edition.

Buch, E., 2000: Air-sea-ice conditions off southwest Greenland, 1981-97. *Journal of Northwest Atlantic Fishery Science*, **26**, 123–136.

Clarke, R. A. and J.-C. Gascard, 1983: The formation of Labrador Sea water, Part I, large-scale processes. *Journal of Physical Oceanography*, **13**, 1764–1788.

Cuny, J., P. Rhines, F. Schott and J. Lazier, 2004: Convection above the Labrador Continental Slope. *Journal of Physical Oceanography*, **35** (4), 489–511.

Cuny, J., P. B. Rhines, P. P. Niiler and S. Bacon, 2002: Labrador Sea boundary currents and the fate of the Irminger Sea Water. *Journal of Physical Oceanography*, **32** (2), 627–647.

Curry, R. and C. Mauritzen, 2005: Dilution of the Northern North Atlantic Ocean in Recent Decades.

Czeschel, L., 2005: The Role of Eddies for the Deep Water Formation in the Labrador Sea. Dissertation, Leibniz Institut für Meereswissenschaften, IFM-GEOMAR.

daSilva, A., A. C. Young and S. Levitus, 1994: Atlas of surface marine data 1994. Tech. rep. 6, U.S. Department of Commerce, NOAA, NESDIS.

Deser, C. and M. Blackmon, 1993: Surface Climate Variations over the North Atlantic Ocean during Winter: 1900–1989. *Journal of Climate*, **6** (9), 1743–1753.

Deser, C., M. Holland, G. Reverdin and M. Timlin, 2002: Decadal variations in Labrador Sea ice cover and North Atlantic sea surface temperatures. *Journal of Geophysical Research*, **107** (C5), 3035.

Dessier, A. and J. Donguy, 1994: The sea surface salinity in the tropical Atlantic between 10 S and 30 N: seasonal and interannual variations (1977–1989). *Deep Sea Res*, **41**, 81–100.

Dickson, R., J. Lazier, J. Meincke and P. Rhines, 1996: *Decadal Climate Variability*, Springer, Chapter Long-term coordinated changes in the convective activity of the North Atlantic, 211–261. Number 44 in Global Environmental Change.

Dickson, R. R., J. Meincke, S.-A. Malmberg and A.-J. Lee, 1988: The Great Sainity Anomaly in the northern north Atlantic 1968 - 1982. *Progress in Oceanography*, **20**, 103–151.

Eden, C. and C. Böning, 2002: Sources of eddy kinetic energy in the Labrador Sea. *Journal of Physical Oceanography*, **32** (12), 3346–3363.

Fasham, M., 2003: *Ocean Biogeochemistry: The Role of the Ocean Carbon Cycle in Global Change*. Springer.

Fischer, J., F. A. Schott and M. Dengler, 2004: Boundary Circulation at the Exit of the Labrador Sea. *Journal of Physical Oceanography*, **34** (7), 1548–1570.

Fratantoni, D. M., 2001: North Atlantic surface circulation during the 1990's observed with satellite-tracked drifters. *Journal of Geophysical Research*, **106** (C10), 22,067–22,093.

Funk, A. and P. Brandt, 2007: The West Greenland Current as a source of interannual eddy kinetic energy variability in the Labrador Sea. *Geophysical Research Letters*, **submitted**.

Ganopolski, A. and S. Rahmstorf, 2001: Rapid changes of glacial climate simulated in a coupled climate model. *Nature*, **409**, 153–158.

Gregory, D. N., 2004: Climate: A Database of Temperature and Salinity Observations for the Northwest Atlantic. Canadian Science Advisory Secretariat Research Document 2004/075, Department of Fisheries and Oceans.

Haak, H., J. Jungclaus, U. Mikolajewicz and M. Latif, 2003: Formation and propagation of great salinity anomalies. *Geophysical Research Letters*, **30** (9).

Häkkinen, S., 1993: An Arctic source for the Great Salinity Anomaly: A Simulation of the Arctic Ice-Ocean System for 1955-1975. *Journal of Geophysical Research*, **98** (C9), 16397–16410.

Häkkinen, S. and P. B. Rhines, 2004: Decline of Subpolar North Atlantic Circulation During the 1990s. *Science*, **304** (555).

Hansen, D. V. and H. F. Bezdek, 1996: On the nature of decadal anomalies in North Atlantic sea surface temperature. *Journal of Geophysical Research*, **101** (4), 8749–8758.

Hasselmann, K., 1976: Stochastic climate models, Part I, Theory. *Tellus*, **28**, 473.

Horne, J. and S. Baliunas, 1986: A prescription for period analysis of unevenly sampled time series. *Astrophysical Journal*, **302** (2), 757–763.

Houghton, R. W. and M. H. Visbeck, 2002: Quasi-decadal salinity fluctuations in the Labrador Sea. *Journal of Physical Oceanography*, **32**, 687–701.

Hurrell, J., 1995: Decadal trends in the North Atlantic Oscillation. *Science*, **269**, 676–679.

IPCC, 2007: Climate Change 2007: Synthesis Report. *Intergovernmental Panel on Climate Change, Fourth Assessment Report, Valencia, Spain.*

Jones, H. and J. Marshall, 1997: Restratification after Deep Convection. *Journal of Physical Oceanography*, **27**, 2276–2287.

Katsman, C. A., M. A. Spall and R. S. Pickart, 2004: Boundary Current Eddies and Their Role in Restratification of the Labrador Sea. *Journal of Physical Oceanography*, **34**, 1967–1983.

Khatiwala, S. P., R. G. Fairbanks and R. W. Houghton, 1999: Freshwater sources to the coastal ocean off northeastern North America: Evidence from $H_2^{18}O/H_2^{16}O$. *Journal of Geophysical Research*, **104** (C8), 18241–18255.

Kortzinger, A., J. Schimanski, U. Send and D. Wallace, 2004: The Ocean Takes a Deep Breath. *Science*, **306**, 1337.

Kwok, R., G. F. Cunningham and S. S. Pang, 2004: Fram Strait sea ice outflow. *Journal of Geophysical Research*, **109** (C01009).

Lab-Sea-Group, 1998: The Labrador Sea Deep Convection Experiment. *Bulletin of the American Meteorological Society*, **79** (10), 2033–2058.

Lavender, K. L., R. E. Davis and W. B. Owens, 2002: Observation of Open-Ocean Deep Convection in the Labrador Sea from subsurface Floats. *Journal of Physical Oceanography*, **32** (2), 511–526.

Lazier, J. R. N., 1973: The renewal of Labrador Sea Water. *Deep Sea Research*, **20**, 341–353.

Lazier, J. R. N., 1982: Seasonal variability of temperature and salinity in the Labrador Current. *Journal of Marine Research*, **40** (Supplement), 341–356.

Lazier, J. R. N., 1988: Temperature and salinity changes in the deep Labrador Sea, 1962 - 1986. *Deep-Sea Research*, **35** (8), 1247–1253.

Lazier, J. R. N., 1995: The salinity decrease in the Labrador Sea over the past thirty years. In: *Natural Climate Variability on Decade-to-Century Time Scales*, National Research Council, 295–304.

Lazier, J. R. N., R. Hendry, A. Clarke, I. Yashayaev and P. Rhines, 2002: Convection and restratification in the Labrador Sea, 1990–2000. *Deep-Sea Research Part I*, **49** (10), 1819–1835.

Lazier, J. R. N. and D. G. Wright, 1993: Annual velocity variations in the Labrador Current. *Journal of Physical Oceanography*, **23**, 659–678.

Le Treut, H., R. Somerville, U. Cubasch, Y. Ding, C. Mauritzen, A. Mokssit, T. Peterson and M. Prather, 2007: *Historical Overview of Climate Change*, Cambridge University Press, Cambridge, United Kingdom and New York, NY, USA, Chapter Climate Change 2007: The Physical Science Basis. Contribution of Working Group I to the Fourth Assessment Report of the Intergovernmental Panel on Climate Change.

Lilly, J. M. and P. B. Rhines, 2002: Coherent eddies in the Labrador Sea observed from a mooring. *Journal of Physical Oceanography*, **32** (2), 585–598.

Lilly, J. M., P. B. Rhines, F. Schott, K. Lavender, J. Lazier, U. Send and E. D'Asarp, 2003: Observations of the Labrador Sea eddy field. *Progress in Oceanography*, **59**, 75–176.

Lilly, J. M., P. B. Rhines, F. Schott, J. Lazier, U. Send, R. Käse, C. Mertens and E. D'Asaro, 2000: The structure and variability of the Labrador Sea eddy field, 1994-1999, Part I: The mooring perspective.

Lilly, J. M., P. B. Rhines, M. Visbeck, R. Davis, J. R. N. Lazier, F. Schott and D. Farmer, 1999: Observing Deep Convection in the Labrador Sea during Winter 1994/95. *Journal of Physical Oceanography*, **29**, 2065–2098.

Lomb, N., 1976: Least-squares frequency analysis of unequally spaced data. *Astrophysics and Space Science*, **39** (2), 447–462.

Loutre, M., A. Berger, P. Bretagnon and P. Blanca, 1992: Astronomical frequencies for climate research at the decadal to century time scale. *Climate Dynamics*, **7** (4), 181–194.

Lu, Y., D. Wright and I. Yashayaev, 2007: Modelling hydrographic changes in the Labrador sea over the past five decades. *Progress in Oceanography*, **73** (3-4), 406–426.

Marshall, J. and F. Schott, 1999: Open-ocean convection: Observations, theory, and models. *Reviews of Geophysics*, **37** (1), 1.

Martin, T. and P. Wadhams, 1999: Sea-ice flux in the East Greenland Current. *Deep-Sea Research Part II*, **46**, 1063–1082.

Mineral Resource Administration for Greenland, 1998: Physical enviroment of eastern Davis Strait and northeastern Labrador Sea, an overview. Technical Report, Mineral Resource Administration for Greenland, Danish Meteorological Institut, Copenhagen, Technical Report Overview.

Moron, V., R. Vautard and M. Ghil, 1998: Trends, interdecadal and interannual oscillations in global sea-surface temperatures. *Climate Dynamics*, **14** (7), 545–569.

Mysak, L. A., R. G. Ingram, J. Wang and A. Van der Baaren, 1996: The anomaluous sea-ice extent in Hudson Bay, Baffin Bay and the Labrador Sea during three simultaneous ENSO and NAO episodes. *Atmosphere Ocean*, **34**, 313–343.

Mysak, L. A., D. K. Manak and R. F. Marsden, 1990: Sea-Ice anomalies in the Greenland and Labrador Seas during 1901-1984 and their relation to interdecadal Arctic climate cycle. *Climate Dynamics*, **5**, 111–133.

Oka, E. and K. Ando, 2004: Stability of Temperature and Conductivity Sensors of Argo Profiling Floats. *Journal of Oceanography*, **60** (2), 253–258.

Peterson, I. K., S. J. Prinsenberg and P. Langille, 2000: Sea ice fluctuations in the western Labrador Sea (1963-1998). Technical Report 208, Canadian Technical Report of Hydrography and Ocean Sciences.

Pickart, R. S., W. M. Smethie, J. R. N. Lazier, E. P. Jones and W. J. Jenkins, 1996: eddies of newly formed upper Labrador Sea Water. *Journal of Geophysical Research*, **101** (C9), 20711–20726.

Pickart, R. S., D. J. Torres and R. A. Clarke, 2002: Hydrography of the Labrador Sea during Active Convection. *Journal of Physical Oceanography*, **32** (2), 428–457.

Prater, M. D., 2002: Eddies in the Labrador Sea as observed by profiling RAFOS floats and remote sensing. *Journal of Physical Oceanography*, **32**, 411–427.

Press, W., B. Flannery, S. Teukolsky and W. Vetterling, 1992: *Numerical Recipes in C: The Art of Scientific Programming*. Cambridge University Press, Cambridge, England, 2nd Edition.

Rahmstorf, S., 2002: Ocean circulation and climate during the past 120,000 years. *Nature*, **419**, 207–214.

Renfrew, I. A., G. W. K. Moore, P. S. Guest and K. Bumke, 2002: A comparison of surface layer and Surface Turbulent Flux Observations over the Labrador Sea with ECMWF Analyses and NCEP Reanalyses. *Journal of Physical Oceanography*, **32** (2), 383–400.

Rudels, B., 1990: Haline convection in the Greenland Sea. *Deep-Sea Research*, **37** (9), 1491–1511.

Sabine, C., R. Feely, N. Gruber, R. Key, K. Lee, J. Bullister, R. Wanninkhof, C. Wong, D. Wallace, B. Tilbrook et al., 2004: The Oceanic Sink for Anthropogenic CO2. *Science*, **305** (5682), 367–371.

Sarmiento, J. and C. Le Quéré, 1996: Oceanic Carbon Dioxide Uptake in a Model of Century-Scale Global Warming. *Science*, **274** (5291), 1346–1350.

Sarmiento, J. L., T. M. C. Hughes, R. J. Stouffer and S. Manabe, 1998: Simulated response of the ocean carbon cycle to anthopogenic climate warming. *Nature*, **393**, 245–249.

Sathiyamoorthy, S. and G. W. K. Moore, 2002: Buoyancy flux at Ocean Weather Station Bravo. *Journal of Physical Oceanography*, **32**, 458–474.

Scargle, J., 1982: Studies in astronomical time series analysis. II- Statistical aspects of spectral analysis of unevenly spaced data. *Astrophysical Journal*, **263** (Part 1).

Schmidt, S., 2003: Frischwassereinflüße auf die Konvektionsaktivität in der Labradorsee. Diplomarbeit, Institut für Meereskunde, Kiel.

Schmidt, S. and U. Send, 2007: Origin and Composition of seasonal Labrador Sea Freshwater. *Journal of Physical Oceanography*, **37**, 24.

Schulz, M. and M. Mudelsee, 2002: REDFIT: estimating red-noise spectra directly from unevenly spaced paleoclimatic time series. *Computers and Geosciences*, **28** (3), 421–426.

Send, U. and J. Marshall, 1995: Inegral effects of deep convection. *Journal of Geophysical Research*, **25** (5), 855–872.

Smith, W. H. F. and D. T. Sandwell, 1997: Global seafloor topography from satellite altimetry and ship depth soundings. *Science*, **v. 277**, 1956–1962.

Stommel, H., 1961: Thermohaline convection with two stable regimes of flow. *Tellus*, **13** (2), 224–230.

STOMMEL, H. and A. ARONS, 1960a: On the abyssal circulation of the world ocean - I. Stationary planetary flow patterns on a sphere. *Deep-Sea Research*, **6**, 140–154.

STOMMEL, H. and A. ARONS, 1960b: On the abyssal circulation of the world ocean - II. An idealized model of the circulation pattern and amplitude in oceanic basins. *Deep-Sea Research*, **6**, 217–233.

Stramma, L., D. Kieke, M. Rhein, F. Schott, I. Yashayaev and K. Koltermann, 2004: Deep water changes at the western boundary of the subpolar North Atlantic during 1996 to 2001. *Deep-Sea Research: Part I*, **51** (8), 1033–1056.

Straneo, F., 2006: Heat and Freshwater Transport through the central Labrador Sea. *Journal of Physical Oceanography*, **36**, 606–628.

Straneo, F. and F. Saucier, 2007: The outflow from Hudson Strait and its contribution to the Labrador Current. *submitted to: Deep Sea Research: Part I.*

TAYLOR, A. and J. STEPHENS, 1980: Seasonal and year-to-year variations in surface salinity at the nine North-Atlantic Ocean Weather Stations. *Oceanologica Acta*, **3**, 421–430.

Wadhams, P., 2000: *Ice in the ocean*. Gordon and Breach Science Publishers, Newark, NJ.

Walsh, J. E. and D. H. Portis, 1999: Variations of percipation and evaporation over the North Atlantic Ocean, 1958-1997. *Journal of Geophysical Research*, **104** (D14), 16613–16631.

Wang, J., L. A. Mysak and R. G. Ingram, 1994: Interannual variability of sea-ice cover in Hudson Bay, Baffin Bay and the Labrador Sea. *Atmosphere-Ocean*, **32** (2), 421–447.

Wong, A., G. Johnson and W. Owens, 2003: Delayed-Mode Calibration of Autonomous CTD Profiling Float Salinity Data by θ–S Climatology. *Journal of Atmospheric and Oceanic Technology*, **20** (2), 308–318.

Wunsch, C., 1999: The interpretation of short climate records, with comments on the North Atlantic and Southern Oscillations. *Bull. Amer. Meteor. Soc*, **80**, 245–255.

Wunsch, C., 2002: What is the thermohaline circulation. *Science*, **298** (5596), 1179–1181.

Zweng, M. and A. Münchow, 2006: Warming and freshening of Baffin Bay, 1916–2003. *Journal of Geophysical Research*, **111**.

Abbreviations

ADCP	Acoustic Doppler Current Profiler
DFO	Department of Fisheries and Oceans Canada
GSA	Great Salinity Anomaly
ICES	International Council for the Exploration of the Sea
ISW	Irminger Sea Water
lADCP	lowered acoustic doppler current profiler
LC	Labrador Current
LC-ic	offshelf Labrador Current
MOC	meridional overturning circulation
NAC	North Atlantic Current
NADW	North Atlantic Deep Water
NAFO	Northwest Atlantic Fisheries Organization
NAO	North Atlantic Oscillation
NCEP	National Center for Environmental Prediction
nWGCb	northern West Greenland Current branch
PALACE	Profiling Autonomous LAgrangian Circlulation Explorer
SFB	Sonderforschungsbereich
SSH	sea surface height
sWGCb	southern West Greenland Current branch
THC	ThermoHaline Circulation
WGC	West Greenland Current
WGC-ic	offshelf West Greenland Current, often called Irminger Current
WGCn	West Greenland Current north of Cape Desolation
WGCn-ic	offshelf West Greenland Current north of Cape Desolation often called Irminger Current

Danksagung

Für die Möglichkeit zur Verfassung dieser Dissertation, Unterstützung und Betreuung möchte ich mich bedanken bei Uwe Send, Martin Visbeck und Jürgen Fischer; desweiteren bei allen Abteilungsmitgliedern und Kollegen, für die vielen offenen Ohren, bezüglich meiner Fragen, sowie Tips und Hilfestellungen ihrerseits. Insbesondere geht hier mein Dank and Tom Avsic der mir immer mit Rat und Tat zur Seite stand und mir die kallibrierten MicroCat Daten zur Verfügung gestellt hat.

Die Abwechslung, Unterstützung und nötige Motivation im Laufe der Arbeit verdanke ich vor allem Katrin, Theda und Jonte Schmidtko, sowie meinen Eltern und vielen Freunden.

Für das Berichtigen meiner Fehler im Englischen danke ich ganz besonders Berit Rabe, Robin Dillaway und Aneurin Henry-Edwards.

Erklärung

Hiermit bestätige ich, dass ich die vorliegende Dissertation selbstständig verfasst und keine anderen als die angegebenen Quellen und Hilfsmittel verwendet habe.
Ich versichere, dass diese Arbeit weder ganz noch in Teilen zur Erlangung eines Doktorgrades an anderer Stelle vorgelegen hat.
Ich erkläre, dass die vorliegende Arbeit gemäß der Grundsätze zur Sicherung guter wissenschaftlicher Praxis der Deutschen Forschungsgemeinschaft erstellt wurde.

Kiel, März 2008

(Sunke Schmidt)